PART - III

PART - III

DISSOLUTION PHENOMENA ON CRYSTAL SURFACES

DISSOLUTION OF CALCITE CLEAVAGES IN AQUEOUS SOLUTIONS OF SODIUM HYDROXIDE

THERMAL ETCHING OF CALCITE CLEAVAGES

STUDIES OF ETCH PATTERNS BY MULTIPLE BEAM INTERFEROMETRY AND SCANNING ELECTRON MICROSCOPY

CHAPTER - VIII

DISSOLUTION PHENOMENA ON CRYSTAL SURFACES (GENERAL)

CHAPTER - VIII

DISSOLUTION PHENOMENA ON CRYSTAL SURFACES (GENERAL)

8.1 INTRODUCTION

When a crystal is attacked by an appropriate solvent which chemically or physically dissolves it, the initial dissolution begins at certain preferential points. This phenomenon is known as etching, which is as old as the art and science of metallography. It gives rise to various types of geometrical features on a crystal surface. The production of conical depressions with regular geometrical outlines on crystal surfaces are usually known as etch pits, etch figures or etch marks. The form and symmetry of etch pits were used by mineralogists to determine crystal planes and their orientation with one another. At that time the production of etch pits on a crystal surface was not understood satisfactorily. Dissolution of crystal surface is now thought to occur by retreat of monomolecular steps, being reverse to that of growth, which takes place due to the motion of steps on a surface. It is believed that when a crystal is exposed to a solvent, the dissolution usually begins by a nucleation of unit pit of one molecular depth at relatively weak spot on the surface. The unit pit grows as steps retreat across the crystal surfaces through the action of kinks.

The understanding of etch phenomenon was enhanced by the recognition of various types of imperfections in a

crystal. The defect points are relatively weakly bound with the crystal surface. They used less energy to dissociate than that required by points (atoms) in regular structure. If chemical or physical change gives sufficient energy to dissociate imperfections from the exposed surface, etch pits or etch figures are observed on it. It is not necessary that the solvent should be present at the time of etching, other appropriate physical conditions such as ionic bombardment temperature etc. also help to form etch pits at preferential points on a crystal surface. Following are the ways of obtaining preferential dissolution on a crystal surface (i) Chemical dissolution (ii) Thermal dissolution (iii) Ionic dissolution (iv) Electrolytic dissolution and (v) Dissolution by dehydration. The chemical etching usually produces a few or all features on a crystal surface mentioned below :

(i) Etch pits, terraced, flat-bottomed and point-bottomed,

(ii) Shallow pits, pits with beaks,

(iii) Linear etch rows and Intersecting etch rows

(iv) Tunnels and dendritic etch figures

(v) Etch hillocks and

(vi) Etch spirals.

8.2 DISLOCATION DELINEATION BY ETCHING

The study of topographical features on crystal surfaces has assumed increasing importance due to the information it provides for defect structure and under favourable circumstances the history of the growth of crystals. There are several methods of studying surface for revealing dislocations ending on the surface. They are (i) Etching technique, (ii) Decoration method, (iii) X-rays and (iv) Electron microscopy. Important experimental studies on microtopographical features were made by utilizing the above techniques. In the present chapter studies of delineation of dislocations by characteristic etch features and also of growth features on crystal surfaces by high resolution optical techniques are reviewed.

The number of papers on observations of dislocations under controlled dissolution which have been published by now is so large that it is impossible to do justice to each one of them in such a short review. It should be emphasized that all methods have contributed and are still contributing valuable information on dislocations in crystals. The experimental investigation of dislocations in any crystalline substance should not be considered as complete until quantitative studies of all facets based by all four methods are over. It is particularly desirable

to employ more than one method of observation of the same distribution of dislocations to establish whether all dislocations are visible and whether the configurations are modified by the method used for observation. Examples of this are etching and decoration, or either etching or decoration and one of the X-ray diffraction contrast methods or electron microscopy.

The essential background of the dislocations theory of the strength of materials was reasonably well established in 1949 although much remained to be done in developing the fundamental ideas for particular application. Heck[1,2] had observed spiral terraces on single crystals of paraffin, and Hemmlein and others had observed similar terraces on carborundum crystals. Honess[3] had published a book on etch pits on habit faces of minerals and Lacombe and Beaujard[4] had reported arrays of etch pits on aluminium crystals. Siedentopf[5], Rexer[6] and Edner[7] had described the decoration on linear imperfections in crystals. Heidenreich[8] had observed imperfections in thin foils of aluminium by using electron microscope.

Apart from speculations by Shockley and Read[9] on the possibility that the etch pits on the surfaces of aluminium crystals observed by Lacombe and Beaujard[4] were associated with dislocations, there appeared to be no

experimental support for dislocation theory. The discussion on crystal growth which was organized by Faraday Society and held at University of Bristol in April 1949 ("Crystal Growth" Discussion Faraday Society) marked the begining of the first phase of rapid development of experimental knowledge of the properties, behaviour and interaction of dislocations in crystals. This represents one of the outstanding advances in physics and chemistry of the solid state. At this conference, Frank[10] pointed out that it was not possible to explain the observed rates of growth of crystals under conditions of low supersaturation unless some crystal defect was present which would facilitate or estimate the need for the formation of two dimensional nuclei on the surfaces of growing crystals. According to theoretical calculations (Burton and Cabrera[11]) supersaturations far in excess of those under which crystals are observed to grow would be required for this. Frank[10] (Loc. cit) proposed real crystals to be imperfect and that crystal imperfection which played important role in crystal growth was screw dislocation. He showed that even the presence of one screw dislocation would eliminate the need for the formation of successive two dimensional nucleus during growth because the crystal would then have only helicoidal surface. He concluded that participation of single screw dislocation

in growth of crystals would be made evident by the presence of a spiral terrace on a surface while pairs of screw dislocations of opposite hand would be associated with succession of closed loops. However, no experimental evidence was immediately forthcoming to support his ideas. Later, Griffin[12] found such features on beryl crystals. Firm confirmation of the validity of the mechanisms proposed by Frank (Loc cit) has proved by topographical studies of spirals on several crystal surfaces (Verma[13] 1951 a,b,c ; 1952 a,b ; Amelinckx[14] 1951, 1952 a,b, 1953 a,c ; Dawson and Vand[15] 1951 a,b).

The work on the correspondence between etch pits and dislocations arose as a nature sequel to the studies of relationship between growth features (spiral terraces) and screw dislocations. The fact that the dissolution of a crystal occurs preferentially at the site of screw dislocations was first established by Horn[16]. Gilman and Johnston[17] studied the behaviour of dislocations in Lithium fluoride crystals and found that well defined etch pits were formed at the points of intersections of dislocations with cleavage surfaces, when Lithium fluoride crystals were immersed in a very dilute aqueous solution of ferric fluoride or in a solution of containing this substance and hydrofluoric acid. They were able to distinguish between dislocations already present in the

crystals and dislocations freshly introduced by plastic deformation and also between edge and screw dislocations.

The first theoretical treatment of the nucleation of etch pits at dislocations was given by Cabrera and Lavine[18]. They postulated that the strain energy localized in the vicinity of a dislocation, lowered the free energy required for the nucleation of dislocation with a crystal surface. This leads to the preferential dissolution of dislocation sites on the surface. Gilman[19] criticized this model because elastic strain energy of a pure screw dislocation is zero at the surface and both types of dislocations (having some finite energy at the surface) seem to be etched in almost identical fashion. He has suggested that the dislocation core energy is more important than the elastic strain energy for nucleation of etch pits. This is supported by the following observations :

(i) The dislocations in metals are more difficult to etch than those in ionic or covalent crystals.

(ii) The core energies of dislocations in metals are less than in other types of materials.

(iii) Since overlapping strain fields of dislocations closed together tend to cancel out, it would be

expected on the basis of Cabrera's model that widely separated dislocations would etch at different rates than ones closely spaced. Contrary to this, it is observed that etch pits at isolated dislocations within the subgrains of a crystal are of the same size as the etch pits in the sub-boundries.

(iv) Dislocations were etched at different rates (Gatos and Lavine[20]). Schaarwachter[21] has modified Cabrera's treatment taking due care of core energy suggested by Gilman. He distinguished three cases depending on the relative importance of the contributions of the dislocation core energy and elastic energy. (a) Only the core energy is important in lowering G (change in free energy of a two dimensional nucleus formed at dislocations). This is probably the case for metals. (b) Both the core and strain energy contribute to lowering of G ; this is possibly the case for ionic and covalent crystals with small Burger Vector. (c) Only the strain energy of dislocation is significant and the cabrera's model is valid. This case applies to materials having large Burger Vectors e.g. organic materials.

8.3 FORMATION OF VISIBLE ETCH PITS

The necessary condition for the formation of visible etch pits is governed by the kinetics of dissolution ledges as they move across the crystal surface during dissolution. Successive monomolecular ledges usually sweep across closed packed surface. In order for an etch pit to be visible under an optical microscope, the slope of the etch planes should be at least 3^{o} with respect to a close packed surface. Experimentally measured etch pit slopes for several successful dislocation etching solutions have indeed, been found to lie in the range of $5 - 12^{o}$. For an etch pit to have sufficiently steep slope the ratio of dissolution velocity V_n (normal to surface) to V_l (lateral or ledge dissolution velocity parallel to surface) must be greater than a certain value 0.1. In addition to this, the normal dissolution velocity at a dislocation (V_{nd}) be greater than the average vertical dissolution velocity (V_{ndf}) of a dislocation-free portion of the surface. The necessary conditions can thus be written as :

$$V_n/V_l \geqslant 0.1 , \qquad V_{nd} > V_{ndf}$$

Recently, Shah[22] found that for better quality of etch pits, on calcite cleavages, the ratio of tangential velocity V_t (or V_l) to V_{ndf} should be greater than 10

and the value of activation energy for tangential movement of steps away from the source, E_t, should be greater than activation energy for surface dissolution, E_s i.e.

$$V_t / V_{ndf} > 10, \quad E_t / E_s > 1$$

For a symmetrical etch pit, all planes forming a pit are equally inclined, while slope of these planes are different for asymmetric pits. A detailed study of slopes of etch pits was systematically carried out by Ives and Mcausland[23]. They have classified pits into three categories, depending upon the various ranges of slopes of pits on (0001) surface of zinc crystals. They reported that planes of the etch pits were vicinal faces.

Impurity may segregate around dislocations in impure crystals. Impurity may enhance greater chemical reactivity, giving rise to preferential two dimensional nucleation in metal crystals. It is normally observed that etch pitting solutions for most of the metals and semiconductors studied so far are strong oxidizing agents. It is considered that the first step in the dissolution process is an oxidation of crystal surface. This is followed by the removal of oxide layers. It was observed that oxide nuclei were formed on pure copper crystals

(Young[24]) and on Ge crystals (Faust[25]). However, these oxide nuclei were not related to dislocations. The influence exerted by impurities on and around dislocations has been discussed in detail by Gilman[26] et al. on LiF crystals which was etched by water with addition of FeF_3, AlF_3 etc. They found that nature of etch pits was dependent on the concentration of FeF_3 solution. The function of FeF_3 is to inhibit the ledge motion. It means that V_ℓ depends upon Fe^{+++} concentration. The Fe^{+++} ion (and such others in about 30 compounds) retards the step motion, apparently by absorption on the steps, but does not seem to effect V_{nd}. Cations (Fe^{+++}, Al^{+++} etc.) are believed to have strong tendency to form (FeF_6), (AlF_6) complexes and that is why they play a major role and anions do not effect the pit formation. Cabrera (1956) examined theoretically the conditions for the formation of etch pits and oxide nuclei at dislocations. Sears[27] reviewed theory of Cabrera and modified it by including the effect of solution poison. Step poison increases the rate of two dimensional nucleation at fixed supersaturation but markedly decreases the rate of step motion or of spreading of newly formed layers. Ives and Hirth[28] studied the etch pit profile as a function of concentration of LiF and FeF_3 in the etching solution. The results were consistent with a mechanistic theory involving

dissociation of LiF from unimolecular steps on it and subsequent diffusion into solution if a time dependent adsorption of FeF_3 poison at the receding unimolecular steps was involved. The above theory deals with " Part diffusion, Part inhibitor control of ledge kinetics". It explain very well other results except slope of pits. According to this theory the slope of a dislocation pit should decrease with decreasing under-saturation of LiF. Experiment showed the pit slope to be essentially independent of LiF concentration. The explanation given for the discrepancy was that the accumulation of an inhibitor on a given ledge increased as the distance between ledge and surface increased i.e. it was a time dependent process. Westwood[29] used aqueous solutions of a long chain fatty acids to reveal the point of emergence of dislocations in LiF. This shows that fatty acid may provide a ready source of potential inhibitor for a variety of crystal-etchant systems. Chemisorption and complex formation in this process is likely to affect the core energy available for the nucleation of kinks. Ives and Ramchandran[30] studied the morphology of etched LiF surface with an electron microscope. It reveals complex structure of surface ledges on (100) cleavage face of this crystal. The ledge structure is complex due to irregular inhibition by ferric ions. Haribabu and

Bansigir[31] after studying the role of poison and understanding of the etching mechanism, concluded that the stability of the complexes formed at the kink site and those formed in the solvent layer very close to the crystal surface played an important role in the formation of etch pit. Frank[32] and also Cabrera and Vermilyen[33] then applied the theory of kinematic waves to the localized dissolution process. They showed that the role of adsorbed impurity was to promote the bunching of the outward spreading dissolution terraces so that sharp edge depressions which were clearly visible in microscope were formed.

8.4 ETCH PITS AND THEIR CHARACTERISTICS

The most noticeable feature on a chemically etched surface consists of etch pits. They represent early stages of crystal dissolution and subsequent information concerning the origin, distribution and other important aspects of pits is sought by many workers. Etch pits are used to locate dislocations terminating on a crystal surface. Density of etch pits usually remains constant for different periods of etching. Generally it is higher in metal crystals (10^5 to 10^7 per cm^2), than in ionic crystals (10^3 to 10^5 per cm^2). Crystals with low dislocation density are desirable for the study of individual dislocations

by etch pit technique. Whether all etch pits reveal dislocations or all dislocations give rise to etch pits is a question, which is not yet fully answered. Dislocation etch pits are usually of same, size and shape but may be of different depth. The difference in the depth may be due to inclination of dislocation line or energy of a dislocation. Patel and Ramanathan[34] observed oppositely oriented triangular etch pits as well as hexagonal etch pits on octahedral cleavages of diamond. They explained these observations by assuming different energies of various dislocations inside the crystal. It is well known that dislocation line never ends within a crystal. However, if it remains inside the crystal it must form a closed loop. The distance between the positions of depth points of a pair of point bottomed etch pits produced on a dislocation loop are varying with etching time and when the loop is exhausted pits coalesce with each other and form a single etch pit. Due to non-existence of dislocation line it becomes shallower on further etching.

The different types of dislocation etch pits (symmetric and asymmetric) were produced on cleavage surfaces of NaCl (Amelinckx[14] 1956) and LiF by Gilman and Johnston (1956). This is found to be due to different inclination of edge and screw dislocations. Gilman and

Johnston have shown that edge dislocation lines lie normal to the plane of observations in LiF crystals, hence symmetric pits arise after heavy etch by CP-4 etchant, while screw dislocations lie 45° to the plane of observation and etching of screw dislocations gives rise to asymmetric etch pits though symmetrical etchant was used in both cases. They could also distinguish between aged and fresh dislocations. Etch pits formed at aged dislocations are shallower than those formed at fresh dislocations. The different types of etch pits corresponding to edge and screw dislocations terminating on grain boundries were distinguished by their varying depths on surfaces of NaCl crystal (Amelinckx, Loc cit). Livingstone[35] developed etching technique to distinguish between positive and negative edge dislocations in copper. He found two different types of pits (light and dark) on (111) surface of copper single crystals, Marukuwa[36] also observed dark and light pits on Cu(111) surface. He concluded that pits at screw dislocations had dark appearance.

It is now known that shapes of etch pits are functions of concentration of etchants, etching time, temperature and other conditions of etching. The shapes of etch pits produced by various etchants of different concentrations on calcite cleavages were studied by Honess and Jones[37],

Keith and Gilman[38], Patel and Goswami[39], Pandya and Pandya[40], Mehta[41] and Shah[22]. The bounding side of a pit may be rectilinear or curvilinear depending upon the energy of an etchant. Tolansky and Patel[42] observed rectilinear etch pits when etching was carried out on octahedral faces of diamond by fused potassium nitrate at temperature below 475° while at 525°C, etching was much faster and the sides of pits become rounded. Pandya[43] has also studied the aspects of curvilinearity of etch pits for various crystals, such as calcite and mica.

Etch pits are usually of three types (1) Flat-bottomed, (2) Point-bottomed and (3) Terraced etch pits. The third type may be further subdivided into (a) flat bottomed with terraced structure, (b) point-bottomed and terraced with closed layers or with spiral formation. Flat-bottomed pits occur on etched surfaces at the sites of point defects. This is due to formation of chemically highly resistant layers after certain dissolution at point defects, where V_n has extremely small value, nearing zero. However rate of surface dissolution, Vs, does not become zero thereby increasing shallowness of flat-bottomed pits. Point bottomed pits are observed at line defects intersecting the plane of observation. Depth of point-bottomed etch pit usually increases with etching time. There is also variation of

normal velocity of dissolution, V_n, with etching time. Hanke[44] observed different slopes of same etch pits for different periods of etching by the same etchant. Terraced etch pits are formed at the dislocations associated with impurities (Gilman[19]). Some times the distance between any two successive layers of terraces are unequal. This was explained on the basis of unequal distribution of impurities around dislocations. Hanke (Loc. cit) has also observed stepped structure of etch pits on cleavage faces of calcite crystals etched by low concentration of glacial acetic acid. He explained that dissociation constant of the etchant at low concentration was more while reaction product was considerably less giving rise to a stepped structure of etch pits.

The eccentricity of an etch pit arises due to the non-coincidence of geometrical centre with depth point, in the plane figure of an etch pit. This is reported in many cases (e.g. on NaCl by Amelinckx 1956, on diamond by Patel[45], on calcium fluoride by Patel and Desai[46], on Gypsum by Patel and Raju[47]). They had explained the formation of the eccentric pits at the site of inclined dislocations ending on the surface and found no effect on eccentricity due to etchant concentration. It was shown very clearly in this laboratory that besides other factors concentration of an etchant does affect the eccentricity

of an etch pit on calcite cleavages.

Etch technique has been utilized to study dislocations and various properties controlled by them. Etch pits essentially reveal the emergent points of dislocations on a surface and therefore, they give a direct measure of dislocation density. Since they have a definite depth, they may also give some useful information about the kind, configuration and inclination of dislocations. Further, etching is also applied to study.

(1) Stress velocity for individual dislocation,

(2) Deformation patterns like pile ups, polygonal walls,

(3) Configuration of dislocations in as-grown crystals,

(4) Dislocation multiplication and movements,

(5) Fresh and grown - in dislocations,

(6) Plastic flow around dislocation,

(7) Radiation hardening,

(8) Fracture and dislocation,

(9) Surface orientation determination,

(10) Polarity of crystal lattice,

(11) Reaction mechanism, and

(12) Grain boundary.

8.5 KINETICS AND MECHANISM OF DISSOLUTION

Inspite of continued efforts over a number of years the exact mechanism of dissolution is not yet well understood. Notwithstanding the formation of guidelines and generalizations in choosing an etchant of the crystal, the selection of an etchant is usually based on a tedious trial and error method. It is often found that many solutions, quite different in composition of their constituents, may give similar results, while with minor changes in the composition or temperature, an etchant which earlier formed dislocation etch pits, may not reveal dislocations or may behave as a polishing solution or vice-versa. Hence a detailed systematic study of reactions occurring on a crystal surface is necessary.

In order to understand the complex reactions occurring on a surface during etching process, one has to consider Laidler's theory of heterogeneous reactions which deals with the dissolution of a solid in a liquid forming products. According to this theory a reaction occurring at the surface may, in general be separated into five steps, the slowest of which will determine the rate of the overall process. The five steps are (Gerasimov et al.,[48]):

(1) Transportation of reactants to the surface (diffusion),

(2) Adsorption of reactants on the surface.

(3) Reaction on the surface,

(4) Desorption of products, and

(5) Transportation of products into the bulk.

Dependening on the conditions under which the process is conducted and its features, one of the five steps may be the slowest. Hence the rate of catalytic reaction may be limited by one of them. The rate of diffusion grows with the temperature according to the law similar to the Arrhenius equation, (Gerasimov et al.,[48]).

$$D = K \exp(-E / kT)$$

It should be noted that the value of E rarely exceeds 1000 - 2000 calories/mole. (0.05 ev - 0.15 ev) i.e. it is only a small fraction of the activation energies of most of the chemical reactions. Consequently, the increase in the rate of diffusion will considerably be slower than the rate of chemical process in most of the reactions. The surface reactions generally have activation energies of the order of 30 Kcal (Or 1.4 ev) whereas for the diffusion processes the values are very small. Diffusion is also frequently the rate determining step in the case of solid liquid reactions owing to its relatively slow rate in solution. In general, the

processes 2 and 4 may be expected to be slow steps in heterogenious reaction, provided the activation energy of adsorption and desorption is high. Because of low activation energy the surface reaction 3 is rapid. Such a rapid reaction is to be expected if the adsorbed particles are atoms, the combination of which requires little or no energy. According to the proposed mechanism, it is very probable that the actual combination of atoms on the surface will be rapid, and hence the slow stage in the reaction should be adsorption of the reactant or desorption of the product.

Viscosity (μ) and diffusion (D) are considered in a chemical process to decide its nature. For liquids having low viscosity at room temperature, the value of its activation energy, E_μ is about 0.14 ev. For denser solutions the graph of log μ versus 1/T is split into two straight lines with different slopes (Sangwal and Arora[49]). If E_μ and activation energies of dissolution happen to be equal, the dissolution kinetics are fully diffusion controlled (Sangwal and Patel[50], Bogenschultz et al.[51]). Further the value of activation energy for a diffusion controlled mechanism is usually less than that kinetically controlled one. (Abramson and King[52]).

The nature of heterogeneous process is greatly

affected by its temperature, pressures of the reactants, rate of flow and porosity of catalyst. When the temperature changes by $10^{o}K$, the rate of diffusion changes approximately by 1.2 times while the rate of reaction by 3 to 4 times. For this reason when the temperature is reduced, the rate of chemical reaction will decrease faster than that of diffusion (Gerasimov et al. loc. cit). Hence the process may have high values of activation energy at low temperatures and conversely. Such behaviour is observed for porus catalysts.

The rate of dissolution depends on the nature of the etchant, temperature and concentration of the etchant. In particular the concentration-dependent etch rate is quite complex showing a maximum at particular concentration. Such peaks in the curves of etch rate versus $CuCl_2.2H_2O$ concentration in alcohols were observed in CaI crystals (Sangwal and Urusovskaya[53], Sangwal et al.[54]) and subsequently in the curves of etch rate versus acid concentration on MgO crystals (Sangwal and Arora loc. cit). The maxima corresponded to a particular etchant concentration ($CuCl_2.2H_2O$ or HNO_3 and HCl) which formed octagonal or circular etch pits on $\{100\}$ faces of MgO crystals. In case of CsI this behaviour was explained on the basis of the influence of copper complexes on the nucleation and movement of dissolution steps on $\{100\}$ surfaces of MgO.

The appearance of maximum was attributed to the adsorption of acid and reaction product. (Sangwal and Arora loc. cit, Sangwal, Patel and Kotak[55]).

A model for dissolution was proposed by Sangwal[56]. The dissolution of crystal surface at crystal-etchant interface involves the following consecutive steps :

(1) Availability of H^+ and anion on the surface.

(2) Capture and migration of H^+ and anions on the surface.

(3) Formation of a complex.

(4) Adsorption of the complex onto the surface.

(5) Formation of an activated complex on the surface.

(6) Adsorption of the activated complex.

(7) Dissociation of the activated complex into reaction products.

(8) Adsorption of reaction products on the surface.

(9) Transport of the reaction products into etchant.

Steps(1) and(9) of the transport of the reacting species are determined by diffusion kinetics while other steps may be regarded to be limited by reaction rate between acid and the solid. On the basis of this model, it was argued (Sangwal 1980) that experimental results obtained from studies on MgO could be understood if adsorption of

the reactants and the complexes formed during the dissolution on a perfect surface and at dislocation sites were taken into consideration. It was concluded that the adsorption processes played an important role in the formation of good, sharp dislocation etch pits and that the adsorption of the activated complex at defect site caused the nucleation of an etch pit (Sangwal, Patel and Kotak, loc. cit).

8.6 FACET FORMATION OF ETCH PIT

Faust[57] studied the reactivity of germanium in various oxidizing and complexing agent and suggested that the shape of a pit was controlled by oxidizing agent and the complexing agent controlled by the rate of attack. Vaghri and Shah[58] studied the effect of different concentrations of oxidizing agents on Bi-Single crystals and suggested that the shape of an etch pit was dependent on the strength of the defects and reactivity of etchant. In contrast to them Bhatt et al.[59] observed that the shape of etch pit was neither dependent on the type of oxident used in the etchant nor on apparent activation energy associated with etching process. Shah[22] concluded that the shape of an etch pit was dependent on the apparent activation energy. Sangwal and Sutaria[60] found that the formation of pits of different morphologies was associated

with different effective undersaturations developed very close to dislocation sites whereas spherulites and hillocks result when effective supersaturation of spherulites and hillocks is considered to be a process similar to overgrowth of MgO itself on its cleavages. They also concluded that etch pits were produced under conditions when the solutions have a low viscosity and the reaction products were moderately soluble and that highly viscous etchant led to the formation of spherulites and hillocks.

Several authors have developed dislocations etchants for calcite. Present author has not come across systematic study on kinetics of etching process of calcite cleavages using strong alkalies. Hence optical study of kinetics and mechanism of dissolution of calcite cleavages by strong alkali is made.

8.7 THERMAL DISSOLUTION

It is known that atoms are bound with one another in a crystal by a comparatively large force of attraction. If a crystal is provided enough energy, against the force of attraction, many of the atoms will leave the surface. One way to provide energy to a crystal surface is by heating it to a certain temperature. If the amount of heat required to raise the temperature of a crystal surface

is properly controlled, those surface atoms having higher energy than others will be first to fly away from the surface. As a result thermal etch marks will be produced at these points. This process is usually referred to as thermal etching. This type of etching is considered to be the reverse of growth of crystals from vapour. Thermal etching is done usually in the desired atmosphere or in vacuum. Various etch features such as spirals, closed loops, etch pits etc. are observed on a thermally etched crystal surface. If thermal etch figures are formed on the dislocations, the movement of dislocations may be observed. Thermal etching and chemical etching have close correspondence e.g. facet formation and visibility of chemical and thermal etch pits. However detailed quantitative study of similar and different features is not yet made.

The study of thermal etching of various crystals is reported by many workers (e.g. Patel et al.[61] ; Deo and Kumar[62] ; Patel et al.[63] ; Ejima et al.[64] etc.) Quantitative study of thermal etching of calcite cleavages was carried out in this laboratory. In continuation of this study the present work on thermal etching of calcite is made more quantitative in nature and is presented in the relevant chapter.

REFERENCES

1. Heck, C.M. — Phys. Rev., 51, 686-90, 1937.
2. [illegible] — Sci. News, Letter, Dec 1936.
3. Honess, A.P. — 'The Nature, Origin and interpretation of etch figures on crystals' (John Wiley & Sons, Inc. N.Y.) 1927.
4. Lacome, P. and Beaujard, L. — Comp. Rend., 221, 414, 1945.
5. Sidentopf, H. — Physik-Z., 6, 855, 1905.
6. Rexer, E. — Z. Physik, 70, 159, 1931. ibid, 75, 177, 1932.
7. Edner, A — Z. Physik, 76, 735, 1932.
8. Heidenreich, R.D. — J. Appl. Phys., 20, 993, 1949.
9. Shockley, W. and W.T. Read — Phy. Rev., 75, 692, 1949. Ibid, 78, 275, 1950.
10. Frank, F.C. — Disc. Faraday Soc., 5, 49, 1949.
11. Burton and Cabrera, N. — Nature (Lond.), 163, 398, 1949.
12. Griffin, L.J — Phil. Mag. 42, 775, Ibid, 42, 330, Ibid, 42, 1337, 1951.
13. Verma, A.R — Nature, 167, 939, Ibid, 168, 430, 783, 1951. Phil. Mag., 42, 1005, Ibid, 43, 441, 1951. Proc. Phys. Soc. London, D65, 806, 1952.

14.	Amelinckx, S.	Nature, 167, 939, 1951. Ibid, 169, 841, 1952. Phil. Mag., 43, 562, 1952. Ibid, 44, 1048, 1953. J. Chem. Phys. 49, 411, 1953. Phil. Mag., 1, 269, 1956.
15.	Dawson, I.M. and V. Vand	Proc. Royal Soc. Lond., A 206, 555, 1951.
16.	Horn, F.H.	Phil. Mag. 43, 1210, 1952.
17.	Gilman, J.J. and Johnston, W.G.	J. Appl. Phys., 27, 1018, 1956.
18.	Cabrera, N. and Lavine, M.N.	J. Chem. Phys. 53, 675, 1956.
19.	Gilman, J.J.	Surface Chem. Metals and Semiconductor Symp. ; John Wiley & Sons. N.Y. 1960.
20.	Gatos and Lavine, M.N.	J Electrochem. Soc 107, 427, 1960
21.	Schaarwachter, B.S.	Phys. Status Solidi, 12, 375, 1965.
22.	Shah, R.T.	Ph.D. Thesis, M.S. University of Baroda, Baroda, 1976.
23.	Ives, M. and Mcausland, D.D.	Surface Sci., 13, 189-200, 1968.
24.	Young, F.W.	Acta. Met., 8, 117, 1960.
25.	Faust, J.W.	Acta. Met., 11, 1077, 1963.
26.	Gilman, J.J.	Trans, AIME, 212, 783-91, 1958.
27.	Sears, C.W.	J. Chem. Phys., 33, 13-17, 1960.

28. Ives, M.B and Hirth, J.P — J. Chem. Phys. 33, 817, 1960

29. Westwood, A.R. — Phil. Mag., 6, 1475, 1961.

30. Ives, M.B. and Ramchandran, J.R. — J. Appl. Phys., 38, 3675, 1967.

31. Haribabu, V. and Bansigir, K.G. — Physica, 30, 2003, 1969.

32. Frank, F.C. — Growth and Perfection of crystals, Wiley, N.Y. P. 411 Eds. Doremus, Roberts and Turnbill.

33. Cabrera, N. and Vermilyen, D.A. — Growth and Perfection of crystals Wiley, N.Y., P. 393, Eds. Doremus, Roberts and Turnbill.

34. Patel, A.R. and Ramnathan, S. — Physica, 30, 2003-4, 1964.

35. Livingstone, J.D. — Act. Met. 10, 229-239, 1962.

36. Marukuva, K. — Jap. J. App. Phys. 6, 944-9, 1967.

37. Honess, A.P and Jones, J.R. — Bull. Geol. Soc. Amer. 48, 667, 1937.

38. Keith, R.E. and Gilman, J.J. — Act. Met., 8, 1, 1960.

39. Patel, A.R. and Goswami, K.W. — Acta. Cryst., 15, 447, 1962.

40. Pandya, N.S. and Pandya, J.R. — Journal of M.S. Univ. of Baroda Baroda, 10, 21, 1961.

41. Mehta, B.J. — Ph.D. Thesis, M.S. Univ. of Baroda, Baroda, 1972

42.	Tolansky, S. and Patel, A.R.	Phil. Mag., 8, 1003-5, 1957.
43.	Pandya, J.R.	J. Tech. and Engg., M.S. Univ. of Baroda, Baroda, 1969
44.	Hanke, I.	Acta. Phys. Austriea, 14, 1, 1961.
45.	Patel, A.R.	Physica, 27, 1097, 1960.
46.	Patel, A.R. and Desai, C.C.	Z. Krist., 121, 55, 1965.
47.	Patel, A.R. and Raju, K.S.	Acta. Cryst., 33, 217. 1967.
48.	Gerasimov Ya ; V. Dreving ; A. Kiselev ; E. Eremin ; V. Lebedev ; G. Panchenkor and A. Shlygin.	Physical Chemistry, Vol. 2, Mir Publishers, Moscow, 1974.
49.	Sangwal, K and Arrora, S.K.	J. Mat. Sc., 13, 1977.
50.	Songwal, K. and Patel, T.C.	Kristall and Technik, 13, 281, 1978.
51.	Bogenschultz, A.F. Locherer, K. and Mussinger, N.	J. Electrochem. Soc., 114, 970, 1967.
52.	Abramson, M.S. and King, C.V.	J. Amer. Chemi. Soc., 61, 2290. 1939.
53.	Songwal, K. and Urusovskaya, A.A.	J. Crystal Growth, 41, 216, 1977.
54.	Sangwal, K., Urusovskaya, A.A. and Smirnov, A.E.	Ind. J. of Pure and App. Phys., 16, 501, 1978.

55. Sangwal, K., Patel, T.C. and Kotak, M.D. — Kristall and Technik, 14, 8, 949-964, 1979.

56. Sangwal, K. — J. Mat. Sci., 15, 237-246, 1980.

57. Faust, J.W. — Reactivity of Solids (Edited by J.W. Mitchell) John Wiley & Sons Inc. N.Y. 1969.

58. Vaghari, D.J. and Shah, B.S. — J. Cryst. Growth, 23, 163-65, 1974.

59. Bhatt, V.P. ; Vyas, A.R. and Pandya, G.R. — Ind. J. Pure and App. Phys., 12, 807-10, 1974.

60. Sangwal, K. and Sutaria, J.N. — J. Mat. Sci., 11, 2271-2282, 1976.

61. Patel, A.R. ; Bahl, O.P. and Vagh, A.S. — Acta Crystallogr. 19, 1025-26, 1965.
Ibid, 20, 914-916, 1966.

62. Deo, P.G. and Kumar, S. — J. Cryst. Growth, 3-4, 694-699.

63. Patel, A.R. and Chaudhari, R.M. — Jap. J. Appl. Phys. 8, 667-671, 1969.
Ibid, 8, 672-676, 1969.
Indian J. Pure and Appl. Phys., 7, 341-344, 1969.

64. Ejima, T. ; Robinson, W.H. and Hirth, J.P. — J. Cryst. Growth, 7, 155-162, 1970.

CHAPTER - IX

DISSOLUTION OF CALCITE CLEAVAGES

IN AQUEOUS SOLUTIONS OF SODIUM HYDROXIDE

CHAPTER - IX

DISSOLUTION OF CALCITE CLEAVAGES

IN AQUEOUS SOLUTIONS OF SODIUM HYDROXIDE

9.1 INTRODUCTION

Applications of selective etching as a tool in the study of dislocation behaviour are well demonstrated[1]. However the basic mechanism of the process is not yet fully understood. Since the classical work of Gilman et al.,[2] much work in this direction has appeared in the literature on alkali halides (e.g. please see Ives[3], Ives and Hirth,[4] Urusovskaya,[5] Hari babu and Bansigir,[6] Bhagwan Raju and Bansigir,[7,8] Sangwal et al.,[9] etc.) as well as on metals (Popkova et al.,[10,11] Bhatt et al.,[12]) in which attempts have been made to understand it.

Etching solutions of alkali halides consists of a solvent (usually some alcohol or organic acid) to which an inhibitor is added. The etchants for metals and semiconductors are relatively complicated and consists of at least two solutions. One of these solutions forms a compound with crystals while the other desorbs it by forming certain complexes. There is another class of etchants which consists of some pure solutions, for example mineral acids strong alkalies for etching of calcite, fluorite, barite, magnesium oxide etc. This class of etchants is suitable for the study of the etching process.

The shape of an etch pit is dependent on the nature, concentration and temperature of etchant. Occurrence of

different shapes of etch pits on calcite cleavage faces due to various types of etchants and their different concentrations are reported (Watt[13] ; Stanley[14] ; Pandya and Pandya[15] ; Mehta[16] ; Shah[17] and Bhagia[18]). In all cases the diluent used to change concentration of an etchant was distilled water in which calcite is sparingly soluble (0.008 gm per litre at 20°C). It is thus clear that with the same etchant, either concentrated or diluted, the chemical reaction is not materially changed. However, the rate of reaction on cleavage face of calcite changes, which in some cases gives rise to production of etch pits of various shapes. This obviously points to the unusual physical, chemical and crystallographic characteristics of calcite in general and its cleavages in particular. It was also reported that even with the same concentration of an etchant, the rate of stirring of the solution has a marked effect on shape/or eccentricity of etch figures (Hanke[19] ; Mehta[16]).

The present author has carried out a detailed systematic study of etch rates on calcite cleavages by employing strong alkalies (sodium hydroxide and potassium hydroxide) as etchants. Doubly distilled water was used as a solvent. It is observed that basically the etching effects of aqueous solutions of sodium hydroxide and potassium hydroxide are almost similar. Further both

are dislocation etchants. The present work, therefore, reports optical study of etch rates as a function of etching time concentration and temperature of etching, carried out by using aqueous solution of sodium hydroxide.

9.2 EXPERIMENTAL

Natural crystals of calcite were obtained from various localities in India (Sivrajpur, Pavagarh, Broach from Gujarat State and from Rajasthan etc). The crystals are fairly big with their sizes ranging from 1 cm to 15 cm with cross sectional area of the order of 3 cm x 3 cm. A big crystal was selected and etching work was carried out on small pieces obtained by cleaving the crystal in the usual way i.e. by giving a sharp blow with a hammer on a razor blade kept in contact with the crystal along a cleavage direction. The cleavage surface was fully immersed in a still etchant of known concentration for desired time of etching at a constant temperature. The temperature of the etchant was maintained to within $\pm$ 0.5^{o}C by a regulator attached to constant temperature water bath for studies at higher temperature. After etching the crystal for a given period, it was kept into a dilute ammonium chloride solution 0.28 M in distilled water at the same temperature as that of sodium hydroxide solution for eight to ten seconds. By keeping etched sample in dilute ammonium chloride solution,

the calcium oxide film formed during etching in sodium hydroxide solution on calcite cleavage gets dissolved. The crystal cleavage was kept in running water for some time and was then dried by hot air blower. The samples etched were optically studied by CZ VERTIVAL microscope described in Chapter 2. The etch pit dimension along direction [110] was measured by using filar micrometer eyepiece (x 750 with least count of 0.2 microns). An accuracy of $\pm$ 0.1 μ can be achieved by this method. The surface dissolution rate was measured by usual weight loss method using a semi-microbalance.

9.3 OBSERVATIONS AND RESULTS

The chemical dissolution of calcite cleavages by dislocation etchant, aqueous sodium hydroxide solution gives rise boat-shaped (pyramidal and flat bottom) etch pits (Pandya and Pandya[15]). Fig. 9.1(a) and 9.1(b) show photomicrographs of oppositely matched cleavage faces of calcite etched in 17 M solution of sodium hydroxide at 70°C for four minutes and six minutes respectively. There is almost one-to-one correspondence of boat-shaped etch pits. In order to bring out correspondence of individual pits on both photomicrographs pits are numbered as shown in fig. 9.1(a) and 9.1(b). Enlarged photomicrograph of one of the etch pits is shown in fig. 9.1(c). The figure clearly

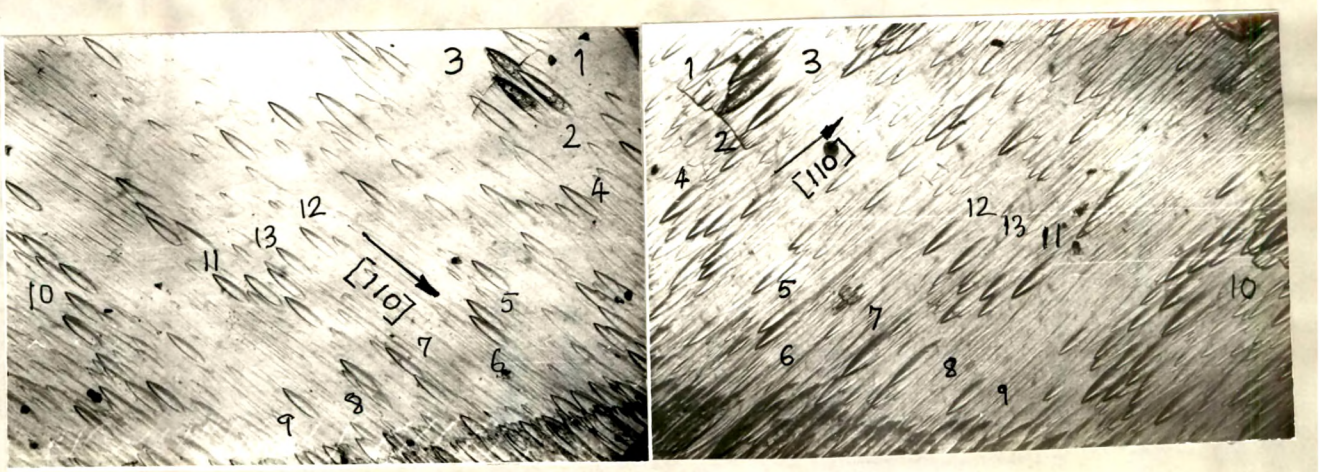

(a) (x 125) (b) (x 125)

Fig. 9.1(a,b) shows photomicrographs of oppositely matched cleavage faces etched in 17 M aqueous NaOH solution at 70°C for 4 min. and 10 min. respectively.

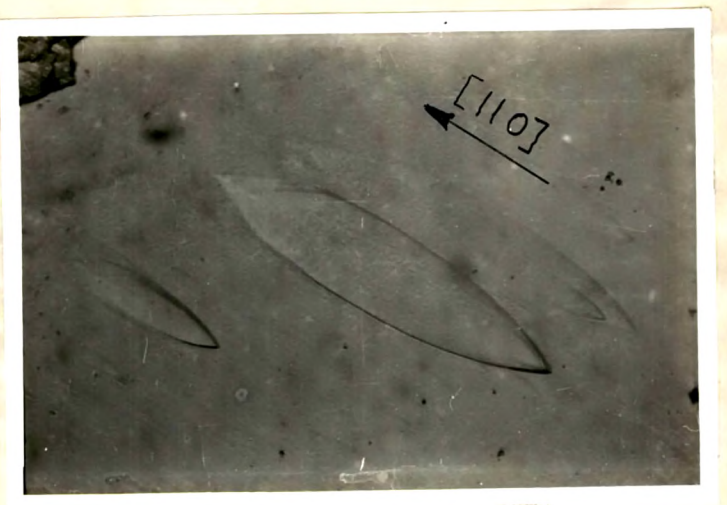

(X 500)

Fig. 9.1 C shows enlarged photomicrograph of etch pit on Calcite cleavage etched in 14.7 M aqueous sodium hydroxide solution at 75°C for 5 min.

reveals sharp ends of boat-shaped pit pointing in direction [110].

9.3.1(a) Effect of etching time on etch pits

Fig. 9.2, 9.3, 9.4, 9.5 show the photomicrographs of calcite cleavage face etched in 12.3 M sodium hydroxide solution at 75°C for 2.0, 4.5, 5.5 and 7.5 minutes respectively. It is clear from the photomicrographs that with the increase in etching time the number and location of etch pits remain unchanged, but the pits grow in size. Further, the cleavage lines (Fig. 9.5) are etched away by successive etching (Fig. 9.3, 9.4). As a result there is a shifting of cleavage line from its original position on the virgin unetched cleavage surface.

9.3.1(b) Effect of concentration on etch pits

Fig. 9.6(a) and 9.6(b) are the photomicrographs of cleavage counterparts etched in 4.8 M and 12.3 M aqueous sodium hydroxide solution for 15 minutes and 5 minutes at 60°C respectively. Also fig. 9.7(a) and 9.7(b) show the photomicrographs of calcite cleavage counterparts etched in 12.3 M and 21.7 M aqueous sodium hydroxide solution for 5 min and 6 min. respectively at 70°C. These photomicrographs indicate that the density of etch pits, on calcite cleavages

Fig. 9.2 (x 125)

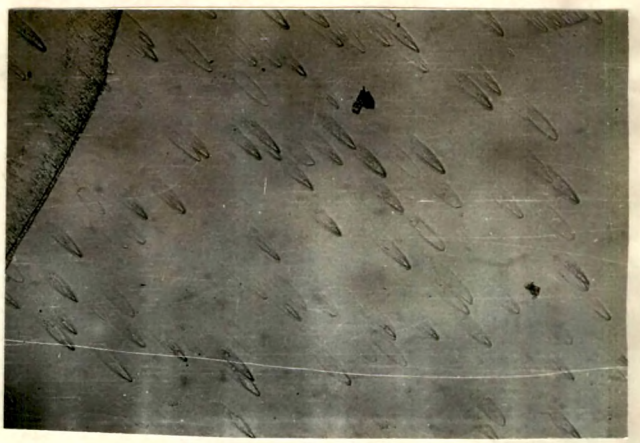

Fig. 9.3 (x 125)

Fig. 9.4 (x 125)

Fig. 9.5 (x 125)

Fig. 9.2, 9.3, 9.4 and 9.5 show photomicrographs of calcite cleavage face etched in 12.3 M aqueous NaOH solution at 75°C for 2.0, 4.5, 5.5 and 7.5 minutes respectively.

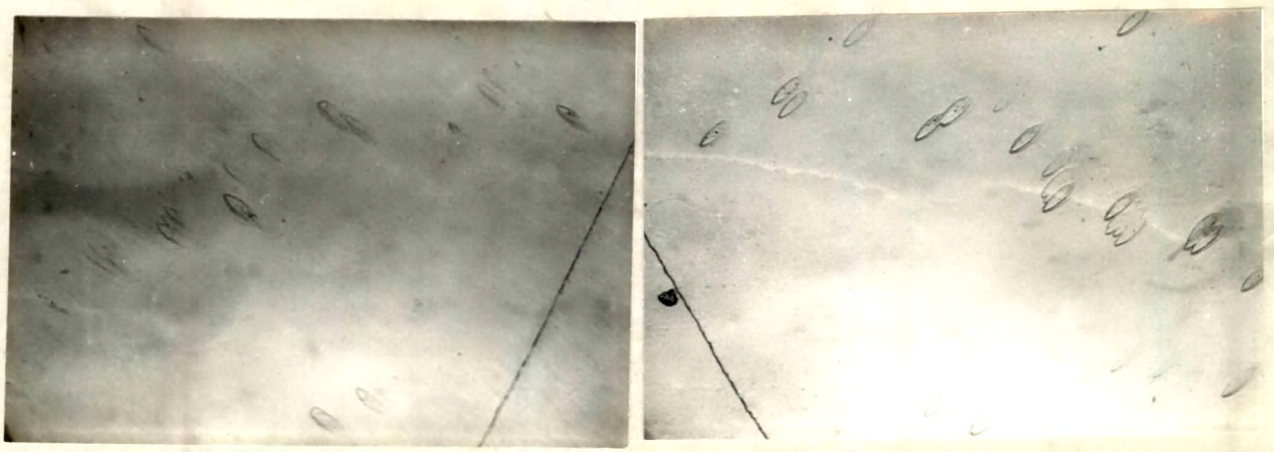

(a) (x 125) (b) (x 125)

Fig. 9.6(a,b) show the photomicrographs of cleavage counterparts of calcite etched in 4.85 M and 12.3 M aqueous NaOH solution at 60°C for 15 min. and 5 min. respectively.

using different concentrations of etchant remain the same. The photomicrographs also show that the plane shapes of etch pits also remain almost identical for different etchant concentrations whereas in case of etchants like acids (Hydrochloric, Acetic, tartaric, Lactic, Formic etc.) show change of shape of etch pits (Mehta,[16] Shah,[17] Bhagia[18]). The photomicrographs fig. 6(a), 6(b) and also fig. 9.7(a) and 9.7(b) show one-to-one correspondence of etch pits. One of the ends of etch pits produced by 21.7 M solution of sodium hydroxide is protruding above the surface, the other is inside the cleavage. surface under observation (fig. 9.15).

In order to assess the influence of concentration of sodium hydroxide solution on etch pits, the temperature of etching was kept constant and the concentration of the etchant was systematically changed.

9.3.1(c) Effect of temperature on etching

Fig. 9.8(a) and 9.8(b) show the photomicrographs of calcite cleavage counterparts etched in 12.3 M sodium hydroxide solution for 10 minutes at 50°C and for 3 minutes at 80°C respectively. Photomicrographs show that at lower and higher temperatures the density of etch pits on cleavage counterparts remains the same. The shapes of pits do not change ; only the pits grow in size at elevated temperatures.

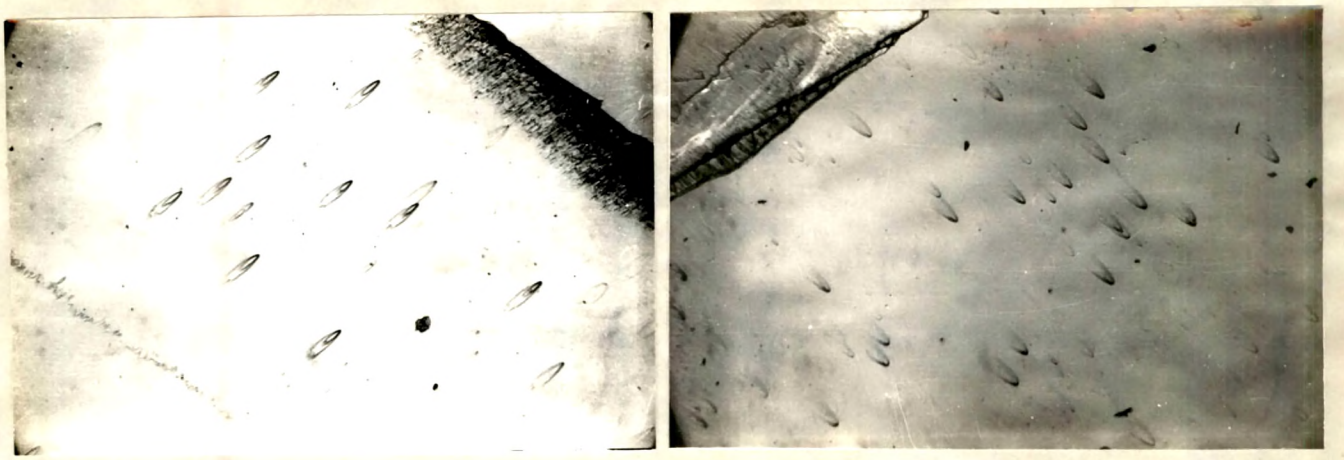

(a) (x 125) (b) (x 125)

Fig. 9.7(a,b) show the photomicrographs of calcite cleavage counterparts etched in 12.3 M and 21.7 M aqueous NaOH solution at 70°C for 5 min. and 7 min. respectively.

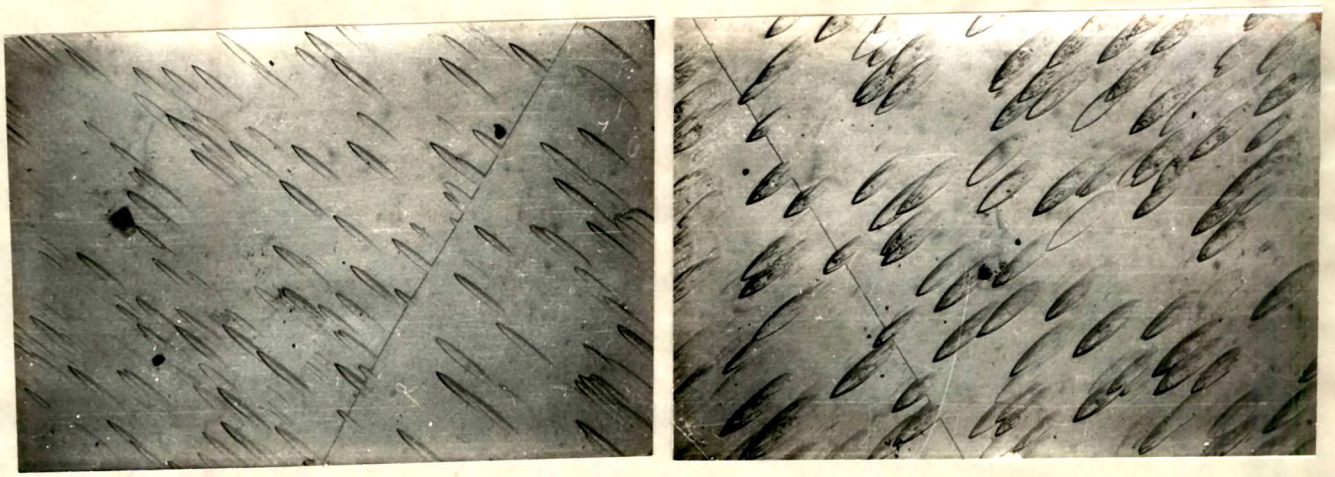

(a) (x 125) (b) (x 125)

Fig. 9.8(a,b) show cleavage counterparts of calcite etched in 12.3 M aqueous NaOH solution at 50°C for 10 min. and at 80°C for 3 min. respectively.

There is almost one-to-one correspondence of etch pits on cleavage counterparts.

9.3.2 Effect of time on etch rates

Several sets of observations of etch pit lengths along direction [110] for different times of etching for various etching temperatures were taken. Table 9.1 present a typical set of observations on length of an etch pit (L) measured along direction [110] and weight loss per cm^2 with etching time at various temperatures of etching using 12.3 M and 21.7 M sodium hydroxide solutions as etchants. Length of etchpit along direction [110] is plotted against etching time (fig. 9.9). It is clear from these plots that length of an etch pit varies linearly with etching time and the straight line passes through the origin. The slopes of these lines give the rate of tangential dissolution, V_t, along [110] at corresponding temperature of etching. Similarly, weight loss per cm^2 is plotted against etching time (fig. 9.10) ; the plots are again straight lines passing through origin. The slopes of these plots give the rate of surface dissolution, V_s in gm per cm^2 per unit time. On dividing this quantity by density of calcite (2.71 gm/cc) one gets the rate of surface dissolution, V_s, in cm/sec. It should be mentioned here that the plots of length of an etch pit (L) and weight loss

Table 9.1

	Concentration C in M	Time t min	Length of Etch pit L x 10^{-4} cm	Wt. Loss gm per cm^2 x 10^{-5}
	12.3 M	10	78	10.05
		20	150	20.4
		30	230	30.1
		40	315	41.09
TEMPERATURE 50°C (323°K)				
	21.7 M	10	38.75	7.6
		20	75.00	14.8
		30	120.00	22.9
		40	156.00	30.5

cont.....

cont.....

	12.3 M	5	80	9.423
		10	152	19.7
		15	240	28.3
		20	321	38.1
TEMPERATURE 60°C (333°K)		30	-	55.6
	21.7 M	5	40.95	7.08
		10	82.00	14.3
		15	120.00	22.0
		20	162.00	28.3
		30		42.5
	12.3 M	3	99.8	10.74
		6	201.0	22.02
		9	305.0	34.21
		12	395.0	45.1
		17	-	63.0
Temperature 70°C (343°K)	21.7 M	3	50.7	9.49
		6	102.0	20.12
		9	155.0	32.14
		12	200.0	40.1
		18	-	57.06

cont.....

cont....

	12.3 M	2	131.5	11.45
		4	260.0	23.4
		6	394.0	35.08
TEMPERATURE		8	525.0	43.4
80°C		12	-	67.2
(353°K)				
	21.7 M	2	63.7	8.96
		4	125.0	18.6
		6	189.0	27.1
		8	260.0	35.7
		12	-	54.1
	12.3 M	45 Sec	87	6.96
		90 Sec	180	13.5
		135 Sec	275	21.3
		180 Sec	352	28.2
TEMPERATURE		300 Sec	-	48.1
90°C				
(363°K)				
	21.7 M	1 Min	58.6	7.6
		2 Min	120.0	14.0
		3 Min	175.0	21.85
		4 Min	243.0	29.00
		6 Min		43.4

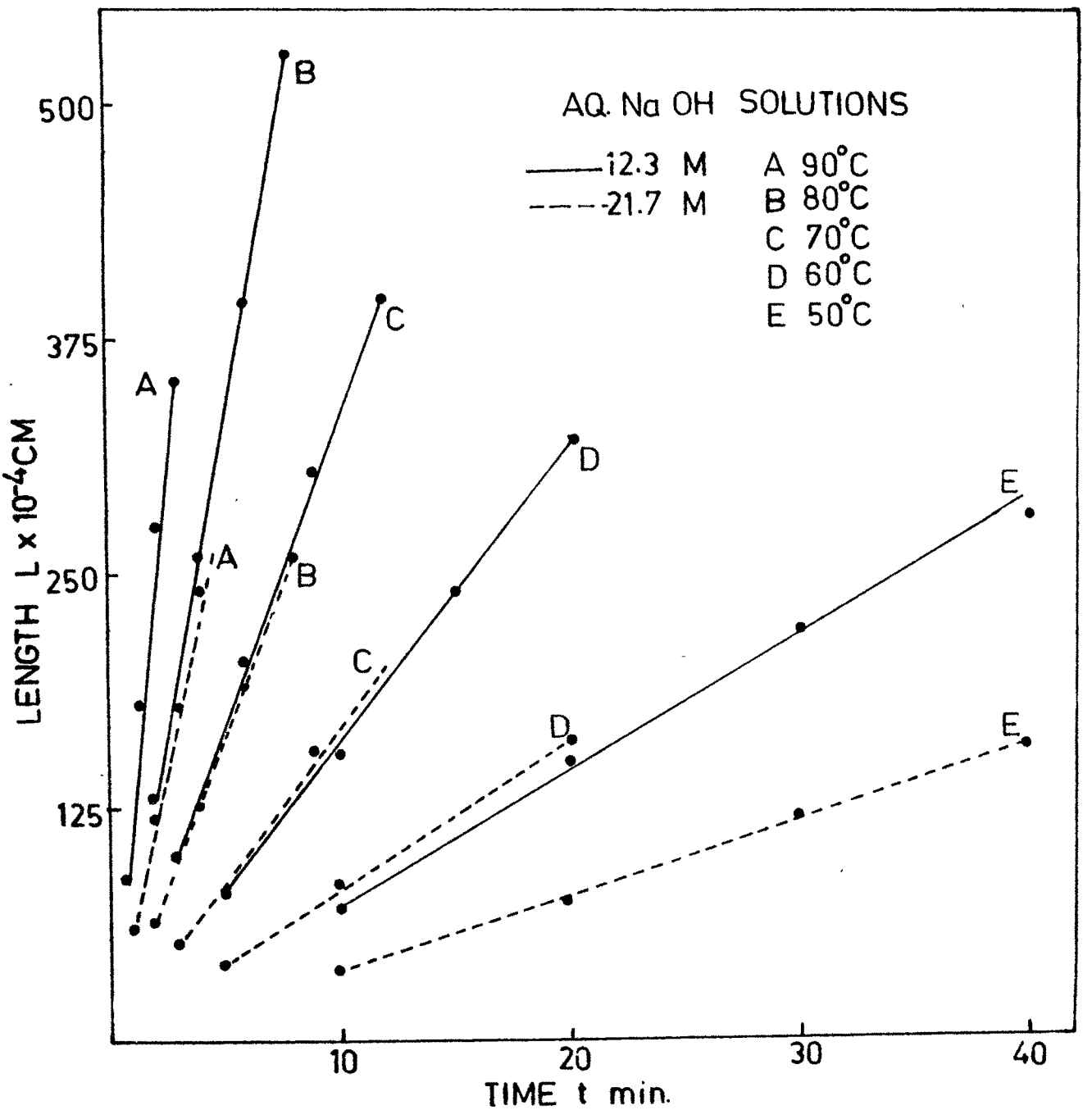

FIG.9·9 PLOT OF LENGTH vs TIME

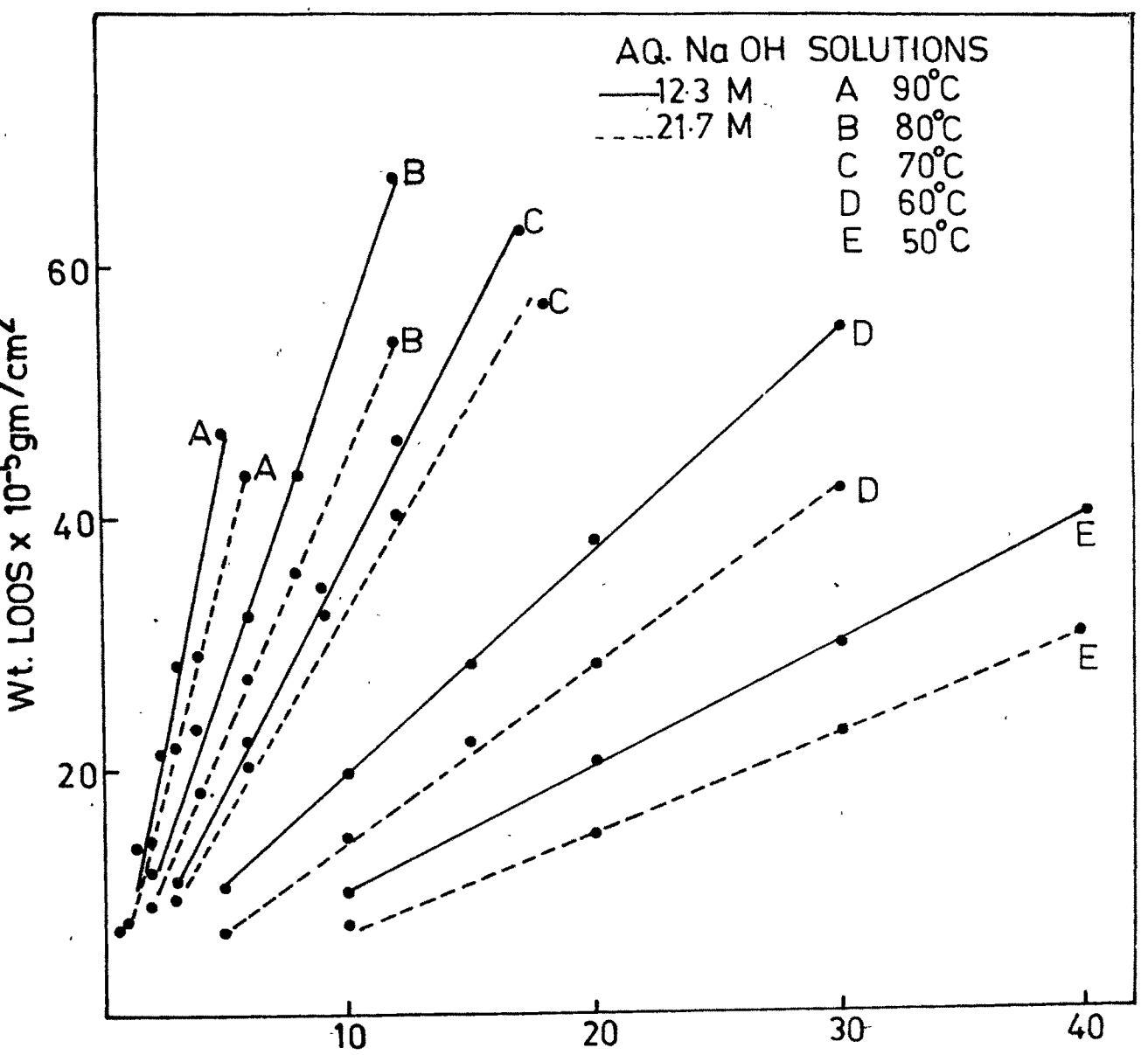

FIG.9·10 PLOT OF Wt. LOOS vs TIME

per cm^2 are always straight lines for all concentrations and temperatures of etching of sodium hydroxide solutions. Straight line plots indicate that rates of tangential as well as surface dissolution are independent of etching time but depend on temperature and concentration of the etchant.

9.3.3 Effect of concentration on etch rates

The dependence of tangential rate (V_t) and surface dissolution rate (V_s) on concentration of sodium hydroxide solution at various temperatures of etching is illustrated by fig. 9.11 and fig. 9.12 respectively. The values of V_t and V_s for various concentrations and temperatures are listed in table 9.2. A careful examination of fig. 9.11 and 9.12 shows that rate of tangential dissolution and that of surface dissolution increases initially with the increase in concentration of the sodium hydroxide solution. After substantial increase, the rate of dissolution decreases at higher concentration of sodium hydroxide solutions. The nature of V_t - C and V_s - C curves is similar. The maximum rate (V_t and V_s) is observed at 17 M concentration at all temperatures of etching. This indicates that the concentration corresponding to maximum rate of reaction does not depend upon temperature of etching.

Table 9.2

TEMPERATURE $T^{o}K$	Concentration C = 485M ; Log C = 0.679						
	$V_t \times 10^{-4}$ cm/sec	Log Vt	$V_s \times 10^{-7}$ cm/sec	Log V_s	$10^3/T$ $^{o}K^{-1}$	V_t/V_s x 10^2	log(V_t/V_s)
323	0.0716	$\bar{6}$.855	0.2818	$\bar{8}$.45	3.096	2.541	2.4050
333	0.1365	$\bar{5}$.135	0.4677	$\bar{8}$.67	3.003	2.918	2.4650
343	0.2512	$\bar{5}$.400	0.7762	$\bar{8}$.89	2.915	3.236	2.5100
353	0.4571	$\bar{5}$.660	1.2001	$\bar{7}$.095	2.833	3.809	2.5808
363	0.7762	$\bar{5}$.890	1.9500	$\bar{7}$.290	2.755	3.981	2.5999

cont.....

Table 9.2 cont.....

Concentration C = 0.3 ; Log C = 0.945

323	0.1047	$\bar{5}$.02	0.3890	$\bar{8}$.59	3.096	2.691	2.4299
333	0.2188	$\bar{5}$.34	0.7244	$\bar{8}$.86	3.003	3.020	2.4800
343	0.4365	$\bar{5}$.64	1.3490	$\bar{7}$.13	2.915	3.235	2.5098
353	0.8414	$\bar{5}$.925	2.3990	$\bar{7}$.38	2.833	3.507	2.5449
363	1.5850	$\bar{4}$.200	4.0741	$\bar{7}$.61	2.755	3.730	2.5717

Concentration C = 12.3M; Log C = 1.038

323	0.1202	$\bar{5}$.08	0.6316	$\bar{8}$.800	3.096	1.903	2.2794
333	0.2661	$\bar{5}$.425	1.0330	$\bar{7}$.09	3.003	2.576	2.4109
343	0.5498	$\bar{5}$.74	2.2091	$\bar{7}$.342	2.915	2.3956	2.3794
353	1.0960	$\bar{4}$.104	3.5210	$\bar{7}$.5471	2.833	3.112	2.4930
363	1.950	$\bar{4}$.29	5.7500	$\bar{7}$.798	2.755	3.390	2.5802

cont.....

Table 9.2 cont...

Concentration C = 14.7 M ; Log C = 1.118

323	0.1202	$\bar{5}$.08	0.6316	$\bar{8}$.91	3.096	1.903	2.2794
333	0.2721	$\bar{5}$.435	1.514	$\bar{7}$.18	3.003	1.797	2.2545
343	0.5623	$\bar{5}$.75	2.754	$\bar{7}$.44	2.915	2.041	2.3098
353	1.072	$\bar{4}$.03	4.677	$\bar{7}$.67	2.833	2.29	2.3598
363	2.042	$\bar{4}$.31	7.943	$\bar{7}$.90	2.755	2.57	2.4099

Concentration C = 17.0 M ; Log C = 1.181

323	0.1413	$\bar{5}$.15	0.9120	$\bar{8}$.96	3.096	1.548	2.1897
333	0.2951	$\bar{5}$.47	1.718	$\bar{7}$.235	3.003	1.717	2.2347
343	0.6026	$\bar{5}$.78	3.126	$\bar{7}$.495	2.915	1.927	2.2848
353	1.175	$\bar{4}$.07	5.495	$\bar{7}$.74	2.833	2.138	2.3300
363	2.138	$\bar{4}$.33	9.120	$\bar{7}$.96	2.755	2.344	2.3699

cont.....

Table 9.2 cont....

Concentration C = 19.1 M ; Log C = 1.2304

323	0.0851.	$\bar{6}$.93	0.5754	$\bar{8}$.76	3.096	1.479	2.1699
333	0.1799	$\bar{5}$.255	1.072	$\bar{7}$.03	3.003	1.678	2.2248
343	0.3589	$\bar{5}$.555	1.950	$\bar{7}$.29	2.915	1.845	2.2649
353	0.6918	$\bar{5}$.84	3.388	$\bar{7}$.53	2.833	2.042	2.3100
363	1.274	$\bar{4}$.105	5.623	$\bar{7}$.75	2.755	2.26	2.3541

Concentration C = 21.7 M ; Log C = 1.2830

323	0.06457	$\bar{6}$.81	0.4677	$\bar{8}$.67	3.096	1.3805	2.1400
333	0.1365	$\bar{5}$.135	0.8710	$\bar{8}$.94	3.003	1.567	2.1950
343	0.2818	$\bar{5}$.45	1.585	$\bar{7}$.20	2.915	1.779	2.2501
353	0.5309	$\bar{5}$.727	2.754	$\bar{7}$.44	2.833	1.927	2.2848
363	0.9772	$\bar{5}$.99	4.677	$\bar{7}$.67	2.755	2.089	2.3199

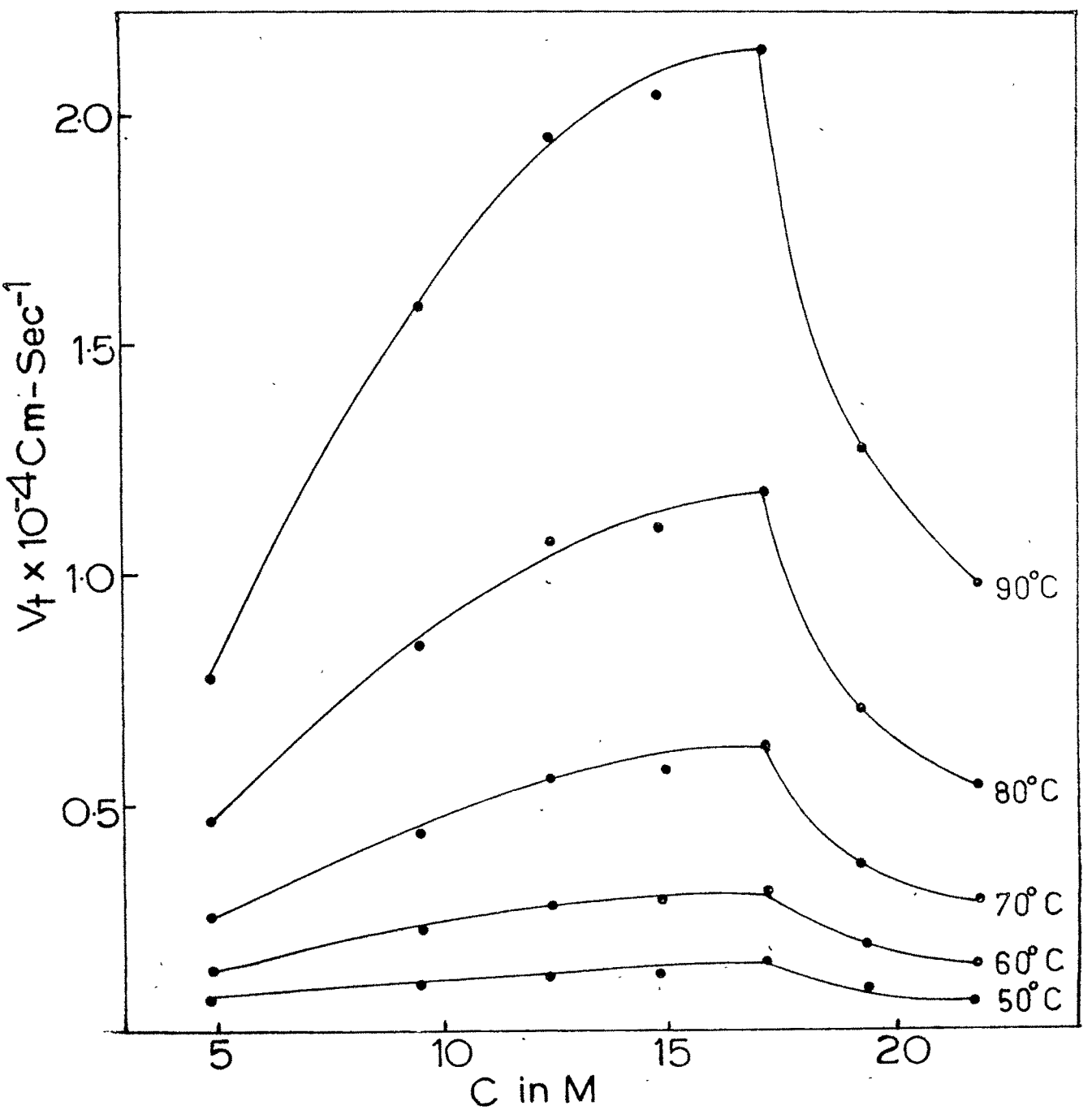

FIG.9·11 PLOT OF V_t vs C

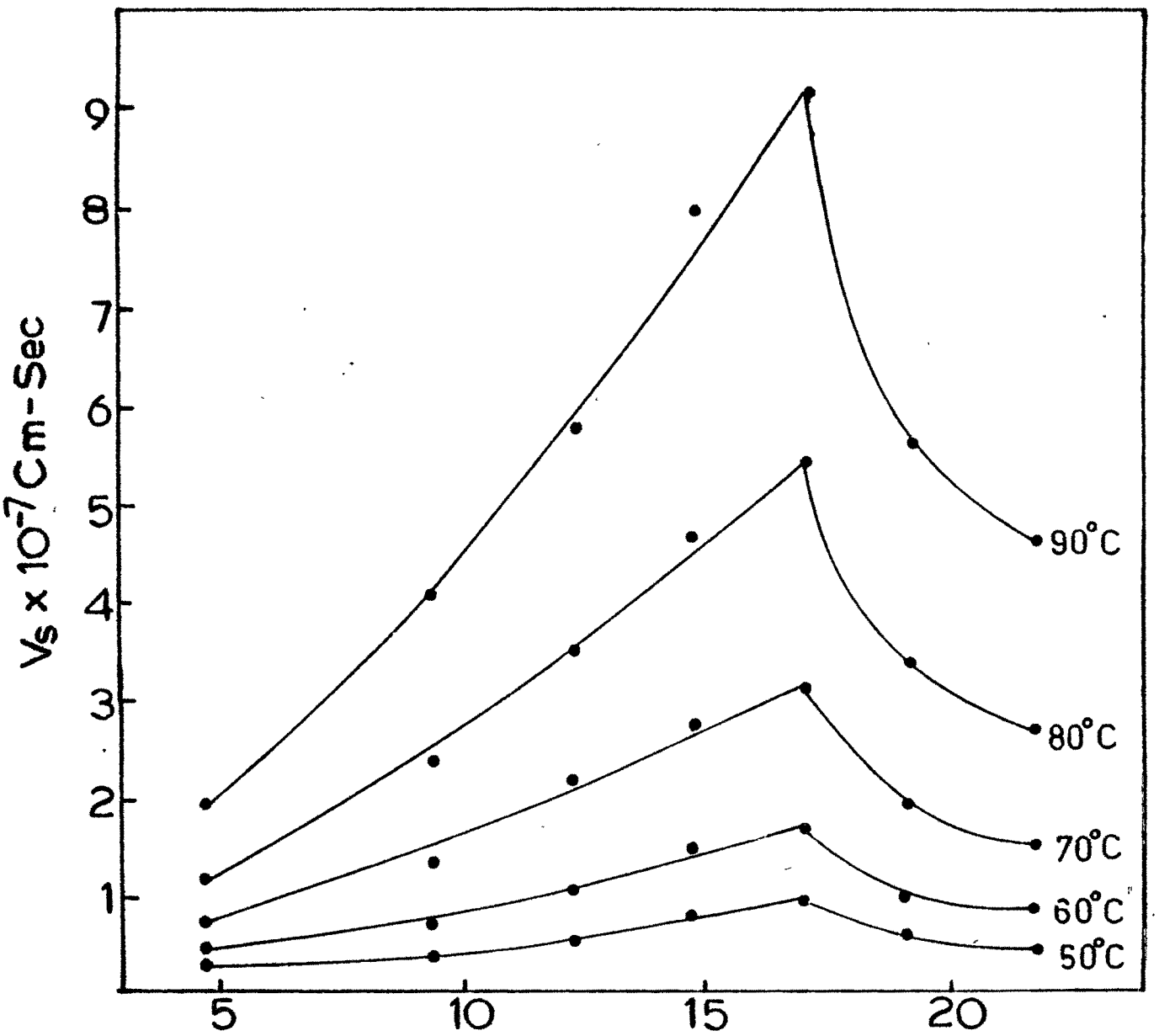

FIG.9.12 PLOT OF V_s vs C

9.3.4 Effect of temperature on etch rates

Table 9.2 shows the rates of tangential and surface dissolution at various temperatures ranging from 50°C to 90°C for various concentrations of sodium hydroxide solutions. Fig. 9.13 and 9.14 show the graphs of Log of etch pit widening rate (V_t) along direction [110] and surface dissolution rate (V_s) against the receprocal of temperatures for various concentrations of sodium hydroxide. According to Arrhenius equation

$$V = A \exp(-E/KT), \quad \ldots\ldots\ldots\ldots\ldots (9.0)$$

the slope of the graph of log V_t (or log V_s) versus 1/T represents the value of E/K, where E is the activation energy of the reacting species and K is the Boltzmann constant. The straight line graphs are observed for each concentration of the etchant and the activation energies for various concentrations are calculated. The energies thus calculated for all concentrations of sodium hydroxide solution are shown in table 9.3.

9.4 DISCUSSION

The observations on matching of etch pits produced by an etchant on oppositely matched cleavage counterparts had shown complete one-to-one correspondence so far as the

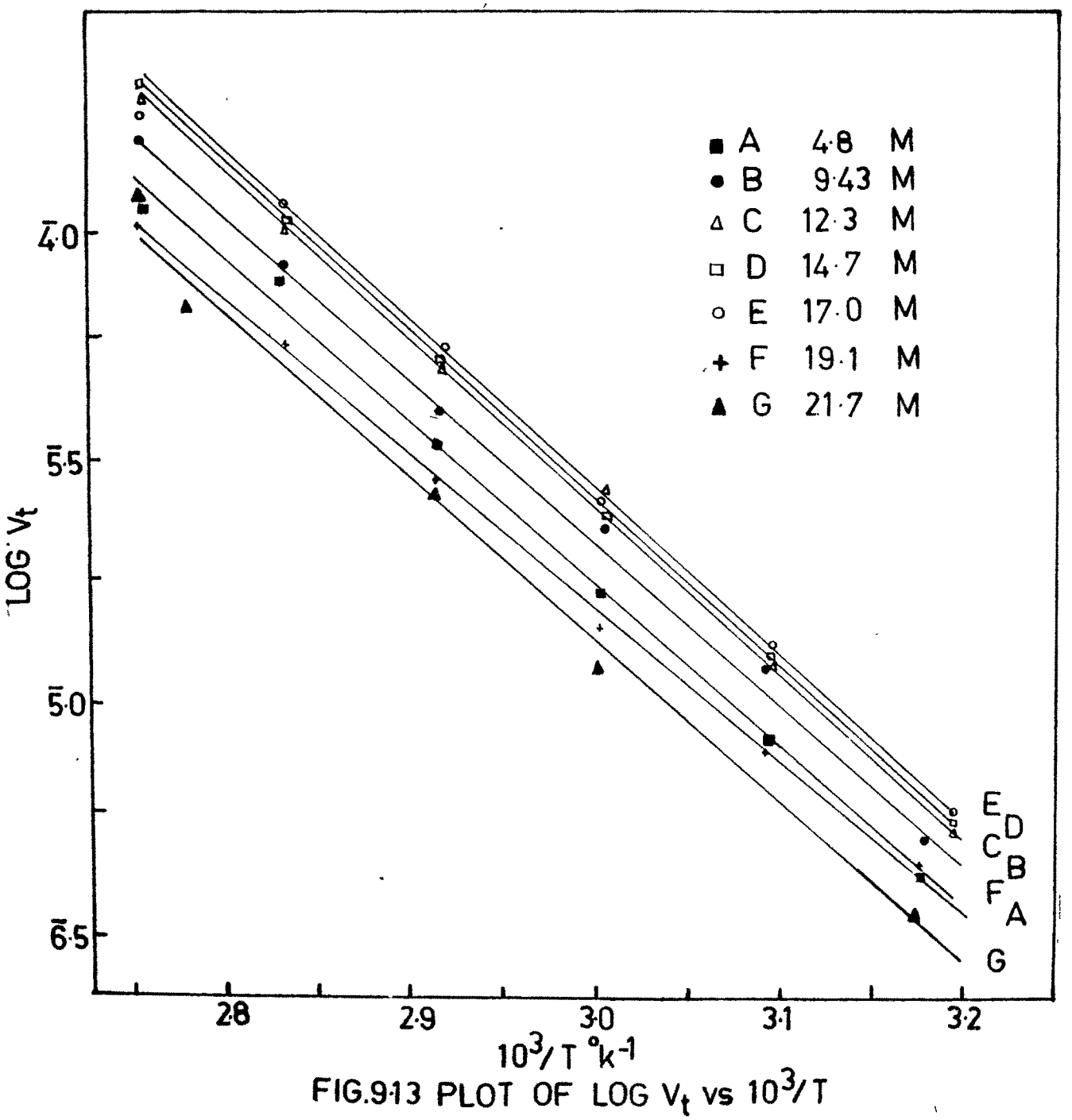

FIG.9·13 PLOT OF LOG V_t vs $10^3/T$

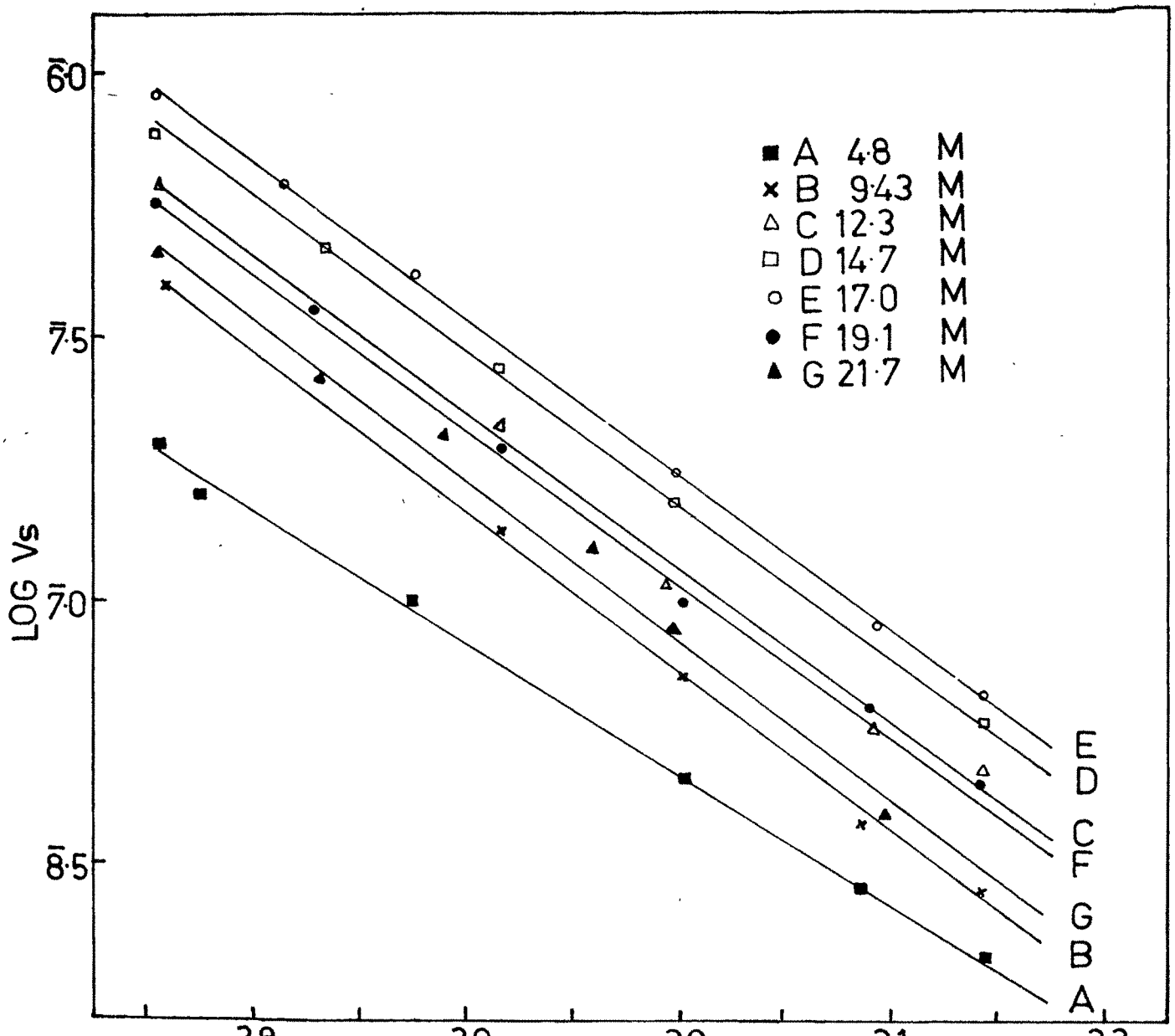

FIG.9·14 PLOT OF LOG Vs vs $10^3/T$

Table 9.3

Concentration C in M	E_t ev	E_s ev	E_t/E_s	E_σ	E_t/E_σ	E_s/E_σ	E_t/E_μ	E_s/E_μ	E_σ/E_μ
2.48	-	-	-	0.13	-	-	-	-	0.68
4.85	0.64	0.48	1.33	0.13	4.92	3.69	3.37	2.52	0.68
9.4	0.69	0.59	1.17	0.20	3.45	2.95	3.63	3.10	1.05
12.3	0.69	0.58	1.19	0.26	2.65	2.23	3.63	3.05	1.37
14.7	0.69	0.57	1.21	0.26	2.65	2.19	3.63	3.00	1.37
17.0	0.69	0.58	1.19	0.26	2.65	2.23	3.63	3.05	1.37
19.1	0.69	0.58	1.19	0.26	2.65	2.23	3.63	3.05	1.37
21.7	0.69	0.59	1.17	0.26	2.65	2.27	3.63	3.10	1.37

Average activation energy of tangential dissolution = E_t = 0.682 ev

Average activation energy of surface dissolution = E_s = 0.567 ev

Activation energy of a viscous solution of sodium hydroxide (19.1 M) = E_μ = 0.19 ev

location, number and orientation of etch pits were concerned. Further, when a cleavage surface was etched by an etchant (NaOH aqueous solutions) and its counterpart by another etchant, the matching of etch pits on identical areas of these counterparts was fairly good. Successive etching of the same cleaved surface by an etchant had produced the growth of etch pits at unchanged positions on the cleavage surface and that no new pits were formed. When thinkflakes (thickness ~ 0.01 mm) were etched, good correspondence of etch pits on the front and reverse faces was also noticed. All these experiments indicate that pits were produced at dislocations terminating on the surface under observation ; hence all etchants reveal dislocations. Whether they reveal all dislocations or not is not considered in the present report. It was mentioned earlier while considering the matching of etch pits on cleavage counterparts that flat-bottomed etch pits on one cleavage surface had correspondence with point-bottomed etch pits on the counterpart. This suggests that a few dislocations of insufficient strength etch out at a faster rate ; hence the flat-bottomed pits are produced at these places. It should be remarked that these points were not studied in detail in the present work.

9.4.1 Requirements of a good etchant

It is well known that the etchant should have following characteristics :

(i) It should be of such a composition that it will give good all round results and reveal the greatest number and variety of structural defects, characteristics and irregularities present. At the same time, it should be able to distinguish its effect from those produced by any of the etchants which can attack only definite types of defects. Thus this selective etching should enable one to study only specific defects.

(ii) It should be simple in composition and stable so that its concentration will not change appreciably upon standing or during use at room temperature and also at moderately higher or lower temperatures.

(iii) It should have constant characteristics at a particular temperature so that the conditions of etching can be easily reproduced. The important conditions of etching are as follows :

(a) Temperature of etching : The rate at which the etchant attacks a specimen depends upon the temperature at which etching takes place. The precise influence of temperature, however varies according to the composition of etchant, amount of impurity present and previous history of the

the specimen. It is, therefore, desirable for reproducible results to carry out etching experiments only at a definite temperature.

(b) Time of etching : The time of etching is perhaps one of the important factors contributing to successful etching and attendent appearance of the structure enabling their detailed study possible with the help of optical techniques. For example, if the time of etching is short as compared to that appropriate for a particular material, the etch structure will not be completely developed nor will there be sufficient details revealed to permit accurate interpretation of the etched area. However, too long time of etching is just as unsatisfactory as one too short, owing to details of surface structure being thereby obscured to varying degrees and frequently some parts of the structure being completely obliterated. The time of etching depends upon the conditions of the surface (freshly cleaved surface, heat treated surface etc.) and the temperature and nature of etchant.

(iv) While etching a specimen etchant should not form products which will precipitate on the specimen

surface, but must have such a composition that reaction products are immediately dissolved chemically or physically in the solution. They must possess closer affinity with the etchant than with the specimen.

(v) It should be non-injurious and non-toxic to the worker conducting work.

(vi) For orientation determination, the etchant should develop etch pits or facets with plane faces accurately parallel to crystallographic planes of low indices.

The above presents, in general, the requirements for the development of a good etchant. In view of these requirements and discussion of the following points, the characteristics of the etchant used in the present investigation will now be considered, by considering

(1) Matching of etch patterns on oppositely matched cleavage faces of calcite and

(2) Quality of etch pits.

In addition to these there are also few noticeable features of dislocation etchant used, which will also be considered.

9.4.1.1(a) Characteristics of aqueous sodium hydroxide solution as the etchant

As far as the location of etch pits is concerned there is almost perfect matching. However, the internal structure of pits is not reflected on either cleavage counterpart. Further the shape of an etch pit is not changed by etching time (fig. 9.2, 9.3, 9.4, 9.5) and also by increasing concentration of solute in fixed amount of distilled water. At higher concentration greater than C_p i.e. 21.7 M concentration solution the pits become more protruding as a result the other end of boat-shaped pit remains undisclosed (Fig. 9.15). Further the number of dislocations (10^4 per cm^2) revealed by aqueous sodium hydroxide solutions is independent of its concentration. The temperature of etching solution also does not change the etch pit shape (Fig. 9.8a & 9.8b) for all concentration of aqueous sodium hydroxide solution.

9.4.1.1(b) Matching of cleavage counterparts etched in aqueous sodium hydroxide solution and glacial acetic acid solution

Fig. 9.16(a) represents photomicrograph of calcite cleavage face etched in 12.3 M aqueous solution of sodium hydroxide at 70°C for five minutes and Fig. 9.16(b) represents

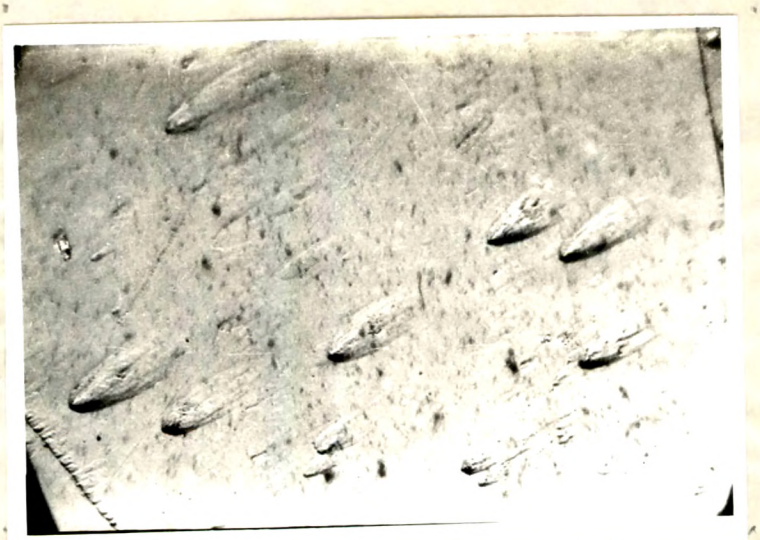

(x 500)

Fig. 9.15 shows photomicrograph of etched cleavage surface in 21.7 M of aqueous NaOH solution at 70°C for 10 min.

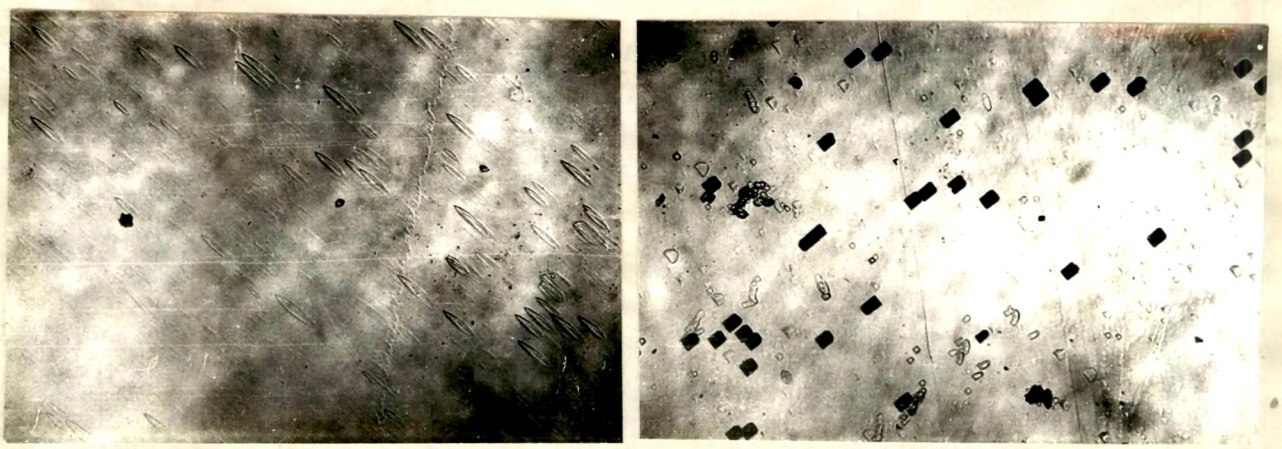

(a) (x 100) (b) (x 100)

Fig. 9.16(a,b) show photomicrographs of cleavage counterparts of calcite etched in 12.3 M aqueous NaOH solution at 70°C for 4 min. and in 10.49 M glacial acetic acid at 30°C for 7 min. respectively.

photomicrographs of its cleavage counterpart etched in 10.49 M glacial acetic acid for six minutes at 30°C. The photomicrographs show one-to-one correspondence of etch pits on cleavage counterparts. This suggests that aqueous sodium hydroxide solution is also a good dislocation etchant for calcite cleavages.

9.4.1.2 Quality of etch pits

The quality of etch pits includes considerations of the shape, size, symmetrical nature and contrast of the pits with respect to the surface. For a given etchant etch pits produced on a cleavage surface are almost of equal sizes.

The condition for the formation of visible etch pits on a crystal surface subjected to etching are (i) $V_n/V_t > 0.1$ and (ii) $V_n/V_s > 1$.[20] Later it was reported[17] that for the formation of visible etch pits, in addition to the above conditions, the ratio of tangential rate of dissolution, V_t, to that of surface dissolution, V_s i.e. V_t/V_s should be greater than 10 and higher the ratio (V_t/V_s) better is the quality of etch pits. A critical study of table 9.2 shows that the ratio V_t/V_s is large. Further the quality of pits improves with increase of temperature of etchant of a given concentration (fig. 9.8a & 9.8b). The ratio V_t/V_s decreases with concentration. This decrease does not reflect

much on quality of etch pits. Thus the ratio V_t/V_s alone cannot account for the quality of etch pits. The combination of V_t, V_s and V_n may enhance the understanding of the quality of etch pits.

9.4.2 Nature of etch rates versus concentration plots

The nature of V-C plots is illustrated in Fig. 9.11 and 9.12. The rate of chemical reaction increases with increase of solute amount in fixed amount of distilled water. It attains maximum value and for higher concentrations (19.1 M and 21.7 M) it decreases. Sanglwal and Patel[9], Sangwal and Arrora[21] reported the occurrence of such peaks in their studies on dissolution of MgO crystal cleavages in HCl, HNO_3, H_2SO_4 and H_3PO_4 solutions. The nature of V - C plots was explained on the basis of adsorption phenomena. The equation of the rate[21,22,23] is given by

$$V = \frac{K C_a}{1 + K_a C_a} \qquad \ldots\ldots (9.1)$$

for moderate adsorption of the reactant and weak adsorption of reaction product(s) where K, K_a are constants and C_a is the acid concentration. It was claimed that equation 9.1 explains the nature of plots. If equation 9.1 explains

the nature of V-C plots, then mathematically the condition for obtaining extremum viz.

$$\left(\frac{dV}{dC_a}\right)_{Ca = 0} = 0 \quad \text{must be}$$

satisfied.

Now differentiating equation 9.1 with respect to Ca yields

$$\left(\frac{dV}{dCa}\right) = K/(1 + K_a C_a)^2$$

and for an extremum

$$\left(\frac{dV}{dC_a}\right) = 0 = K/(1 + K_a C_a)^2$$

This implies that K must be zero or C_a must be infinite. None is possible in view of the finite value of V (Equation 9.1). Thus equation 9.1 is not able to explain nature of V-C plots.

The characteristics of V-C plots (Figs. 9.11 and 9.12) are as follows :

(i) Etching rate increases with temperature of etching.

(ii) The increase is non-linear in nature.

(iii) The rate has a maximum value for a given temperature.

(iv) The maximum value increases with etching temperature.

(v) For all etching temperatures, the maximum value C_p (or within a small concentration range around C_p) of etchant.

(vi) It then falls to a lower value in a non-linear manner.

There are several factors which appear to be responsible for these characteristics. They are as follows :

(1) Availability of ions in the etchant.
(2) Ionic conductivity of the etchant.
(3) Viscosity of the etchant.
(4) Inhibition of reaction products.
(5) Chemical nature of crystal and arrangement of atoms on the cleavage surface.

The increase of reaction rate (V_t or V_s) with increase of etchant concentration may be due to increase of ions reacting with crystal surface. However the pH of these solutions (etchants) does not show any change in their values from 14. With increase of solute in fixed amount of solvent (distilled water) the reactivity of the etchant increases. This may be responsible for increase of rates. It is clear (table 9.2) that the ratio (V_t/V_s) decreases with increase of etchant concentrations. This indicates

that with increase of concentration greater than C_p, V_s is more dominant than V_t, removing larger number of surface layers than those at lower concentrations.

Optical study of etch phenomena is mainly concerned with the study of etch patterns at preferential points. However along with the etching of specific points general dissolution of the surface takes place. Hence it is desirable to study the variation of ratio of $(V_t)_{max}$, to $(V_s)_{max}$ i.e. the ratio Vtm/Vsm with etchant concentration. The plots of (Vt/Vs) vs. concentration and also of log (V_t/V_s) vs. log C for different etching temperatures are curves with two points of inflection (fig. 9.17 and 9.18). On the same plots are shown by dotted lines, plots of Vtm/Vsm vs. concentration and log (V_{tm}/V_{sm}) vs. log C (fig. 9.17 and 9.18). It should be noted that these latter plots are straight lines. For the purpose of comparison such plots are also given wheh lactic and formic acids are used as etchants for studying etching of cleavage faces of calcite.[18] The characteristics of these plots (for acidic etchants), are similar to those observed for alkaline etchants. However it should be noted that for lactic acid and the straight line plot of (V_{tm}/V_{sm}) vs. concentration (fig. 9.19) exhibits scattering of points around the line more noticeable than those observed for aqueous solutions of NaOH and formic acid. This appears to be due to peculiar temperature dependent structural

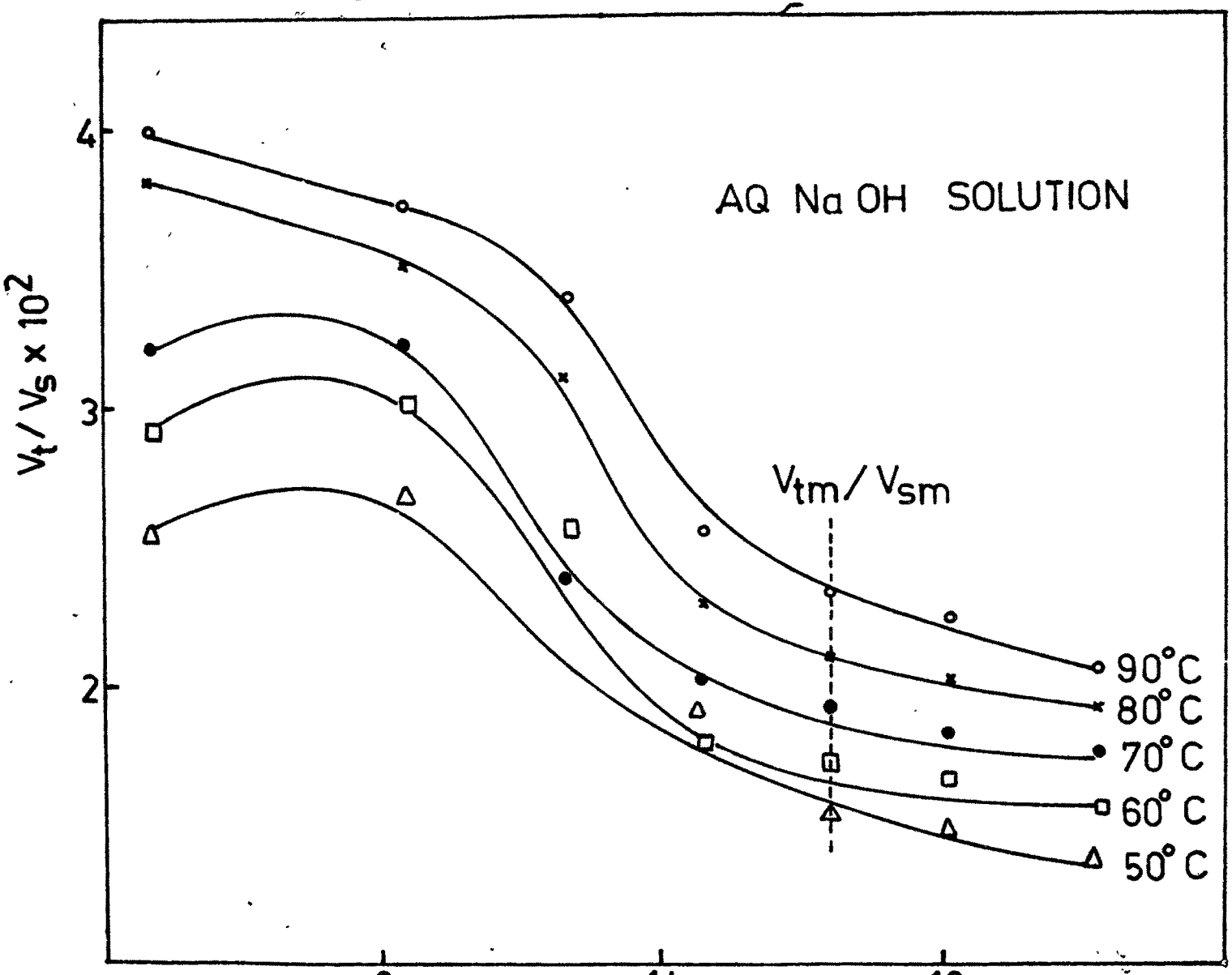

FIG.9·17 PLOT OF V_t / V_s vs C

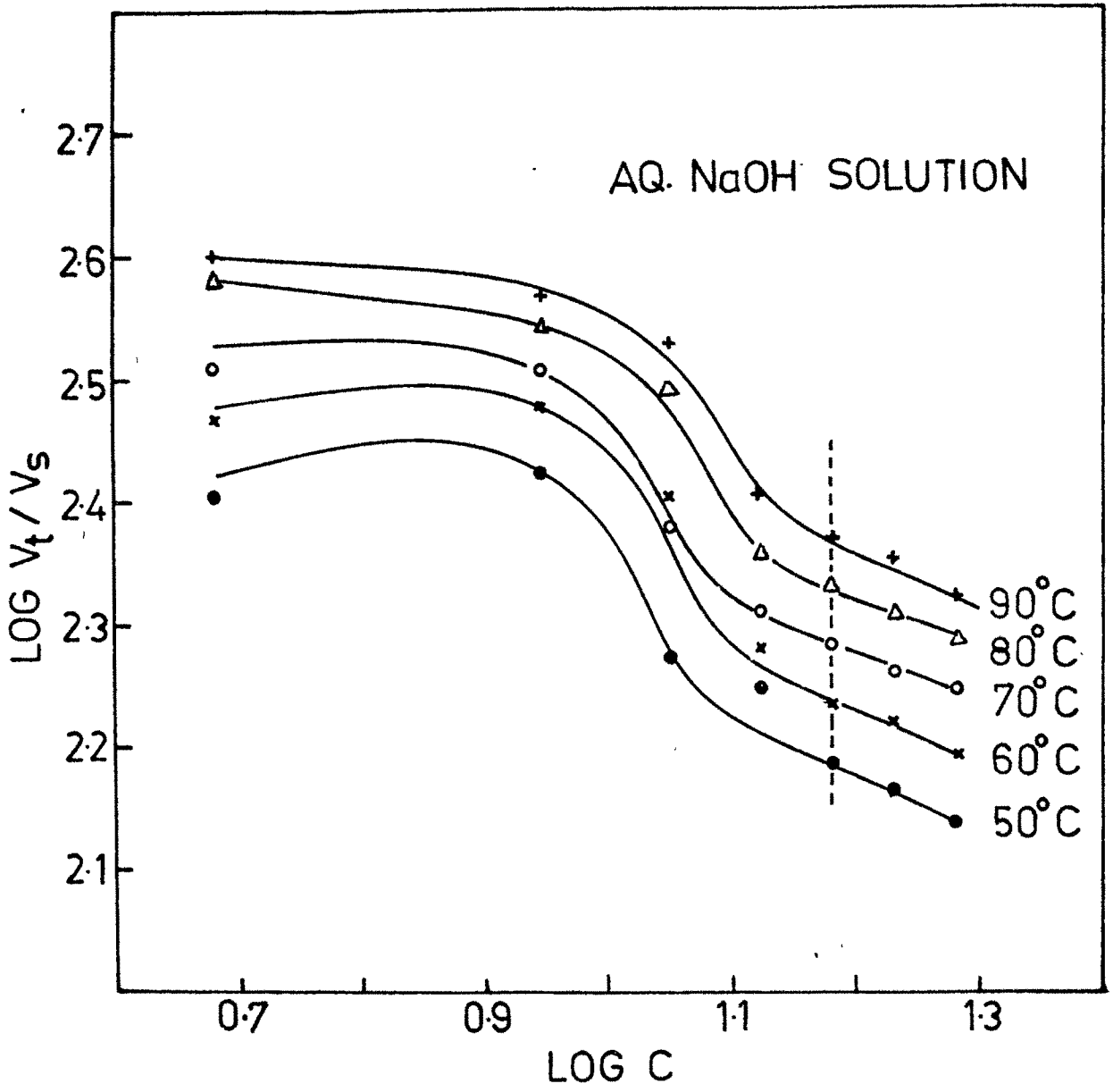

FIG. 9·18 PLOT OF LOG V_t / V_s vs LOG C

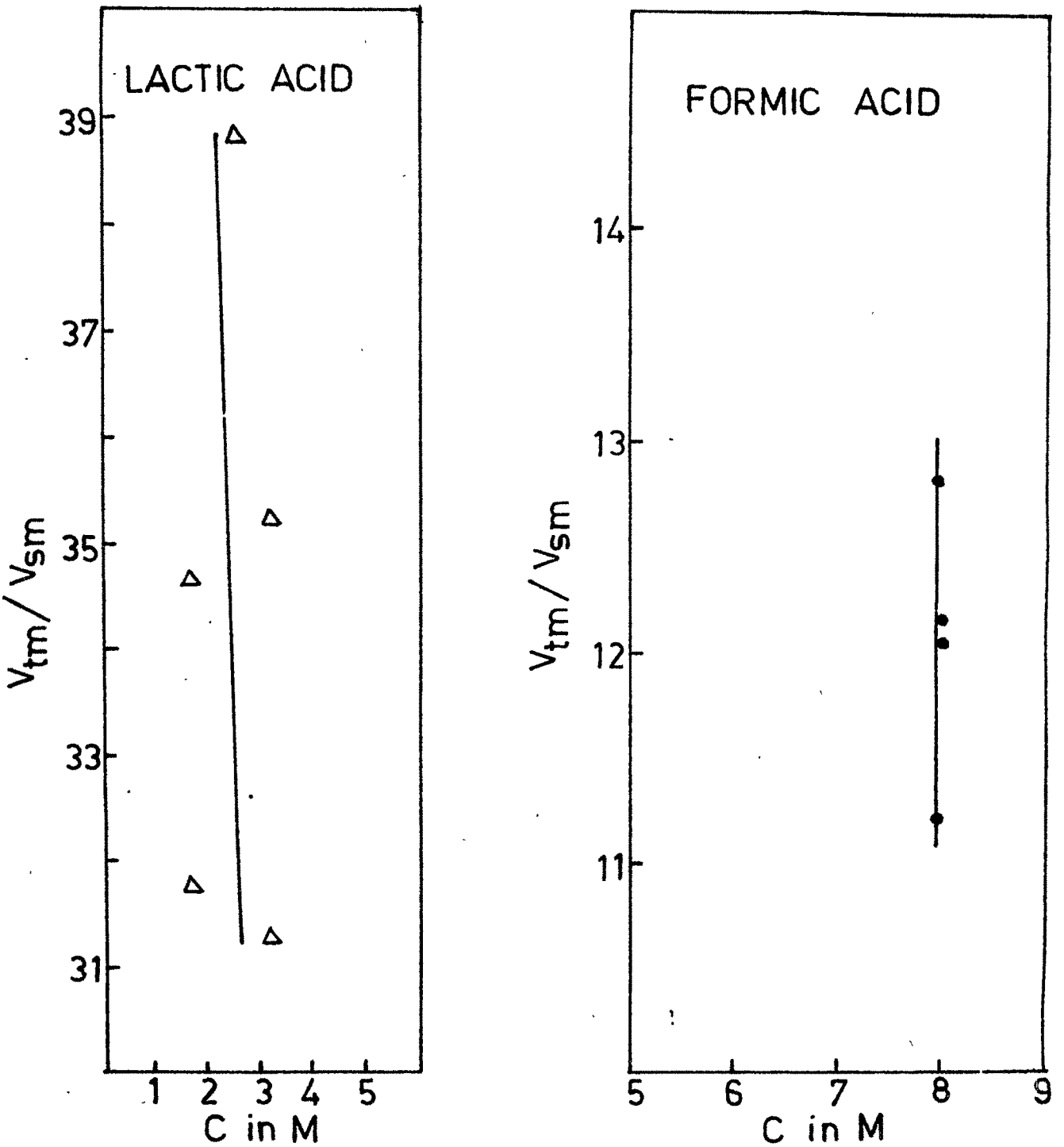

FIG. 9·19 PLOT OF V_{tm}/V_{sm} vs C

property of Lactic acid. The general conclusion which can be drawn from a study of variation of (V_t/V_s) with concentration and etching temperature of the alkaline and acidic etchants, is that for all dislocation etchants the plots of (V_{tm}/V_{sm}) vs. concentration should have linear relation irrespective of the etching temperature and chemical character (acidic or alkaline) of the etchant.

9.4.3. Electrolytic conductivity of the etchant

The ionic mobility and availability of ions is related to electrical conductivity of an electrolyte (the etchant). Elnico Conductivity bridge (cf. Chapter 2) was used to determine electrical conductivity (σ) of the etchant of different concentrations at different etching temperatures (T) (table 9.4). The variation of σ with C (fig. 9.20 and 9.20a) was graphically studied. The salient features of the plots are as under :

(a) Non-linear increase of σ with C and also with T.

(b) Maximum values of σ for different values of T.

(c) Occurrence of maximum values at the same concentration C_σ (NSM) (or within a small concentration range round C_σ).

These features more or less correspond to those reported in the literature (table 9.5). The plot of log σ

Table 9.4

TEMPERATURE $T^{o}K$	Concentration C = 2.48 M ; Log C = 0.3945		
	σ milli mho cm^{-1}	log σ	$10^3/T$ $^{o}K^{-1}$
310.5	293	2.466	3.225
312.0	305	2.484	3.205
315.0	315	2.498	3.169
318.0	325	2.512	3.144
320.5	335	2.525	3.120
322.0	343	2.535	3.105
325.5	355	2.55	2.072
329.0	379	2.578	3.039
	Concentration C = 4.85 ; Log C = 0.679		
310.5	379	2.578	3.225
313.0	390	2.591	3.1948
315.5	410	2.613	3.169
318.0	422	2.625	3.144
320.5	439	2.642	3.120
323.0	457	2.659	3.096
325.0	472	2.674	3.077
326.5	483	2.684	3.0627
329.0	475	2.695	3.0395

cont.....

Table 9.4 cont....

	Concentration C = 9.4 M ; Log C = 0.945		
313.0	340	2.53	3.195
315.5	358	2.55	3.169
318.0	382	2.582	3.144
320.5	405	2.607	3.120
323.0	426	2.629	3.096
325.5	438	2.641	3.072
328.0	449	2.652	3.048

	Concentration C = 12.3 M ; Log C = 1.038		
310.5	270	2.43	3.225
313.0	291	2.463	3.195
315.5	314	2.497	3.169
318.0	335	2.525	3.144
320.5	354	2.549	3.120
323.5	369	2.567	3.091

cont.....

Table 9.4 cont.....

	Concentration C = 19.1 M ; Log C = 1.2304		
313.0	229	2.359	3.195
315.5	245	2.389	3.169
318.0	275	2.439	3.144
320.5	294	2.468	3.120
322.5	309	2.489	3.100
325.0	330	2.568	3.077

	Concentration C = 21.7 M ; Log C = 1.2830		
313.0	210	2.322	3.195
315.5	236	2.372	3.169
318.0	256	2.408	3.144
320.5	278	2.444	3.120
323.0	304	2.483	3.096
325.5	329	2.517	3.072
328.0	354	2.549	3.048
330.5	371	2.569	3.025
333.0	376	2.575	3.003

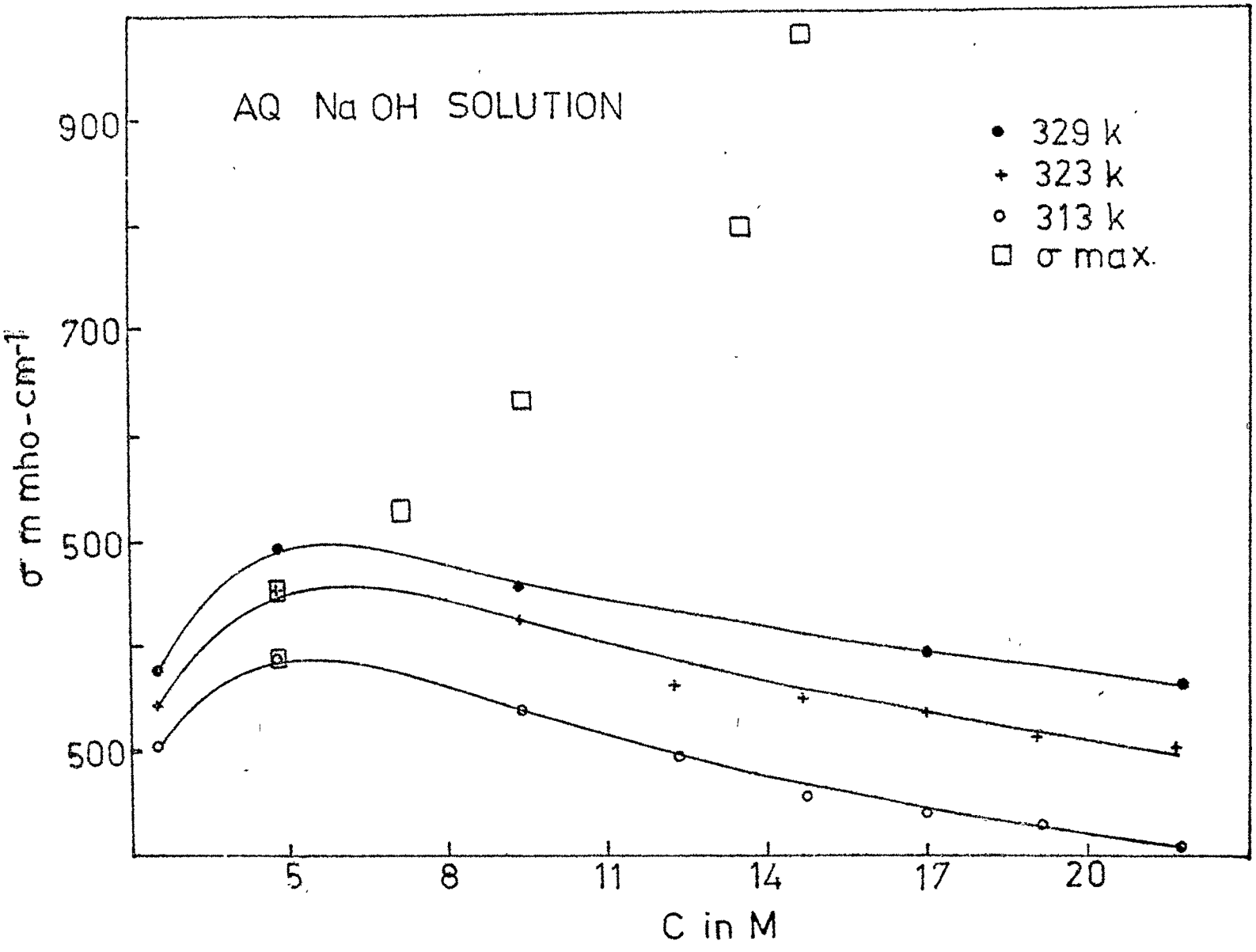

FIG.9·20 PLOT OF σ m mho-cm^{-1} vs C

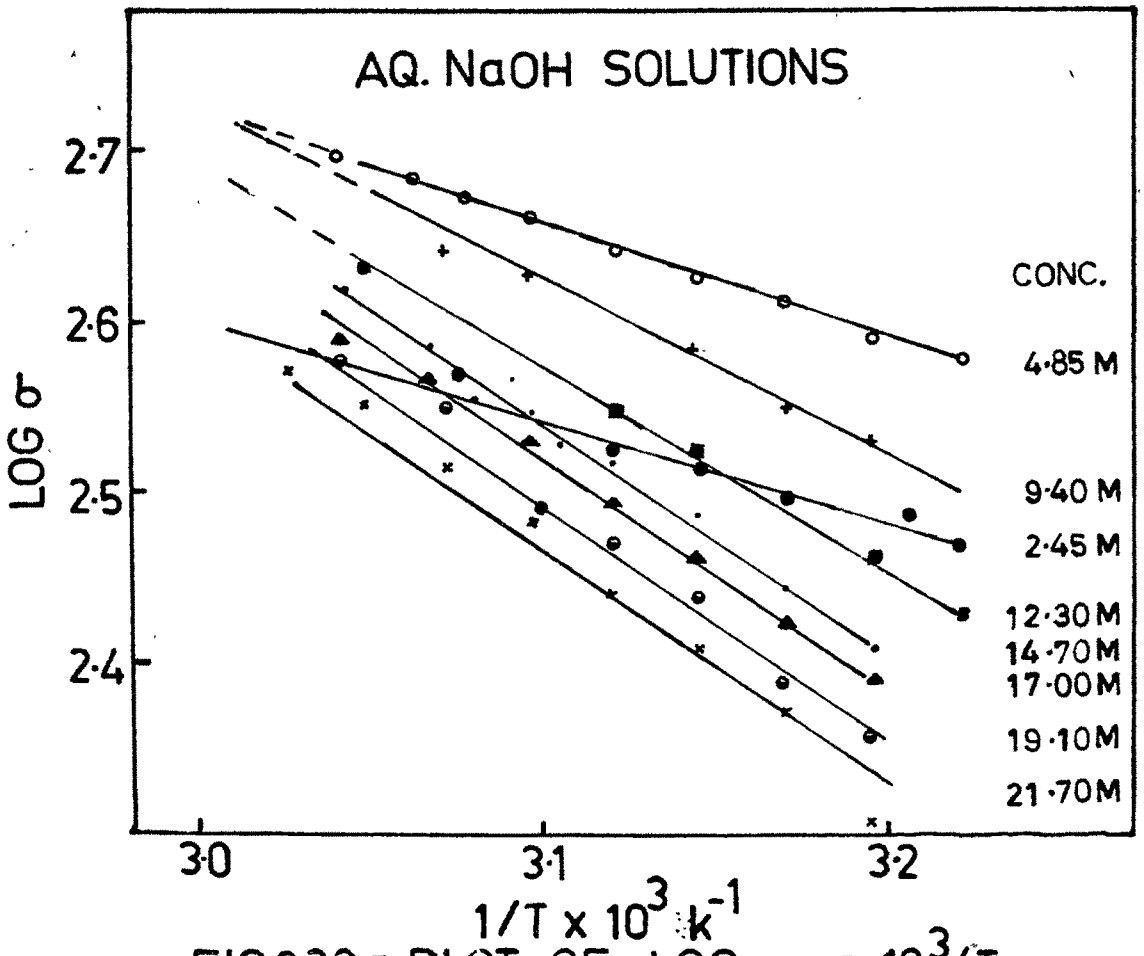

FIG.9·20a PLOT OF LOG σ vs $10^3/T$

versus log C (fig. 9.21) indicates clearly that instead of a sharp maximum, similar to those observed in plots of log V - log C (fig. 9.21a, b) a plateau is observed. The broad maximum suggests that instead of a single maximum value there is a range of maximum values corresponding to a range of concentrations. This behaviour of etchant is different from that of Lactic and Formic acids.[24] Furthermore the concentration values for maximum etch rate and maximum conductivity are different for this etchant (table 9.6) whereas for acidic etchants (lactic and formic) the etch rates become maximum at a concentration at which the electrical conductivity of the same etchant attains maximum value. Thus the correlation for maximisation of etch rates with peak value of electrical conductivity does not exist for the alkaline solutions. This is in sharp contrast with the acidic behaviour of etchants (Lactic and Formic acid).[24]

The maximum value of electrical conductivity (σ m) at a certain concentration for a fixed etching temperature is associated with large value of ionic mobility and number of ions. Further (V_t/V_s) is also associated with the availability of ions for chemical reaction between an etchant and a crystal surface. Hence the relation between σ m and concentration value for σ m should be linear. This is indeed the case not only for alkaline etchant

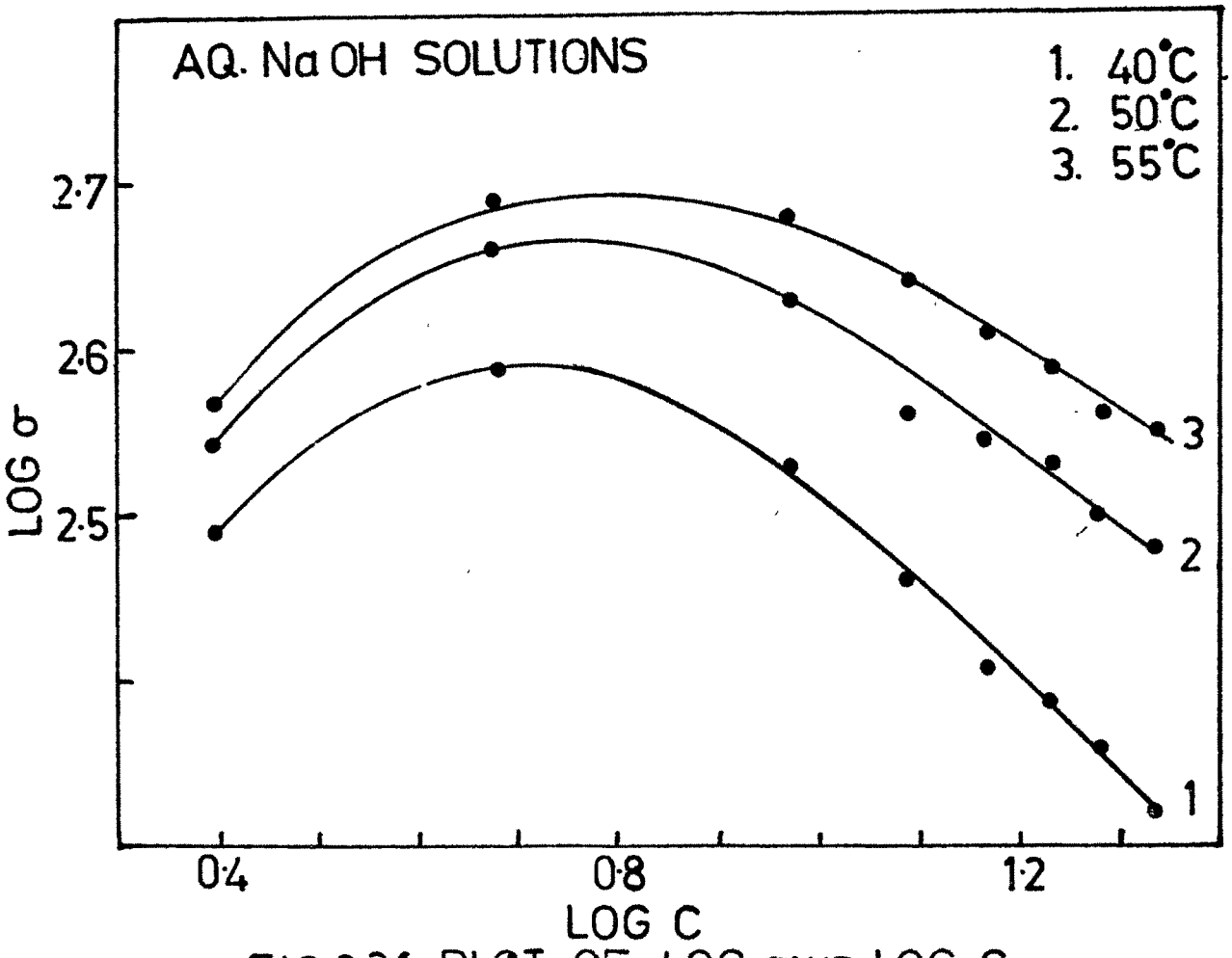

FIG.9·21 PLOT OF LOG σ vs LOG C

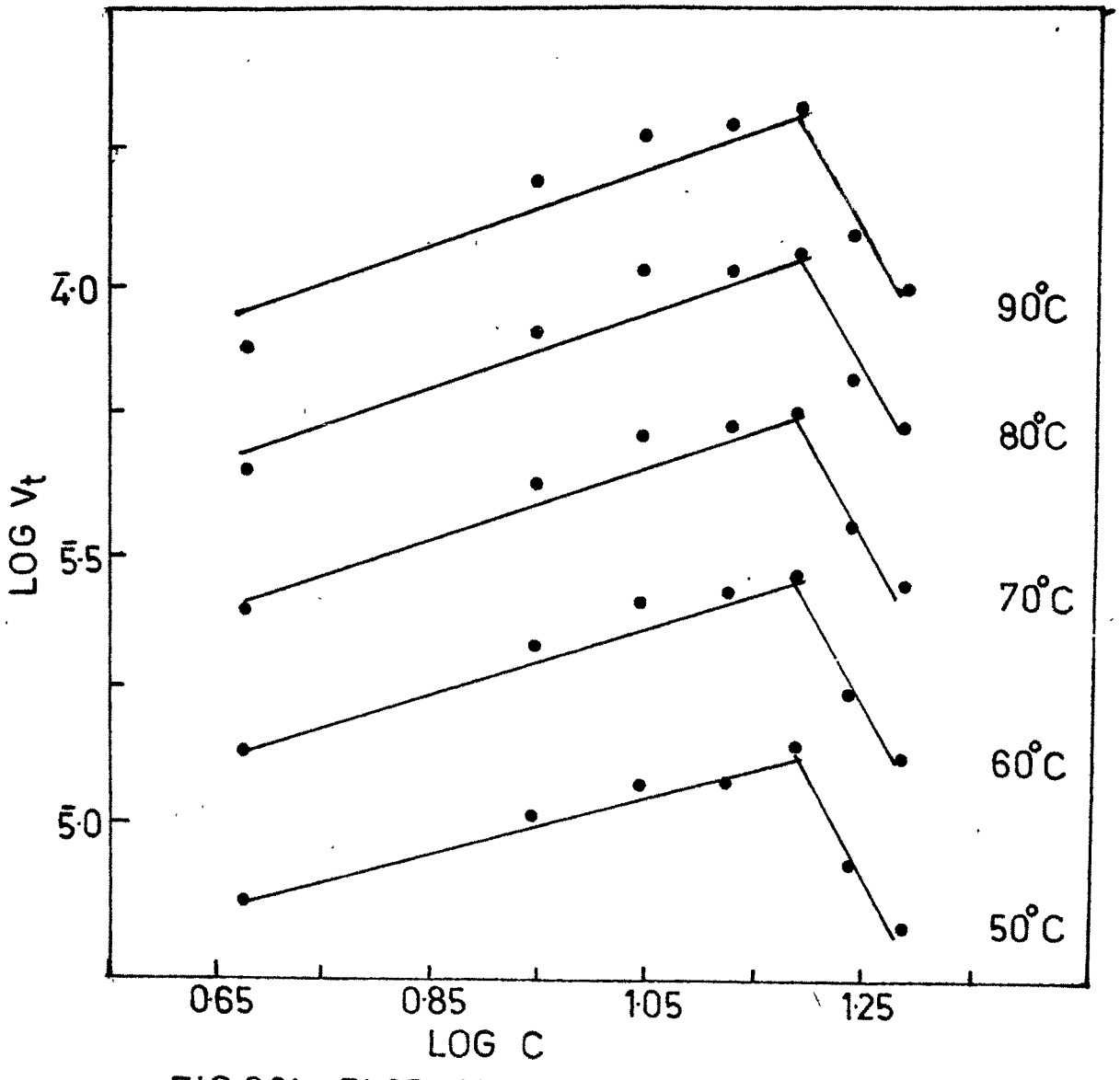

FIG. 9·21a PLOT OF LOG V_t vs LOG C

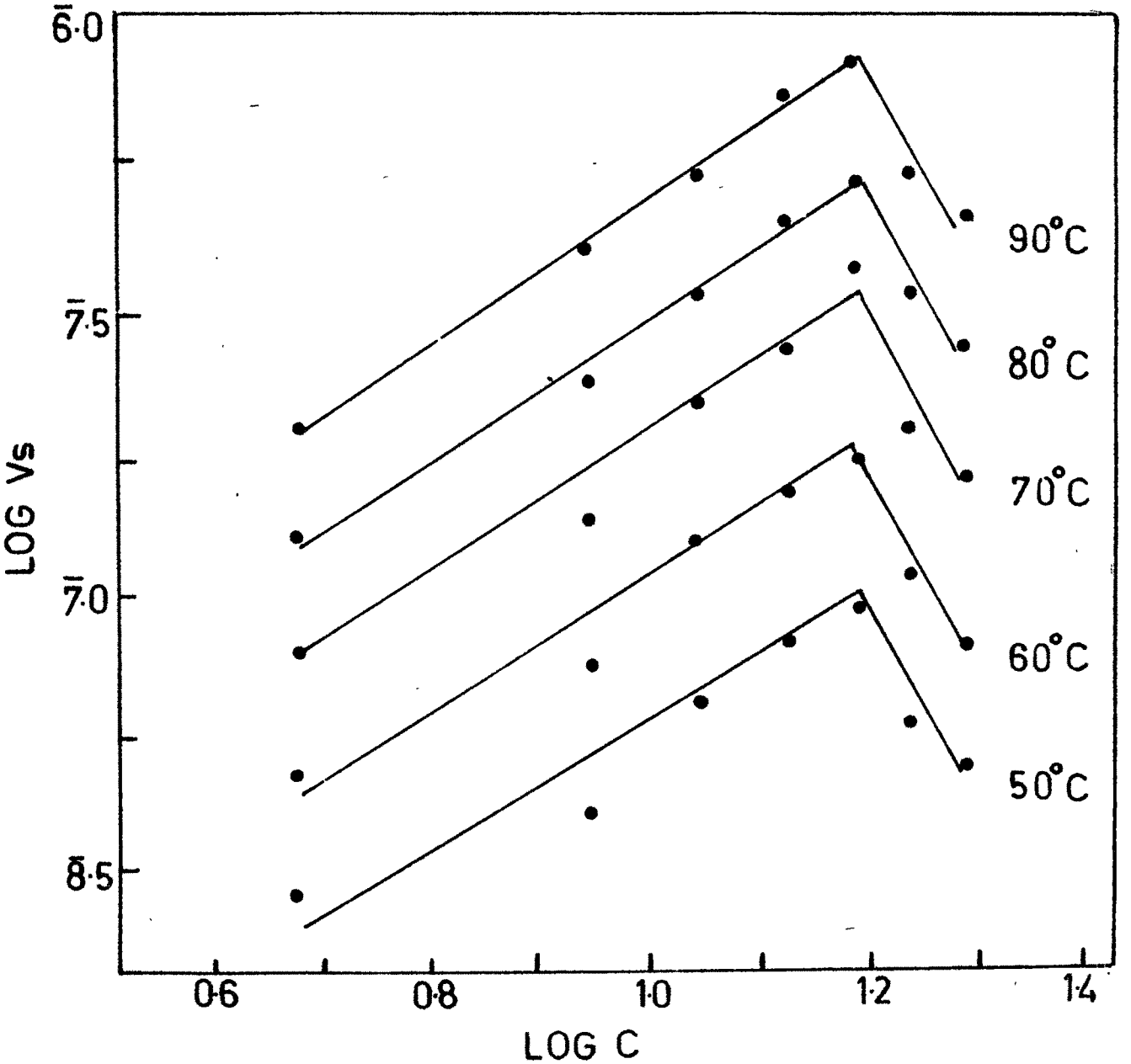

FIG.9·21b PLOT OF LOG Vs vs LOG C

(sodium hydroxide)(fig. 9.20) but also for acidic (Lactic and Formic) etchants (fig. 9.22). This suggests that for all dislocations etchants the relations between (V_{tm}/V_{sm}) and concentration and also between σ_m and concentration are linear and independent of etching temperature and chemical nature of the etchant. However (V_{tm}/V_{sm}) and σ_m do not occur for identical concentration values (table 9.6) This indicates that the viscosity of an etchant could be a factor responsible for this behaviour of etchants.

9.4.4 Viscosity of the etchant

It is well known that viscosity of a solution varies with concentration and temperature-and that for a fixed temperature it increases with concentration, whereas for a fixed concentration of solution, it decreases with increase of temperature. This general feature is true for aqueous solutions of sodium hydroxide (table 9.7a, b) (fig. 9.23 and 9.24). The (V_{tm}/V_{sm}) has different values (varying over a small range) at a concentration of 17 M of aqueous solution of sodium hydroxide and for different etching temperatures, whereas for concentrations varying from 4.85 M to 14.7 M has different maximum values (varying over a large range) for different etching temperatures studied in the present investigation. Further V_t and V_s decrease with concentration beyond 17 M whereas σ decreases beyond σ_m for a certain concentration (table 9.4). However viscosity

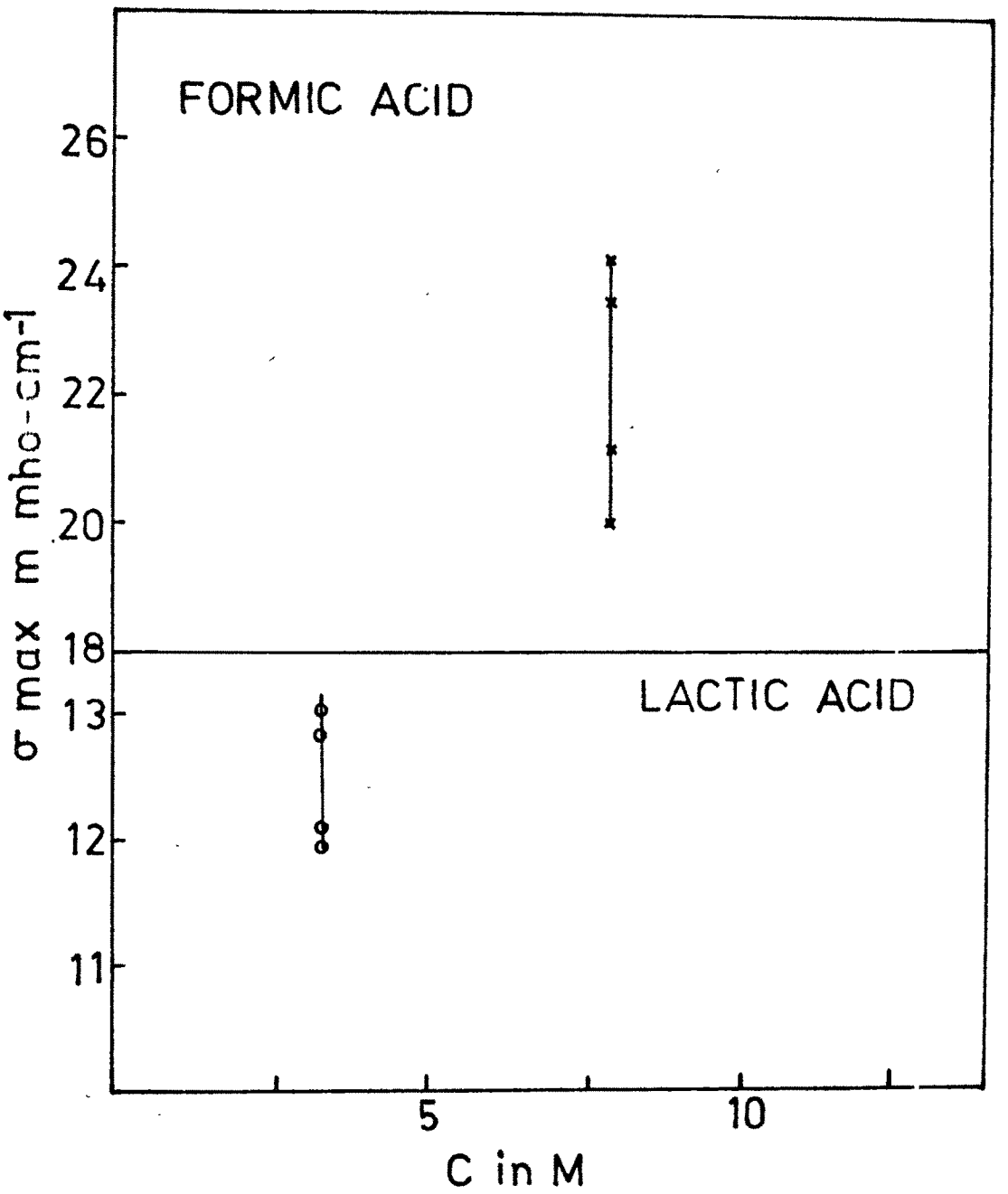

FIG. 9·22 PLOT OF σ m vs C

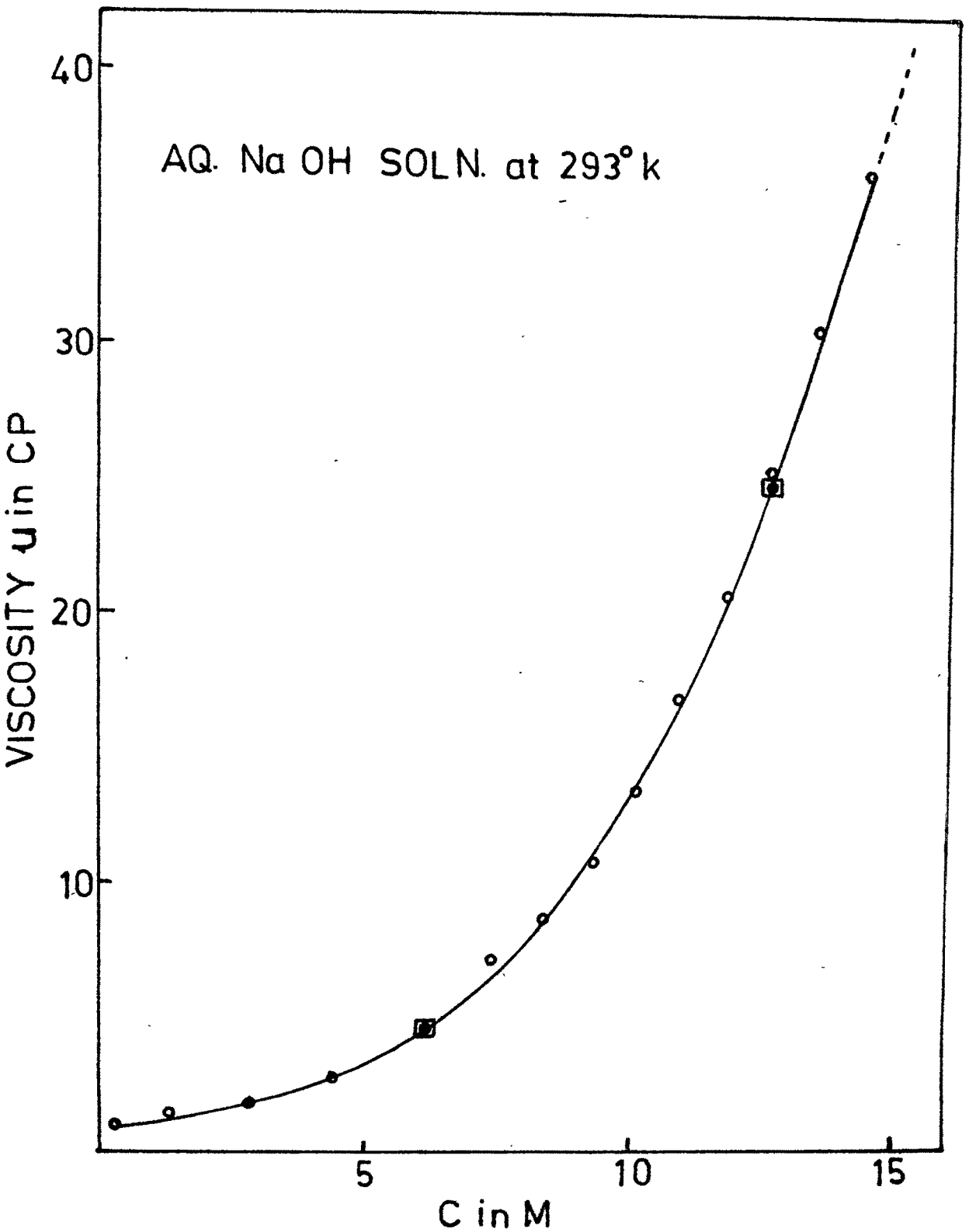

FIG. 9·23 PLOT OF VISCOSITY vs CONC.

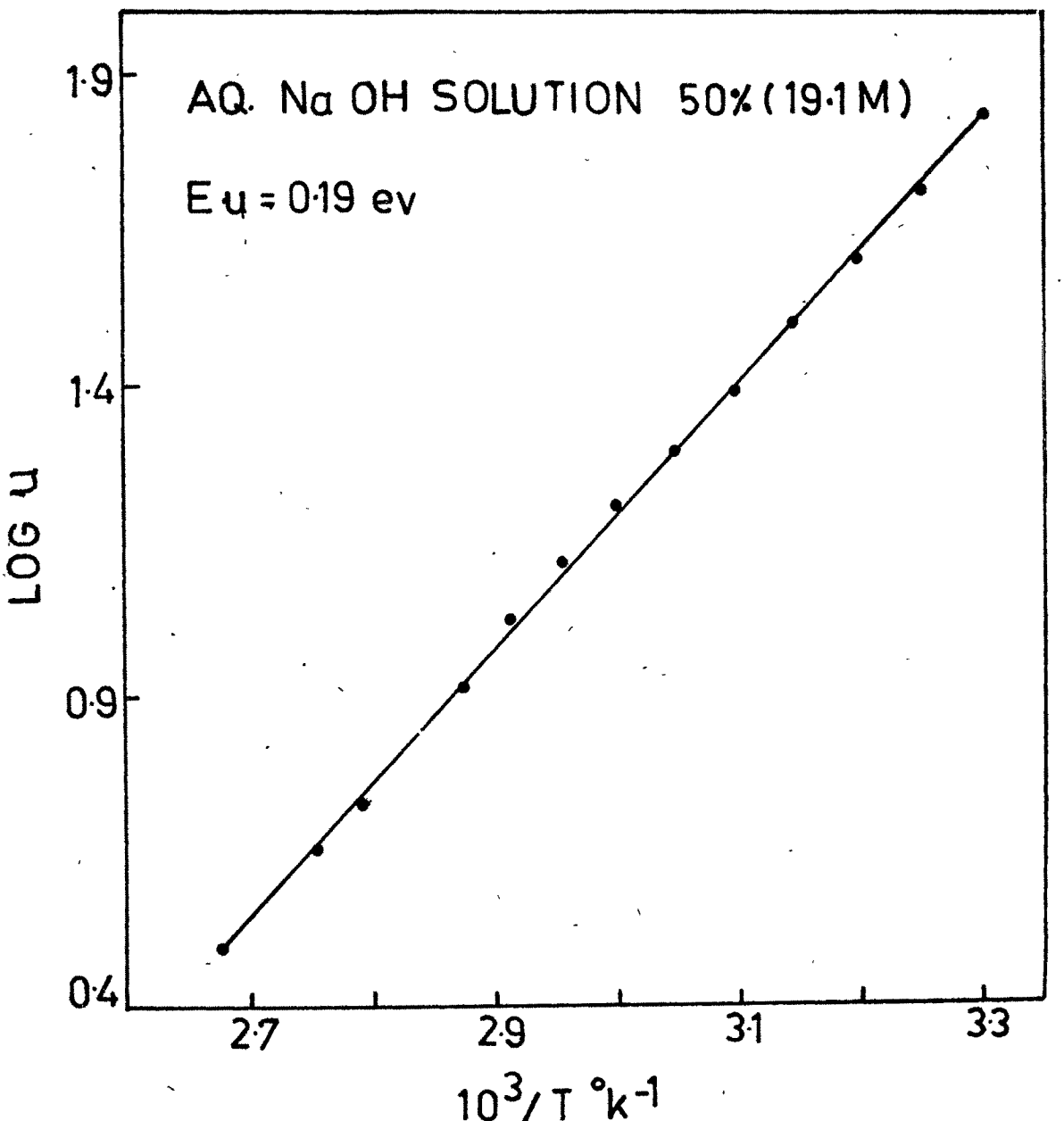

FIG. 9·24 PLOT OF LOG u vs $10^3/T$

Table 9.7a * Viscosity of NaOH solutions at $20^{o}C$

Concentration C in %	in M	Log C	Viscosity in centipoise
1	0.25	$\bar{1}$.3979	1.054
5	1.3	0.1139	1.328
10	2.75	0.4393	1.881
15	4.3	0.6335	2.787
20	6.05	0.7818	4.618
24	7.3	0.8633	7.102
26	8.3	0.9191	8.741
28	9.2	0.9638	10.834
30	10.0	1.0000	13.513
32	10.8	1.0334	16.835
34	11.7	1.0682	20.746
36	12.5	1.0969	25.316
38	13.4	1.1271	30.48
40	14.3	1.1553	36.36

* Values taken from CRC Hand book, Chemistry and Physics, Weast 57th Edition, 1976.

Table 9.7b *Viscosity of 50% (19.1 M) solution at different temperatures

TEMPERATURE $T^{o}K$	Viscosity μ cP	Log μ	$10^3/T$ $^{o}K^{-1}$
303	65	1.8129	3.3
308	52	1.7160	3.246
313	40	1.6021	3.195
318	32	1.5051	3.144
323	24.8	1.3944	3.096
328	20	1.3010	3.048
333	16	1.2041	3.003
338	13.1	1.1172	2.958
343	10.5	1.0211	2.915
348	8.25	0.9164	2.873
353	6.75	0.8293	2.833
358	5.35	0.7283	2.793
363	4.5	0.6532	2.755
368	3.7	0.5682	2.717
373	3.05	0.4842	2.681

* Values taken from Chemical Engineers Handbook by Perry John Howard, 4th Edition P, 3-196, McGraw Hill Book Co.

increases for all concentrations mentioned above i.e. from 4.85 M to 14.7 M and beyond these values, at a constant etching temperature.

The reaction between calcite and aqueous solution of sodium hydroxide is as follows :

$$CaCO_3 + 2\,NaOH \longrightarrow Na_2CO_3 + Ca(OH)_2$$

$$Na_2CO_3 + Ca(OH)_2 \longrightarrow Na_2CO_3 + CaO + H_2O$$

Sodium carbonate dissolves in the solution whereas the second reaction product namely calcium oxide is sparingly soluble in the solutions of sodium hydroxide and sodium carbonate. Thus during etching of cleavage face of calcite, a thin film of calcium oxide is formed on the surface. This film is removed by rinsing the etched sample in dilute solution of ammonium chloride (0.28 M).

The study of V-C plots (figs. 9.11 and 9.12) shows that tangential and surface dissolution rates increase with etchant concentration and etching temperature and becomes maximum at a certain concentration C_p. Further $V_t >> V_s$. This suggests that the film formation does not obstruct preferential and surface dissolution of calcite cleavages. With the progressive increase of etchant concentration beyond C_p (17 M) at a constant etching

temperature, etch rates (V_t and V_s) become smaller and smaller and etchant viscosity becomes larger and larger. Further for the concentration values less than 17 M, electrical conductivity is significantly decreasing which in turn indicates that the free ion concentration and ionic mobility are decreasing. It is thus apparent that the higher viscosity ($>$60 CP at 293°K) of the etchant with concentrations $\geq$ 17 M arrests the etch pit growth and decreases ionic mobility and concentration due to the formation of a thin film of a definite thickness [given by $(Vs)_{max}$] at a certain etching temperature, e.g. 0.912×10^{-7} cm/sec. (0.912 millimicron per second) at 50°C (323°K) (table 9.2), for 19.1 M and 12.5 M concentrations of sodium hydroxide solution having viscosity 24.8 CP at 323°K and 293°K respectively (fig. 9.23 and fig. 9.24). The film thickness increases with etching temperature (table 9.2) e.g. it is 9.12 millimicron per second at 90°C (363°K), for etchant concentrations 19.1 M and 6.1 M having viscosity 4.5 CP at 363°K and 293°K respectively (fig. 9.23 and fig. 9.24). The acidic etchants also show similar, but subdued behaviour (table 9.6) it is because of the mild behaviour [due to comparatively smaller values of viscosity (cf. table 9.6)] that the maximum values of V_t/V_s and electrical conductivity occur at the same value of etchant concentration whereas for alkaline etchant V_{tm}/V_{sm} and σ_m occur at different

concentrations e.g. at etching temperature 323°K they occur at 17 M and 4.85 M etchant concentrations (table 9.6). Hence due to larger value of viscosity of 17 M concentration much greater than 4.85 M, less number of ions with reduced mobility are available. Further among acidic etchants lactic acid has comparatively higher viscosity (30 Cp at 25°C) ; its etching behaviour shows greater resemblance with that of alkaline etchant. It should be remarked here that viscosity values are comparatively much smaller than those of common highly viscous liquids e.g. castor oil with viscosity 1027 Cp at 19.5°C. Thus for a still etchant (i.e. having zero relative velocity between etchant and crystal) acting chemically on a cleavage face of calcite, higher viscosity of etchant having concentration 17 M favours formation on the surface, a thin film of reaction product with thickness greater than the optimum value. This optimum thickness is a function of etchant concentration and etching temperature. Thus when aqueous solution of sodium hydroxide was used as a dislocation etchant, etch rates V_t and V_s $[$with $(V_{tm}/V_{sm}) \gg 1]$ increase and etch pits grow at thicknesses of thin films less than the optimum and conversely. The reaction product also helps in deciding the degree of adsorption.

9.4.5 Reaction product inhibition

The inhibition of reaction products is a possible

factor for decrease of etch rates at concentrations greater than C_p. The dependence of reaction of etching time (t) for weak and strong adsorption of reaction products on a crystal surface is given by

$$\delta_\omega = K_1 t \qquad \ldots\ldots (9.2)$$

$$\delta_s = K_2 t \qquad \ldots\ldots (9.3)$$

where δ is desorption rate ; suffixes ω and s indicate desorption to be weak and strong respectively. K_1 and K_2 are constants. If the adsorption of reaction products is weak, the plot of reaction versus time should be a straight line (cf. eqn. 9.1). In the present case work, the graphs (fig. 9.9 and 9.10) of length of an etch pit along direction [1$\bar{1}$0] and weight loss per cm^2 against etching time are straight lines. Hence adsorption of reaction products is weak in dissolution of calcite in aqueous solutions of sodium hydroxide. For strong adsorption the plot of reaction versus etching time should be a parabola, which is not found to be the case for the range of etchant concentrations and etching times and temperatures studied in the present investigation. Thus the reaction product does not inhibit the chemical reaction rate i.e. V_s. This can be seen from the fact that after etchant concentration 17 M, V_t and V_s decrease and (V_t/V_s) decreases from its

value V_{tm}/V_{sm} (table 9.8), thereby showing dissolution of greater number of surface layers and less dissolution at preferential points. The etching temperature is also an important parameter in the etching process. This can realised from a study of Arrhenius plots. However if the effects of V_t and V_s are independently considered, the reaction product does inhibit the chemical reaction after a concentration of 17 M of sodium hydroxide solution.

9.4.6 Arrhenius plots of etch rates

Most of the etchants dissolves a crystal surface independently of line defects producing etch pits. The surface dissolution has been attributed (Gilman[25] 1960, Ives and Plews[26] 1965) to the presence of other short-lived defects such as lattice impurities. It plays important role in the etching process. Hence the determination of the activation energies for dissolution of surface, E_s and for tangential movement of steps away from the nucleus, E_t is likely to enhance the understanding of etching process.

The temperature of etching affects the plane shape of etch pits. For a definite concentration of the etchant (acetic acid)[17] and for temperatures within a given temperature range plane shape of an etch pit is invariant within the limits of optical resolution in this range.

Hence activation energy is constant. The changes in activation energy are also seen with gradual changes in range of temperature. The plane shape of etch pits depends upon concentration range at a constant temperature. This was established[16] in this laboratory using, hydrochloric acid and glacial acetic acid. Using organic acids such as Lactic and Formic, Bhagia[18] studied etch pits shape with concentration. However the strong alkaline etchant (aqueous NaOH solution) does not show change of shape for various temperatures and concentration range. Table 9.3 show the activation energies E_t and E_s for various concentrations of NaOH solutions. The same value of E_t are found for almost all concentrations of the etchant. Similarly almost the same values of E_s are also found for concentrations of the etchant. This strengthens the view that activation energy remains constant for identical shapes (plane) of etch pits.

Chemical kinetics of etch pits with rhombic outlines obtained by using 0.078 M acetic acid and 0.0275 M hydrochloric acid solution in distilled water[17] and also by using 0.111 M Lactic acid solution[18] and saturated solution of ammonium chloride (9 M) was optically studied. The activation energies, E_t for rhombic shapes are 0.68, 0.02, 0.99 and 0.35 ev respectively. This indicates that for identical shapes of etch pits, the activation energies

for different etchants on calcite cleavages are different. Similarly boat shaped etch pits can be produced by different concentrations of NaOH solutions and lactic acid[18] (1.64 M solution). The values of activation energies are 0.62 and 0.20 ev respectively. Thus these different values E_t and E_s for a given shape of etch pit are dependent on etchant only. This suggests that different etchants attack the surface in a manner which is characteristic of the etchant and not of the crystal.

The quality of etch pits and symmetry of etch pits can also be predicted on calcite cleavages. It was concluded[17] that for better quality of etch pits ratio E_t/E_s is greater than one ; higher is the ratio better the quality. In the present work the quality of etch pits is observed to be superior (table 9.3).

9.5 MECHANISM OF DISSOLUTION

Any catalytic reaction proceeds in the following steps.[23] (i) diffusion of reacting species, (ii) adsorption on the surface, (iii) reaction on the surface, iv) desorption of reaction products and (v) diffusion of products away from the surface.

Depending upon the condition in which the process is conducted, a reaction can be diffusion controlled or

kinetically controlled. The rate of diffusion changes with temperature according to the law similar to the Arrhenius equation.[23]

$$D = K \exp(-E/RT) \qquad \ldots\ldots (9.4)$$

where D = diffusion rate

K = constant having same dimension as that of D

E = activation energy for diffusion process

R = universal gas constant

T = temperature in ^{o}K.

It should be noted that the value of E rarely exceeds 1000 - 2000 calories per mole (0.05 - 0.10 ev) i.e. it is only a small fraction of the activation energies of the most of the reactions. Consequently the rate of diffusion will increase with temperature considerably slower than the rate of chemical reaction. Viscosity and diffusion are correlated (Laidler[27]). From the plot of log μ versus receprocal of temperature (fig. 9.24) activation energy, E_μ can be determined. It is 0.19 ev. For liquids which have low viscosity at room temperature, the value of activation energy E_μ is usually 0.14 ev. For denser solution two values are reported.[21] If E_μ and

activation energy of dissolution E_s happen to be equal, the dissolution kinetics are fully diffusion controlled (Sangwal and Patel[9] ; Bogenschultz et al.[28]). Further the activation energy for a diffusion controlled mechanism is usually less than that of kinetically controlled one (Abramson and King[29]). In the present case the activation energies of surface dissolution and tangential dissolution are three times the activation energy (table 9.3) of the viscous etchant (sodium hydroxide solution). Hence in the present case the chemical dissolution of calcite in sodium hydroxide solution is kinetically controlled. It is also possible to determine the order of the kinetically controlled chemical reaction by the equation

$$V = A C^n \quad \ldots\ldots \quad (9.5)$$

where V is the etch rate, A is a constant and C is the concentration of the etchant and n is the order of chemical reaction. However this information does not appear to enhance the understanding of the mechanism of etching of cleavage faces of calcite by aqueous solution of sodium hydroxide.

9.6 CONCLUSIONS

(1) Plane shape of an etch pit produced by different concentrations of NaOH solutions in cleavage face of

calcite is independent of concentrations. The pits at the highest concentration exhibit sharp beak ; however the shape is not changed.

(2) Etch rates are independent of time.

(3) Dislocation etch pit dimensions (lateral and tangential) attain the maximum value at certain concentration C_p (17 M) of the etchant.

(4) The C_p value of the etchant is independent of temperature of etching.

(5) Beyond C_p the etch rates decrease with increase of concentration.

(6) The electrical conductivity of the etchant (aqueous solution of sodium hydroxide) attains a maximum value of etchant concentration which is different from the value of concentration at which etch rates become maximum.

(7) In the study of etch phenomena, the ratio V_{tm}/V_{sm} should be considered. For all dislocation (alkaline solutions, Lactic and Formic acids) etchants the relation between V_{tm}/V_{sm} and etchant concentration and also between σ_m and concentration are linear and independent of etching temperature.

(8) Higher viscosity and thin film formation of calcium oxide are responsible for the dissimilar values of etchant concentrations at which V_t, V_s and σ attain maximum values (cf. 3 and 7).

(9) The thickness of thin film of calcium oxide formed on a cleavage face is a function of etchant concentration and etching temperature.

(10) For good visibility of etch pits, the ratio E_t/E_s should have values greater than one.

(11) The chemical dissolution of calcite in sodium hydroxide solution is kinetically controlled.

REFERENCES

1. Johnston, W.G. — J. App. Phys., 27, 1018, 1952.
2. Gilman, J.J. — Trans. AIME, 212, 783-91, 1958.
3. Ives, M. and Mcausland, D.D. — Surface Sci., 13, 189-207, 1963.
4. Ives, M.B. and Hirth, J.P. — J. Chem. Phys., 33, 817, 1960.
5. Urusovskaya, A.A. — Sov. Phys. Cryst., 10, 437-41, 1965.
6. Haribabu, V. and Bansigir, K.G. — Physica, 30, 2003, 1969.
7. Raju, I.V.K. Bhagvan, Sankaram, T. Bhima and Bansigir, K.G. — J. Phys. D, 3(12), 1796-7, 1970.
8. Raju, I.V.K. Bhagvan and Bansigir, K.G. — J. Cryst. Growth, 11(2), 171-6, 1971.
9. Sangwal, K. and Patel, T.C. — Kristall and Technik, 13, 281, 1978.
10. Popkova, E.G. ; Predvoditelev, A.A. — Kristallografiya, 1970, 15(1), 91-7 (Russ), 1970.
11. Popkova, E.G. ; Matveeva, G.S. and Predvoditelev, A.A. — Kristallografiya, 1969, 14(1), 53-8, (Russ) 1969.
12. Bhatt, V.P ; Vyas, A.R. and Pandya, G.R. — Ind. J. Pure, App. Phys., 12, 807-10, 1974.

13. Watt, H. — Nature (London), 163, 314, 1959.

14. Stanley, R.C. — Nature (London), 182, 1584, 1959.

15. Pandya, N.S. and Pandya, J.R. — Jour. of M.S. Univ. of Baroda, Baroda, 10, 21, 1961.

16. Mehta, B.J. — Ph.D. Thesis, M.S. Univ. of Baroda, Baroda, 1972.

17. Shah, R.T. — Ph.D. Thesis, M.S. Univ. of Baroda, Baroda, 1976.

18. Bhagia, L.J. — Ph.D. Thesis, M.S. Univ. of Baroda, Baroda, 1983.

19. Hanke, I. — Acta. Phys. Austrica, 14, 1, 1961.

20. Robinson, W.H. — Techniques for the direct observation of structure and imperfections (John Wiley & Sons, Inc. N.Y.) 1968.

21. Sangwal, K. and Arrora, S.K. — J. Mat. Sci., 13, 1977-85, 1978.

22. Sangwal, K. ; Patel, T.C. and Kotak, M.D. — Kristall and Technik, 14, 8, 949-964. 1979.

23. Gerasimov, Ya. ; V. Dreving ; A. Kiselev ; E. Eremin ; A. Shlygin and G. Panchenkov — Physical Chemistry Vol. 2, Mir Publishers, Moscow, 1974.

24. Bhagia, L.J. and Pandya, J.R. — Surface Technology, 19, 187-192, 1983.

25. Gilman, J.J. — Surface Chemi. Metals and Semi conductor Symp., John Wiley & Sons, N.Y. 1960.

26. Ives, M.B. and Plew, J.T. — J. Chem. Phys. 42, 293, 1965.

27. Laidler, K.J. — Chemical Kinetics McGraw Hill Book Co., 1950.

28. Bogenschultz, A.F., Locherer, K. and Mussinger, W. — J. Electrochem. Soc., 114, 970, 1967.

29. Abramson, M.S. and King, C.V. — J. Amer. Chem. Soc., 61, 2290, 1939.

CHAPTER - X

THERMAL ETCHING OF CALCITE CLEAVAGE SURFACES

CHAPTER - X

THERMAL ETCHING OF CALCITE CLEAVAGE SURFACES

10.1 INTRODUCTION

It is well-known from the theory of growth of perfect crystals that the time required to grow a crystal of ordinary, normal size in a laboratory at low super-saturations is abnormally very high. However, in actual practice, this time is very small of the order of a few minutes or a few hours. This therefore, clearly suggests that real crystals are imperfect. In nature and even under controlled conditions in laboratories, it is not possible to obtain crystals free from all defects. Thus all crystals whether grown in the laboratory or obtained in nature invariably contain some kind of defects. Various methods now available for detecting and studying various types of defects are (i) Chemical etching, (ii) Thermal etching, (iii) Ionic etching, (iv) Dehydration etching, (v) Decoration technique, (vi) X-ray diffraction, (vii) Electron-microscopy and (viii) Field-ion-microscopy.

Chemical etching is extensively used for a large number of crystals for revealing dislocations and is discussed in earlier chapters. In this chapter work on thermal etching will be briefly reviewed alongwith the work carried out by the author on thermal etching on calcite cleavages.

The principle of thermal etching is the evaporation of thermally activated molecules/atoms under controlled condition from comparatively highly strained regions on a crystal surface such as impurities, defects sites and in particular non-equilibrium line defects commonly known as dislocations terminating on the surface under observations. At elevated temperatures movement of atoms may take place to establish a mechanical balance between the surface tension and the line tension of dislocations. Movement of molecules is usually rapid at defects in crystals raised to a temperature near the decomposition temperature or melting point. Hence etch pits may form at these sites. Thermal etching is employed to reveal and study dislocation patterns in crystals. It should be noted that correlation between thermal etch pits and dislocations has not yet been successfully well-established for all crystals.

In a number of cases the observations on the same crystal surfaces by two or more different methods (such as X-ray diffraction, etching etc) have been well correlated. Dislocations in Si and Ge surfaces were revealed by chemical etching. Dash[1] had used decoration technique to study the same surface of Si crystal by diffusing impurities at higher temperatures. He had also used X-ray methods to study this surface, and could obtain good correlation by these methods.

Espange[2] has used transmission electron microscopy to find spacing between crystal planes, whose value is in accordance with X-ray determination. Spivak et al.[3] preferred ionic etching to chemical etching because ionic bombardment can be used over wide range of temperatures. Further chemical etching is usually applied to a heat treated sample on the assumption that no change in the crystal structure of metal due to this treatment is introduced. The thermal etch treatment for a number of single crystals of metals has been extensively studied by many workers. The low index faces of metal crystals develope a hill and valley structure when heated in a desired atmosphere. Such changes in surface topography (usually called faceting) together with the development of grain and twin boundaries and grooves are the usual patterns produced by thermal etching. When a crystal surface is heated, there is a possibility of evaporation or decomposition or polymorphic transformation of the surface. Evaporation of a crystal is usually more at defect sites than at perfect lattice regions. There is a finite probability for etch pit formation on faces similar to chemical etch pit formation. Thermal etch pits are also observed in polymorphic transformation. Thermal decomposition of the crystal also produces etch pits. All these processes usually come under the general term 'thermal

etching'. In proper sense thermal etching may be termed as the spontaneous change of the topography of a planar solid surface at elevated temperatures.

Before the concept of dislocation was introduced in the defect study of crystals, review on thermal etching of metal crystals was given by Shuttleworth[4]. He has suggested that the boundary grooves and striations are formed mainly by the surface migration of metallic ions until an equilibrium surface of minimum energy is attained. Hendrickson and Machlin[5] developed thermal etching technique for revealing dislocations in silver single crystals. A large number of microscopic thermal etch pits were formed whose density is constant and is independent of etching time. When a silver crystal was bent, it was found that density of excess thermal etch figures depended inversely upon the radius of bending. Hirth and Vassamillet[6] have concluded from their observations, that there is not an exact correlation between thermal etch pits and dislocations. In addition, it is shown that the size and distribution of etch pits is a function of orientation of silver single crystals. In other metals such as antimony Shigeta and Hiramatsu[7] found thermal etching technique to be unsatisfactory for revealing dislocations. This was based on the observation of lower density of thermal etch pits than

that of chemical etch pits which revealed dislocations. Bunten and Weintroub[8] has described sensitive thermal etching technique for revealing the grain size structure of the antimony single crystal. It is clear from above observations on various crystals that thermal etching is not likely to be an exact method to reveal dislocations in metal crystals.

During the past few years much work on thermal etching of ionic crystals in general and on alkali halide crystals in particular has been carried out. Smakula and Klein[9] observed that thermal etching carried out in vacuum occurred preferentially at distorted points in thalium halide crystals. They observed that etching proceeded in a regular manner forming pits bound by $\{110\}$ planes. They noted that high temperature produced disordered etching and surface striations.

Freshly cleaved surfaces of NaCl single crystals thermally etched at 750°C in air showed circular etch pits produced at the sites of dislocations ending on the faces (Patel et al.,[10]). They also observed little correspondence of thermal etch patterns on matched halves. Evaporation spiral and circular terraced pits were observed on cleavage faces of KCl single crystal (Patel et al.,[10] 1966). They

attributed the formation of terraces of etch pits at two dislocations very near to each other. Budke[11] observed three types of etch pits on thermally etched NaCl crystal in vacuum (10^{-5} torr), (i) crystallographically oriented square pits, (ii) pits with edges rounded and (iii) shallow pits having no observable fine structure except at their centres.

Takeda and Kondoh[12] used thermal etch technique to reveal dislocations in nickel oxide in the temperature range 1550° - 1650°C. They found square and retangular crystallographic etch pits, and a good correspondence of thermal etch pits with chemical etch pits, thereby suggesting the formation of these pits at dislocations. Voitsekhovskii[13] reported use of evaporation figures for finding orientation of crystals. Another oxide which is very well-known is ice, which melts at low temperature (0°C). Thermal etching of ice crystals at about -15°C in a low vacuum (10^{-2} torr) was reported by Michell et al.,[14] They suggested the stepwise propagation of etching.

Decomposition of a crystal is also due to thermal etching. Here crystals dissociate into new substances. In evaporation there is only a phase change i.e. from solid to vapour. Thermal treatment may give rise to polymorphic transformation. Kennedy and Patterson[15] worked on thallous

nitrate and observed thermal etch pits after polymorphic transformations. They concluded that preferential thermal etching occurred around dislocations in the polymorphic transformation.

When intermetallic compound surfaces are heated up to a decomposition temperature of one constituent the decomposition rate of both the cleaved surfaces may not be the same. Due to different decomposition rates thermal etch pits are formed on a fast evaporating surface at a relatively low temperature. Millea and Kyser[16] reported thermal decomposition of GaAs surfaces. As(111) face decomposes at a higher rate than the Ga(111) surface at a temperature of 750°C. At 800°C the decomposition rates of both faces are nearly equal. In the above process dislocations do not appear to act as nucleation sites. Surface kinks, mechanical scratches and unknown microtopography of surface produced by chemical etching have been observed to act as nucleation sites for thermal decomposition. Regular tetrahedron whose sides are Ga⟨111⟩ are formed on As(111) surfaces, the decomposition rate of the 110 face is intermediate between the As(111) and Ga(111) faces. Density of thermal etch pits is also found to depend on the temperature of decomposition. Hillocks are formed along with thermal etch pits in the above compound. The temperature at which hillocks are

formed is usually higher than the temperature at which etch pits are formed. The octahedron (III) faces of Indium antimonide appear to be an exceptional case. In this crystal hillocks are formed at temperatures lower than those required for etch pit formation. They are explained on the basis of breaking of bonds. In the above cases compound decomposes into their constituents.

In the following cases solid A decomposes into solid B + gas C which usually goes to the atmosphere. Singh[17] studied the decomposition phenomenon of mercury fulminate in which critical size was needed for explosive decomposition. He observed the preferential decomposition along (010) and (110) planes as well as along the growth features on the surface of crystals. He suggested sites of nuclei to be probable points of emergence of dislocations on the surface. Jach[18] has studied thermal decomposition of dehydrated nickle oxalate and suggested preferential decomposition at dislocations. He remarked that linear kinetics resulted from the preferential decomposition and this type of mode was energetically more favourable than at regular reactant product interfaces. Electron microscope study was carried out on the partly decomposed crystals of CdI_2 (Bristow and Rees[19]). They observed white patches on partly decomposed faces of above crystals, which were associated with dislocation lines. CdI_2 decomposes into

cadmium and iodine vapour. The same type of reaction was observed in calcite crystals. Calcite decomposes fully at 850°C into solid calcium oxide and carbon dioxide gas. Impurity within a crystal sometimes plays a dominant role in the process of thermal etching, e.g. it lowers the temperature at which thermal etching commences. Varshavskii[20] observed that a pure diamond crystals could be etched in air at 850°C while thermal etching of impure crystals took place at a lower temperature. In thermal etching decomposition process should be unidirectional otherwise growth features along with etch figures may be observed and it is difficult to differentiate both features if they are of the same form. Neutron irradiation favours the unidirectional decomposition (Jach 1962).

Thomas and Renshaw[21] studied the decomposition phenomenon in single crystals of calcite. They suggested the thermal pits observed at 500°C in vacuum to be at dislocations terminating on the surface. Cutler and Kovalenko[22] in the same year found strong dependence of thermal pits on calcite cleavage surfaces, on prehistory of specimen surface and on impurity associated with dislocation. Hirth et al.,[23] found thermal etch rate measurements to be consistent with the terrace ledge kink model of sublimation in case of cadmium selenide single crystal. Moller et al.,[24] calculated activation energy

for cross-slip of screw dislocations to be 3.6 ± 0.3 ev for Germanium crystals when extrapolated to zero stress. Parasnis et al.,[25] observed no correspondence of thermal etch pits on cleavage counterparts with dislocations in silver chloride monocrystals. Robertson[26] determined activation energy and surface diffusion coefficient in thermal etching and grain grooving of polished polycrystalline specimens of silicon ceramics. They found grain boundary grooving formed by an evaporation process similar to that for decomposition. In this laboratory thermal etching of calcite cleavage surfaces was optically studied (Mehta[27]). The thermal etch pits did not show any correspondence on matched halves. On multiple etching of the same cleavage surface little increase in etch pits density was observed. The detailed comparative study of chemical and thermal etch pits has shown that thermal etch pits on calcite cleavage surfaces are produced at dislocation-free impurity sites. In continuation of this work the present study was carried out by determining the thermal activation energy and comparing it with the chemical activation energy required to produce dislocation etch pits on calcite cleavages.

10.2 EXPERIMENTAL PROCEDURE

In the present study freshly cleaved surface of natural calcite was thermally etched in the range of

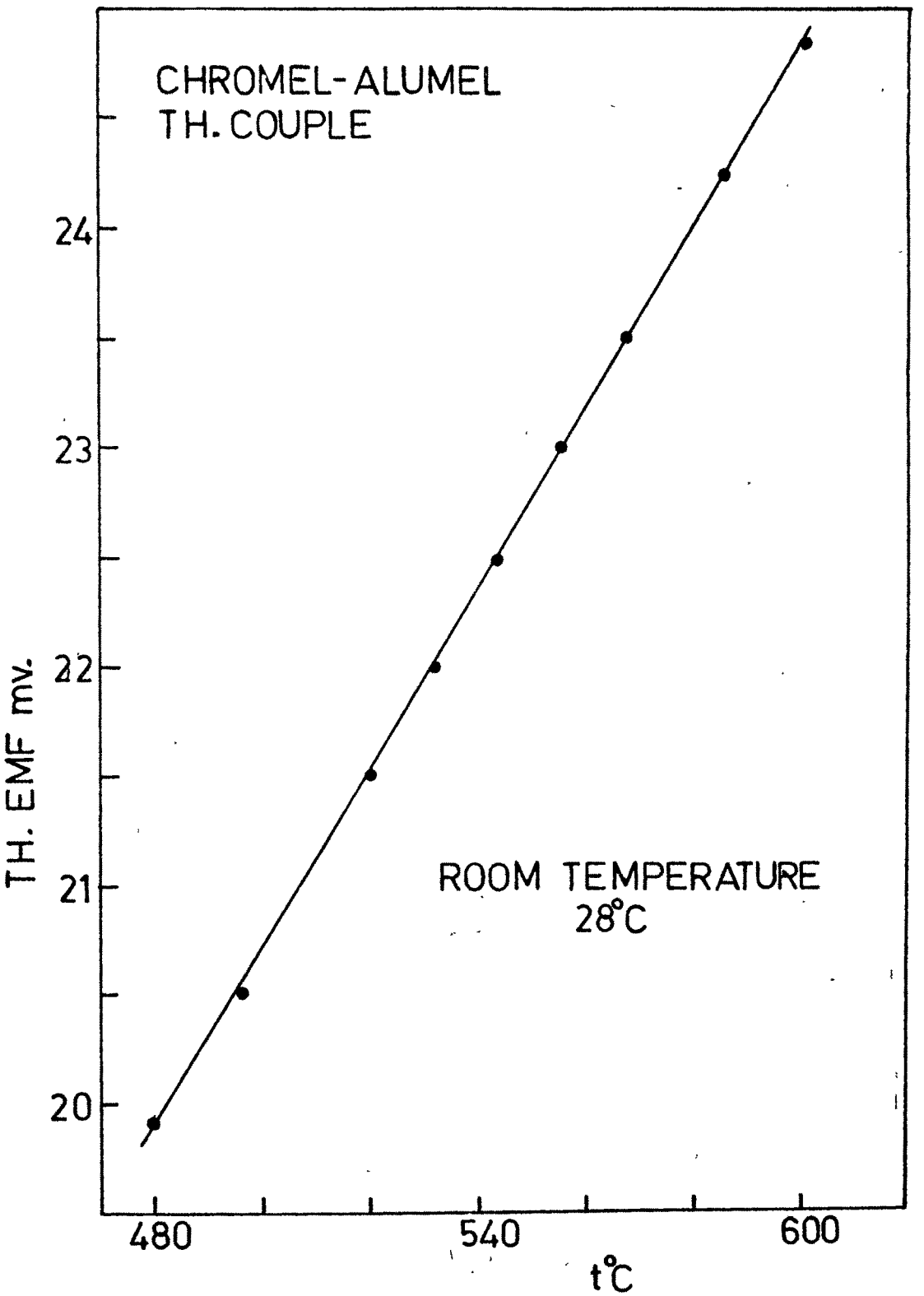

FIG.10·1 PLOT OF TH. EMF vs TEMP.

temperature 535°C to 605°C in an energy regulated vertical temperature gradient furnace (fig. 2.13). The energy regulator unit (dial) of the furnace is calibrated interms of temperatures so that the desired temperature can be obtained and maintained constant for long period of time. The temperature record was done by sensitive millivoltmeter using chromel-alumel thermocouple. The millivoltmeter was calibrated for given range of temperatures with standard pyrometer. The graph of thermo emf against temperature (fig. 10.1) shows the recorded calibrated plot of thermo emf shown in millivoltmeter against temperature of the given furnace. The furnace was attended throughout the run of the experiment and for any undesirable changes in temperature due to reasons beyond control of the present author, the observations were rejected. The stabilized power was used throughout the experiment to operate the furnace. Every time freshly cleaved sample of calcite crystal was placed in a porcelein crucible at a definite place in the furnace in such a manner that the cleavage surface was always exposed to the atmosphere in the furnace. The temperature of the furnace was slowly raised to a desired value and maintained constant by constant and adequate supply of heat energy by energy regulator. The required temperature was obtained in two hours. On attaining the desired temperature, etching time was counted. After thermal etching

of the crystal surface for a given time, the furnace was shut off and brought to room temperature. The crystal was very carefully weighed using semimicrobalance (fig. 2.12) before and after thermal etching. Etch pit dimensions were measured by an optical microscope. The least count of the filar micrometer eyepiece was 0.4 micron. The same sample was successively etched three to four times.

10.3 OBSERVATIONS AND RESULTS

It is reported in literature that calcite decomposes at 850°C. These crystals were therefore kept well below decomposition temperature, say 650°C, for one hour, when the crystals were taken out from the furnace, surfaces were found covered with white layer. From the chemical test it was found that this layer consisted of calcium oxide only. The crystals became so soft that slight force by the forcep can cleave them very easily. Further this surface did not exhibit any meaningful micro topographical features. It is now well-established in this laboratory that (Mehta 10c cit) within a given range of concentration of a dislocation etchant, plane shape / out line of an etch pit on calcite cleavage faces remains unchanged. Just as a gradual change from one range of concentration of a dislocation etchant to another (Mehta 1972) or a change in etching temperature of a dislocation etchant (Shah[28] 1976)

produces a change in the plane shape of a pyramidal or flat-bottomed etch pit, the change of etching temperature from 520°C to 530°C and from 530°C to 540°C creates respectively circular, hexagonal and rhombic outline of pyramidal or flat-bottomed thermal etch pits on calcite cleavage surface (Mehta loc cit). The variation in etching time for a given etching temperature does not produce any change in shape. Further the plane shape of thermal etch pit does not show any change beyond 540°C. The kinetics of thermal etching is studied by the present author from 536°C to 605°C by optical measurements of lengths of diagonals of etch pits and weight-loss in successive etching of the same sample at the given temperature.

Fig. 10.2a and Fig. 10.2b shows the matched halves of calcite cleavage surfaces etched at temperature 572°C for six hours. It is seen from these photomicrographs that the thermal etch figures do not show any correspondence and that they are of assorted sizes. Besides large figures are formed on cleavage lines ; the figures are also observed at places free from cleavage, slip or twin lines. The figures having rhombohedral out line with slopping faces meeting at a point. This point coincides with the geometrical centre of the rhombic figures. Thus eccentricity of a thermal pit is zero. This is one of the basic characteristics of a thermal etch pit (Mehta and Pandya[29]

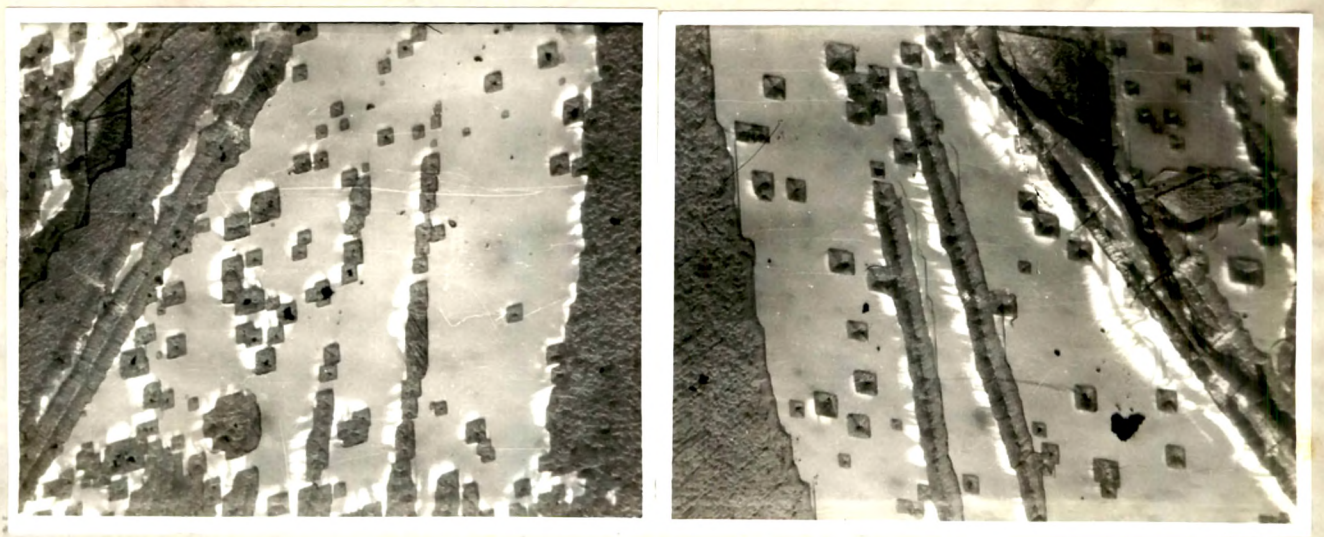

(a) (x 40) (a) (x 40)

Fig. 10.2 (a,b): Photomicrographs of thermally etched cleavage counterparts at 572^{o}C for six hours.

1982 ; Mehta[30] 1981) on a cleavage face of calcite. It differentiates a thermal pit from a chemical etch pit having concentration dependent eccentricities (Mehta and Pandya[31] 1981, Mehta[32,33] 1980, 1981a,b) and orientations (Mehta and Pandya[34,35] 1981 , 1982b). The sides of these pits are parallel to the edges of the crystal i.e. to $\langle 100 \rangle$ whereas longer and shorter diagonals are parallel to directions $[1\bar{1}0]$ and $[110]$ respectively. The density of these marks varies from 10^3 to 10^4 per cm^2.

10.3.1 Effect of time and temperature of etching

Many workers have shown from etching study of different crystals that if the pits represent the sites of line defects, the repeated etching of these crystals surfaces should not show any change in the number, position and orientation of these pits. Fig. 10.3(a,b,c) represent photomicrographs of freshly cleaved surface successively thermally etched at 583°C for 10 hours (5 + 5 hours), 15 hrs. and 20 hrs. respectively. It is unusually clear from all these figures that although these etch marks which are of different sizes increase in dimensions with increase of etching period, yet a few new etch figures are found in the second stage of etching such as x, y, z fig. 10.3 (a) The density of thermal figures on this surface is slightly increased. The cleavage line PQ, RS, TU are unaffected by

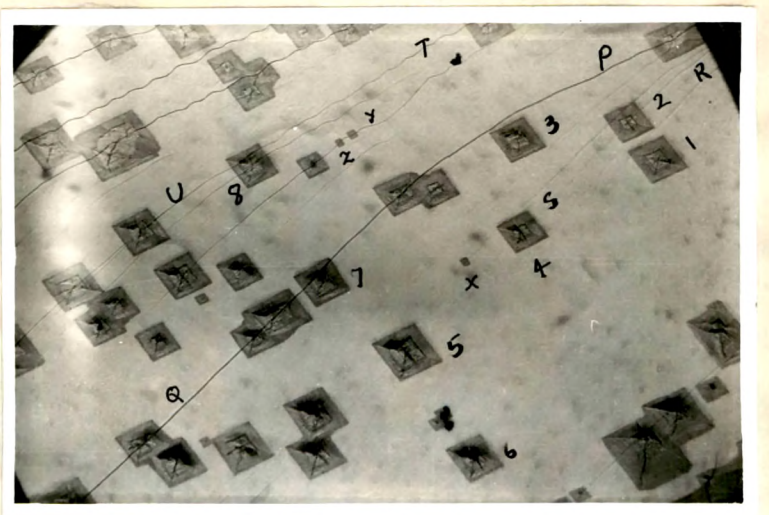

(a) (x 50)

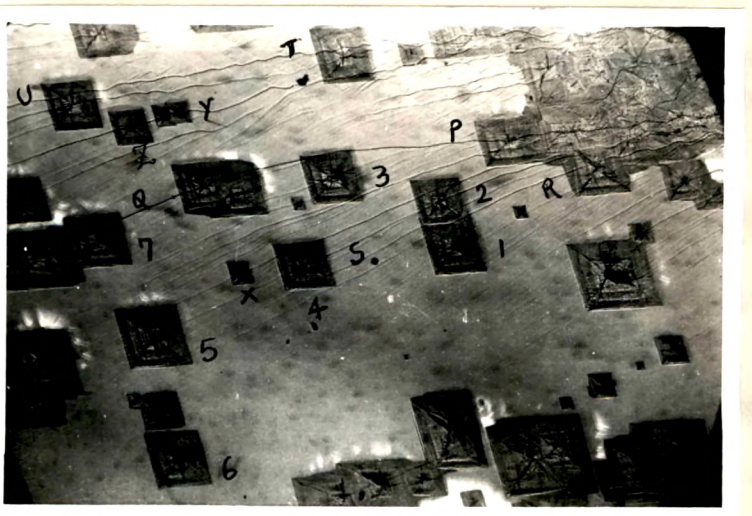

(b) (x 50)

(c) (x 50)

Fig. 10.3 (a,b,c) shows successive thermal etching at 583°C for 10 hrs (5hr + 5hr), 15 hrs and 20 hrs respectively of the same cleavage surface.

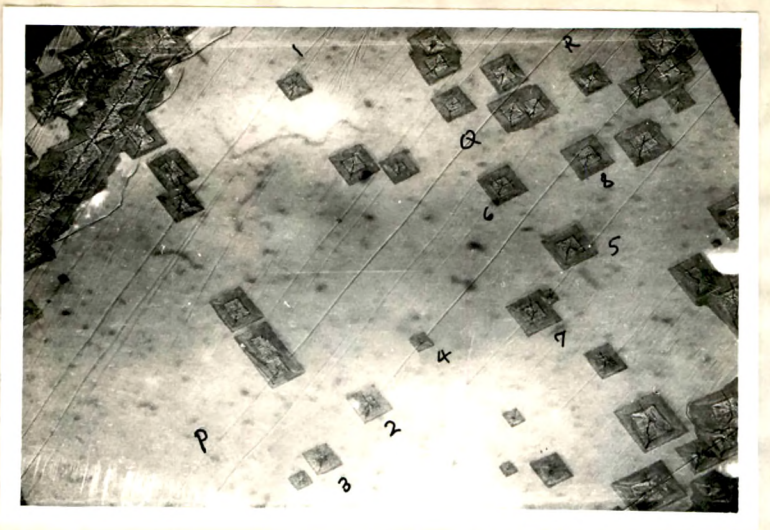

(a) (x 50)

(b) (x 50)

(c) (x 50)

Fig. 10.4(a,b,c) shows photomicrographs of successive thermal etching of the same cleavage surface at 583°C for 10 hrs (5 hrs + 5 hrs), 15 hrs and 20 hrs respectively.

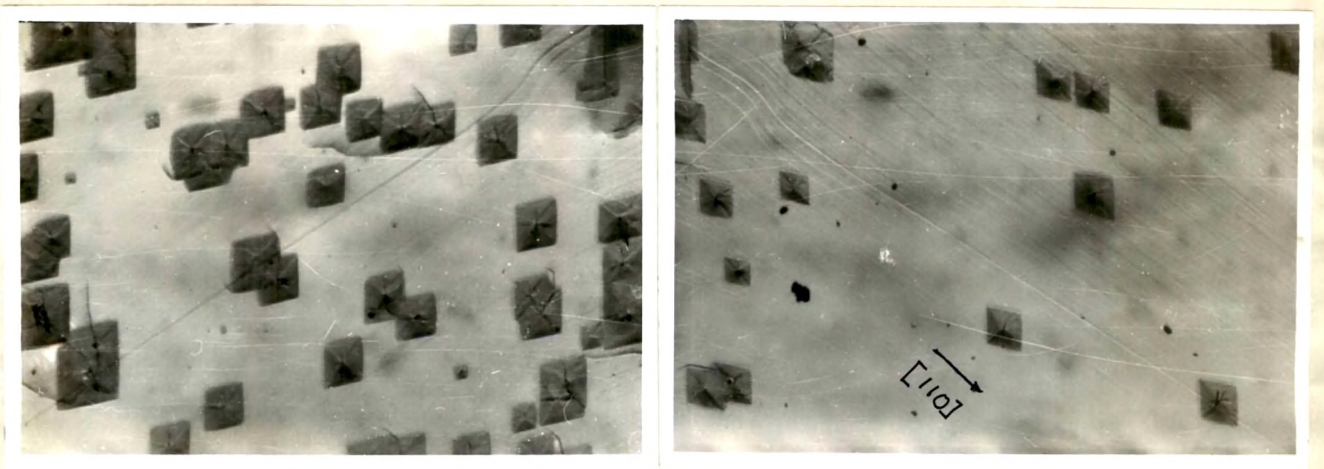

(a) (x 50) (b) (x 50)

Fig. 10.5(a,b) shows photomicrographs of thermal etching on cleavage counterparts at 560^{o} and 548^{o}C for 7 hrs and 8 hrs respectively.

(a) (x 50)

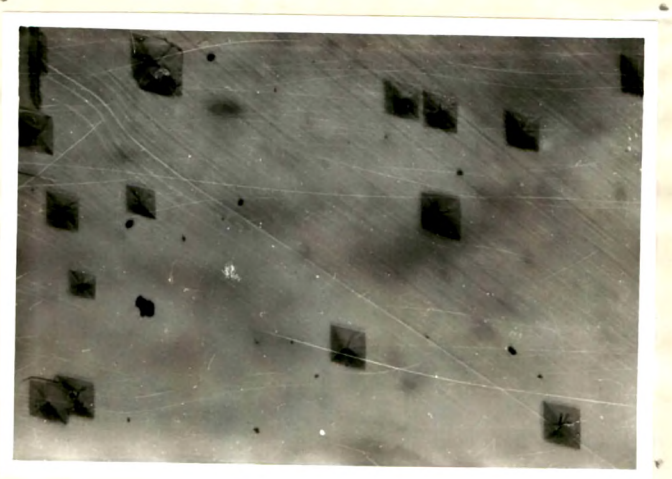

(b) (x 50)

Fig. 10.6(a,b) shows photomicrographs of successive thermal etching at 548^{o}C for total period of 32 hrs and 8 hrs respectively of the same cleavage surface.

thermal etching and do not shift from their position as is usually found in the case of chemical etching (Tolansky and Patel[36] ; Pandya[37]).

The neighbouring pits enlarge on repeated etching and coalesce to form bigger pits of varying sizes. The internal structure of these figures also change with repeated etching. On multiple etching the number of cracks within thermal etch figures increases with time of etching. In these figures the diagonals of the rhombic etch figures are seen clearly. Fig. 10.4 (a,b,c) also shows the repeated etching of freshly cleaved surface at same 583°C for 10 hrs. (5 hrs. + 5 hrs.), 15 hrs. and 20 hrs. respectively. The diagonals of rhombic thermal etch figures numbered 1 to 9 in Fig. 10.4 (a,b,c) and numbered 1 to 9 in Fig. 10.3(a,b,c) are measured in the usual way by micrometer eyepiece. Fig. 10.5 (a,b) shows matched pair of freshly cleaved samples etched at 560°C for seven hours and at 548°C for eight hours respectively. The density of pits seems slightly more on the sample etched at 560°C than the one at 548°C. The cleavage lines are unaffected by variation of temperature. Fig. 10.6a (x50) exhibits photomicrograph of repeated etching of a sample at 548°C for total time of 32 hrs. in four equal intervals of time period i.e. after eight hrs. of etching the microtopography of the cleaved sample was optically studied. In this way the sample was studied four

times, with the final topography as shown in Fig. 10.6a. Fig. 10.6b shows one etched at 548°C for eight hours. In this repeated etching the density of pits has increased.

Several sets of observations of etch pit diagonals for different etching times and etching temperatures were taken. Table 10.1 presents a typical set of observations on variation of length of etch pit diagonals (L_1 and L_2) and weight loss per cm^2 with time at various temperatures of etching. As the thermal etch pits are of assorted sizes, the large number of pits were considered for measurement and a few categories of pits like A, B, C are made. The statistical average lengths of diagonals were taken for different categories. Fig. 10.7 and 10.8 shows plots of length of etch pits along $[1\bar{1}0]$ and along $[110]$ directions against etching time. It is clear from these plots that length of both diagonals of pits varies linearly with etching time. The slopes of these lines give the rates of tangential dissolution, V_t along specified directions at corresponding temperatures of etching. The rates of tangential dissolution along shorter diagonals are found to be less than that along longer diagonals. Similarly weight loss per cm^2 is plotted against etching time (Fig. 10.9) ; the plots are again straight lines. The slopes of these lines give the rate of surface dissolution, Vs, in gm/cm^2 per unit time. Division of this quantity by density of calcite (2.71 gm/cc)

Table 10.1 Thermal Etching of Calcite Cleavages

	Time in hours		Diagonal length $L \times 10^{-4}$ cm		Wt. loss $\frac{gm}{cm^2} \times 10^{-3}$
			Longer	Shorter	
Temperature of Etching 548°C	8 hrs	A	42.00	33.81	
		B	36.85	32.55	2.22
		C	29.4	23.52	
	7.5 hrs	A	67.3	57.33	
		B	62.68	51.45	5.3
		C	54.6	46.41	
	8 hrs	A	93.45	80.43	
		B	87.36	74.76	7.4
		C	78.75	69.51	

Cont....

Table 10.1 cont...

		A	42.42	35.28	
Temperature of Etching 560°C	7 hrs	B	32.97	27.99	3.05
		C	24.78	19.95	
		A	92.4	77.7	
	7 hrs	B	84.0	70.77	6.2
		C	73.5	60.9	
		A	140.7	117.18	
	7 hrs	B	130.2	108.36	9.3
		C	122.64	99.12	
		A	58.8	49.56	
Temperature of Etching 572°C	6 hrs	B	43.26	34.65	3.26
		C	31.5	25.2	
		A	140.7	117.6	
	6 hrs	B	122.85	103.95	7.18
		C	111.93	92.4	
		A	223.65	185.85	
	6 hrs	B	202.65	172.2	10.89
		C	193.2	160.65	

Cont...

Table 10.1 cont...

		A	123.48	103.32	
Temperature of Etching 583°C	5 hrs	B	92.4	77.28	7.152
		C	68.88	58.8	
		A	249.9	212.1	
	5 hrs	B	224.7	187.74	16.501
		C	191.94	170.10	
		A	374.85	319.2	
	5 hrs	B	349.65	294.0	24.681
		C	320.25	278.25	
		A	38.64	36.97	
Temperature of Etching 595°C	2 hrs	B	32.55	30.45	5.472
		C	28.14	27.09	
		A	124.32	110.25	
	2 hrs	B	117.18	103.95	11.0
		C	107.1	100.8	
		A	209.58	184.8	
	2 hrs	B	201.6	180.6	16.7
		C	189.9	176.4	

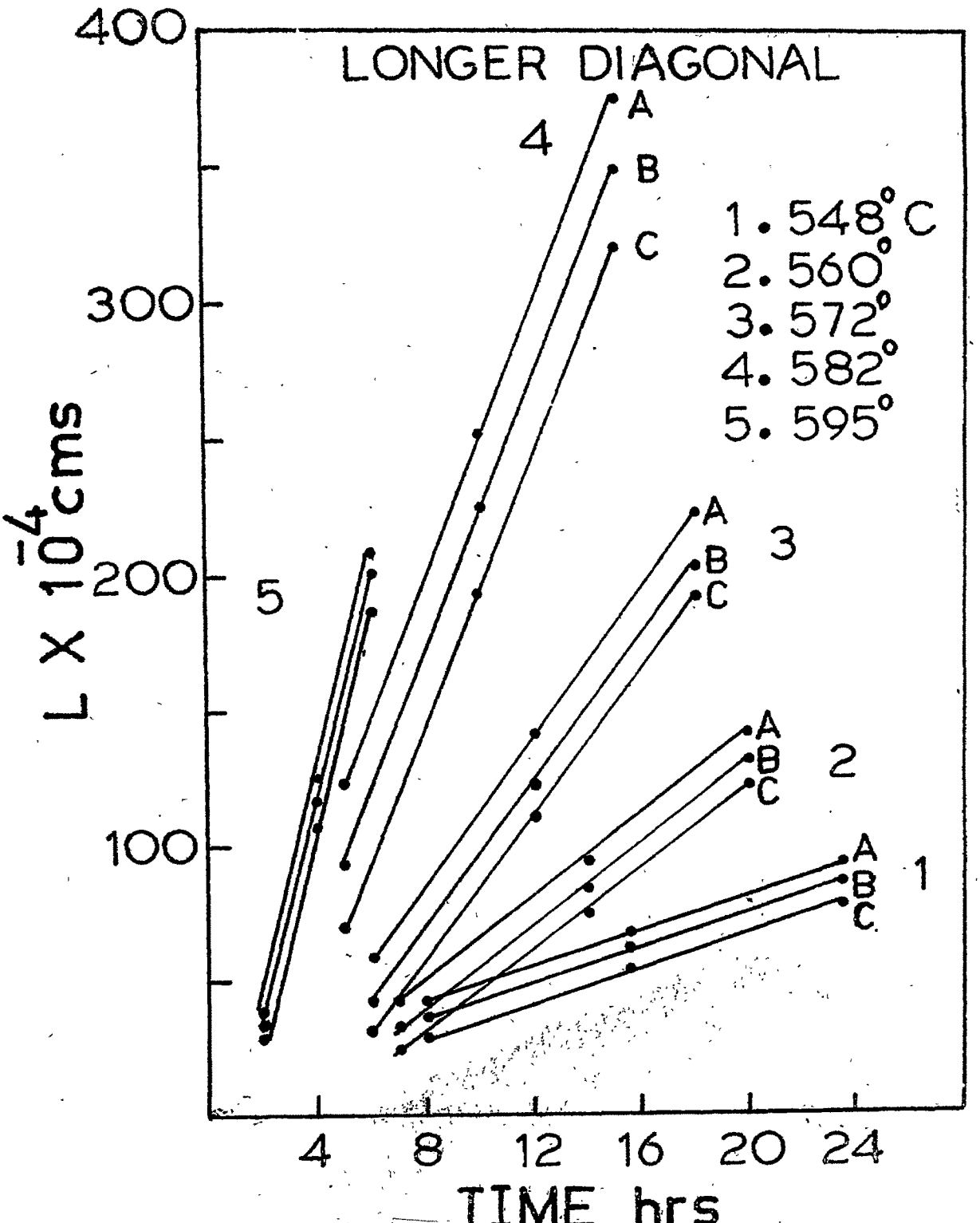

FIG.10.7 PLOT OF LENGTH vs TIME

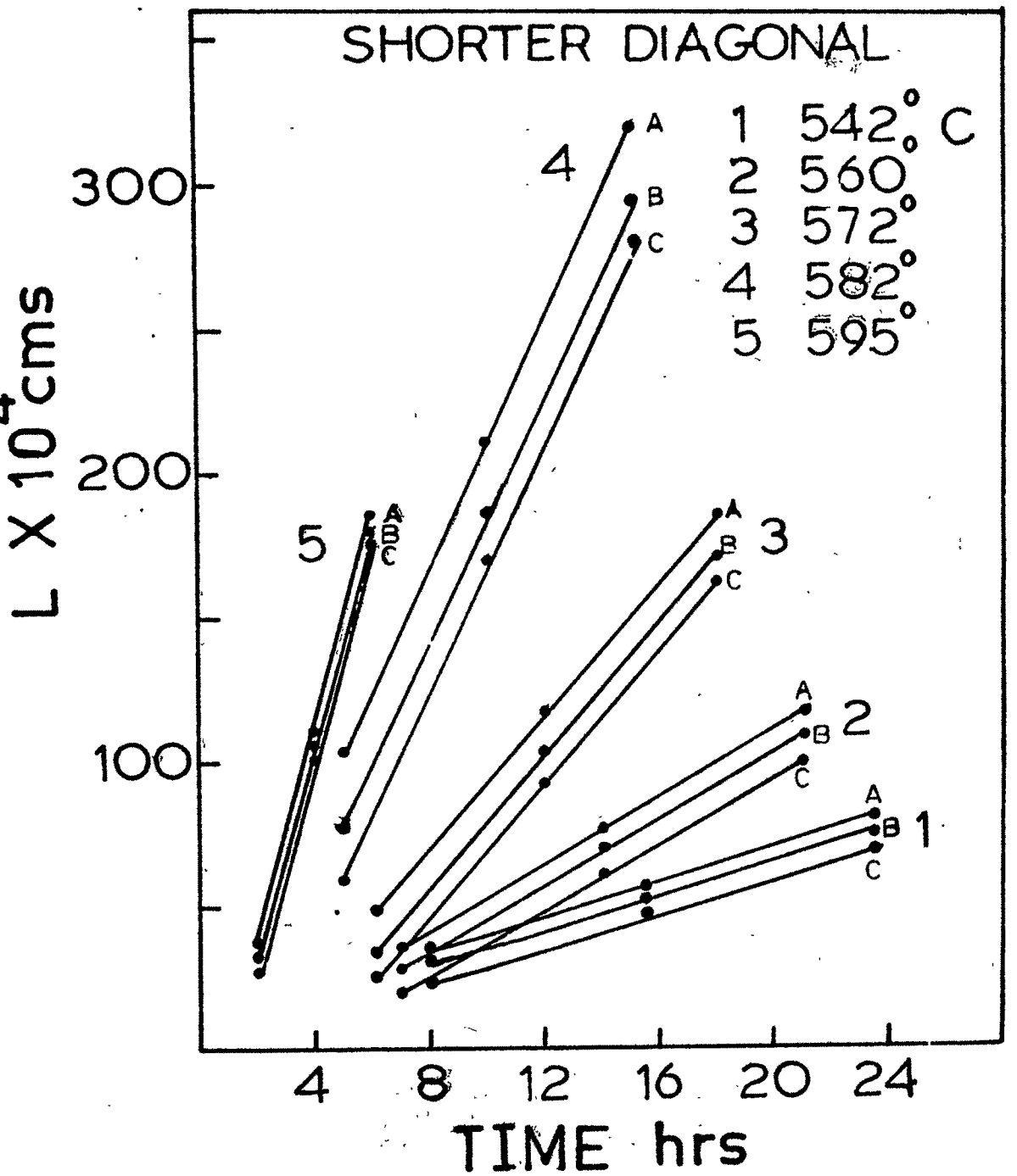

FIG.10.8 PLOT OF LENGTH vs TIME

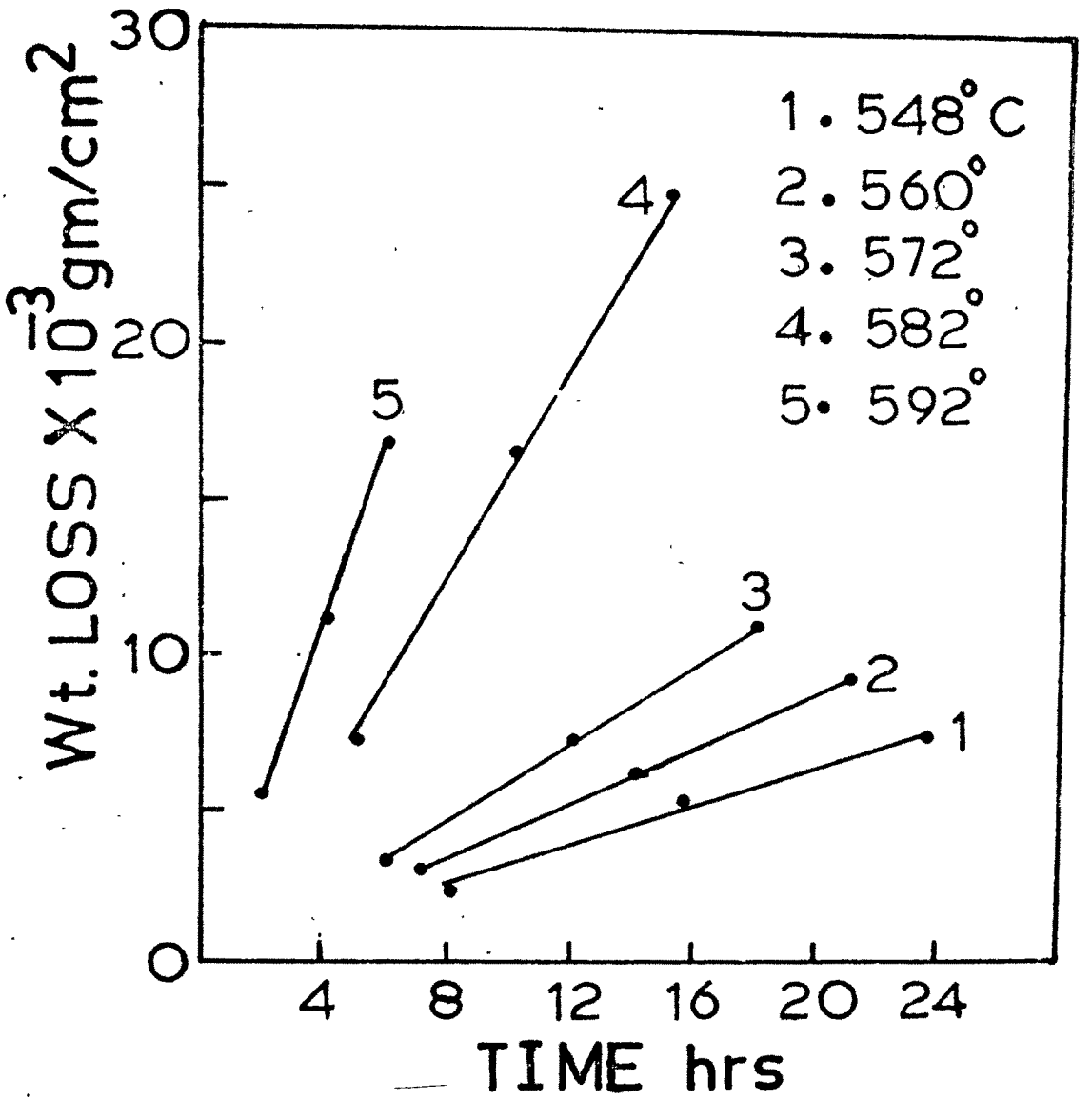

FIG. 10.9 PLOT OF WT LOSS vs TIME

yields the rate of surface dissolution, Vs, in cm per second. The straight line plots indicate that rates of tangential as well as surface dissolution are independent of etching time but depend on temperature of etching. Table 10.2 shows the rate of tangential and surface dissolution at various etching temperatures ranging from 536°C to 605°C. Fig. 10.10 shows the graphs of the log of time rate of increase of pit diagonals (V_{t1} and V_{t2}) along $[1\bar{1}0]$ and $[110]$ Vs receprocal of etching temperature T°K and log of surface dissolution rate versus (1/T) plotted on the assumption that Arrhenius equation for chemical dissolution is also applicable to thermal dissolution.

According to Arrhenius equation,

$$V = A \exp(-E/KT),$$

the slope of the graph of log Vt (or log Vs) versus 1/T represents the value of E/k, where E is the activation energy of the process and K is Boltzman constant. The activation energies thus calculated for thermal etching are shown in Table 10.2. The table also shows the preexponential factors ($A_{t_{th}}$ and $A_{s_{th}}$) for tangential and surface dissolution rates.

10.4 DISCUSSION

Thermal etching may initiate at the imperfections in

Table 10.2

Temp. ^{o}K	$V_{t1} \times 10^{-7}$ cm/sec	log V_{t1}	$V_{t2} \times 10^{-7}$ cm/sec	log V_{t2}	$V_s \times 10^{-7}$ cm/sec	log V_s	$10^3/T$ $^{o}K^{-1}$
809	-	-	-	-	0.0576	$\bar{9}$.7602	1.236
821	0.933	$\bar{8}$.9699	0.7648	$\bar{8}$.8835	0.1422	$\bar{8}$.1529	1.218
833	1.960	$\bar{7}$.2923	1.5968	$\bar{7}$.2032	0.2213	$\bar{8}$.3450	1.200
845	3.7310	$\bar{7}$.5718	3.1580	$\bar{7}$.4994	0.3095	$\bar{8}$.4907	1.184
856	7.0000	$\bar{7}$.8451	6.0291	$\bar{7}$.7802	0.8383	$\bar{8}$.9234	1.168
868	11.4300	$\bar{6}$.0580	10.3090	$\bar{6}$.0132	1.2300	$\bar{7}$.0900	1.152
880	-	-	-	-	1.4760	$\bar{7}$.1691	1.136

Calculated activation energies and preexporential factors

$E_{t\ th}$ = 3.303 ev ; $A_{t\ th}$ = 8.128×10^{12} ; 7.203×10^{12}

$E_{s\ th}$ = 2.97 ev ; $A_{s\ th}$ = 2.089×10^{10}

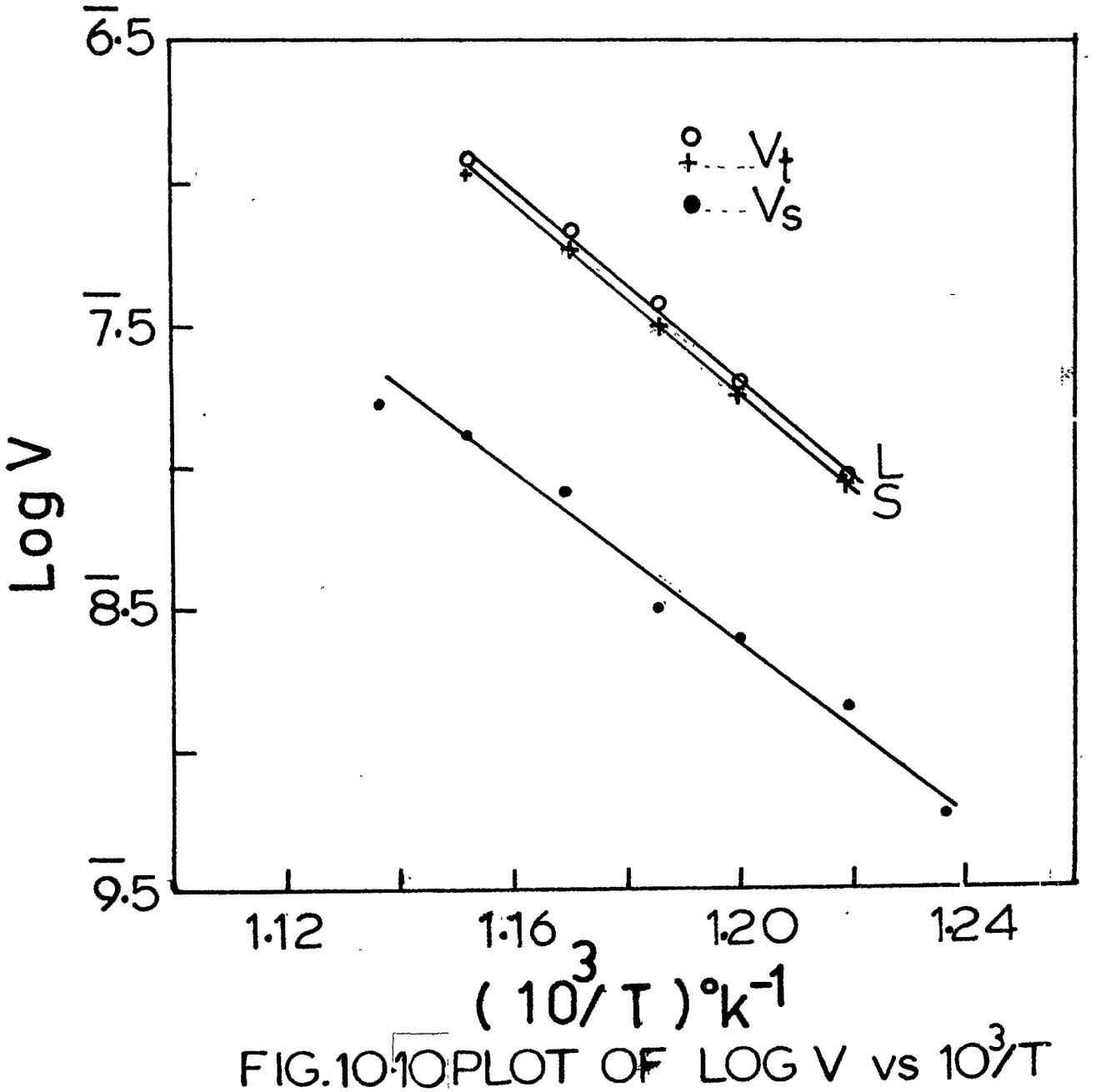

FIG.10·10 PLOT OF LOG V vs $10^3/T$

crystals. Microtopographical changes of surfaces are of two types : (1) Formation of thermal etch pits and/or formation of thermal grooves. The kinetics of atomic migration on a crystal surface, experiencing unbalanced exchange of material with its environment may produce etch pits. The reduction in surface energy with the orientation of the plane may create faceting in the crystal. Faceting is generally observed on a low index plane. The progressive widening of the facets was due to the separate action of evaporation and condensation. Imperfections are associated with strain field and the local free energy of the crystal surface is greater near the neighbourhood of imperfections than for the perfect surface region. If the rate of evaporation is same for imperfect and perfect surfaces, general evaporation takes place. In this case dislocations may or may not act as nucleation sites for production of thermal etch pits. It may be due to higher amount of thermal energy than dislocation energy or dislocation is mobile and its free energy becomes less when dislocation is at a higher temperature. It is clear from the above that controversial results are found in cases of thermal etching of metal crystals, [Hendrickson et al. (Loc. cit) and Hirth et al. (Loc. cit)] like silver crystals. For many ionic crystals such as NaCl, KCl, Cu_2O, thermal etch pits due to evaporation of material of high temperatures are formed at dislocations. Spiral etch pits

formed on NaCl or KCl (Patel et al., 1965, 1966) have no correlation with screw dislocations. Thermal decomposition of intermetallic compounds does not initiate at dislocations. The thermal pits at dislocation sites were reported by Jach (Loc. cit) in dehydration of Nicle oxalate. Mehta (1972) concluded, by studying matched cleavage counter parts of calcite, one thermally etched and the other chemically etched, the thermal pits to be at impurity centres. With these controversies on origin of thermal pits. The activation energies of thermal dissolution may unfold more information about the process. Table 10.3 shows the activation energy values for tangential dissolution and surface dissolution due to thermal etching. These values $E_{t\ Th}$ and $E_{s\ Th}$ are 3.3 ev and 2.97 ev respectively. Table 10.3 shows the activation energies of tangential dissolution and surface dissolution due to chemical etching of calcite cleavages by different chemical etchants. The table also shows the ratio of E_t/E_s in chemical etching and thermal etching For well defined geometrical chemical etch figures E_t/E_s ratio should be greater than 1 (Shah[28] 1976). The present study indicates that it is also true for well defined rhombic thermal etch figures on calcite cleavages.

The values of the activation energies $E_{t\ Ch}$ and $E_{s\ Ch}$ for tangential dissolution and surface dissolution using

Table 10.3 Activation Energy Values

	Etchant		Chemical Etching			Thermal Etching		
			$E_{t\ ch}$ ev	$E_{s\ ch}$ ev	$\frac{E_{t\ ch}}{E_{s\ ch}}$	$E_{t\ th}$ ev	$E_{s\ th}$ ev	$\frac{E_{t\ th}}{E_{s\ ch}}$
1.	Aq. Sodium hydroxide solution		0.62	0.52	1.192	3.3	2.97	1.11
2.	Aq. Potassium hydroxide solution		0.62	0.49	1.266			
*3.	Acetic acid	0.45%	0.68	-	-			
*4.	Acetic acid	60%	0.54	0.31	1.742			
*4.	Formic acid	100%	0.56	0.42	1.334			
*5.	Ammonium chloride saturated solution		0.35	0.23	1.526			

* Values obtained by different students in this laboratory using different chemical etchants.

Acetic acid	R.T. Shah	Ph.D. Thesis, M.S. Univ. of Baroda, 1976.
Formic acid	L.J. Bhagia	Ph.D. Thesis, M.S. Univ. of Baroda, 1982.
Ammonium chloride soln.	Shripad Khisti	Private Communication.

different etchants which reveals dislocations are fairly low. The thermal activation energies for controlled thermal dissolution are comparatively very large. This indicates that more energy is consumed to move ledges producing pits. It also indicates that those points/regions on the surface with energy values from 0 to about 3 ev will be thermally activated. Since dislocations terminating at points on surface, revealed by etch pit formation required small energy values of the order of a few hundreds of millielectron volts, they would be rapidly swept away by thermal energy. Quantitatively this can be understood by taking the ratios of tangential dissolution energy values and also the ratio of surface dissolution energy values for the process of thermal and chemical etching, viz. $E_{t\ th}/E_{t\ ch}$ and $E_{s\ th}/E_{s\ ch}$. The table 10.3 shows these values. It is clear from these values that the activation energies for thermal dissolution are larger by a factor six than the chemically activated energy values. This is obvious in view of the fact that the chemical dissolution occurs at a faster rate than the thermal dissolution (cf. tables 9.2 & 10.2). Further it has been shown qualitatively, that the controlled chemical dissolution reveals dislocations terminating on the cleavage surface under observation.

This conclusion was obtained in a qualitative manner

(Mehta, 1972). Quantitative support is now fairly well established by the present investigation.

10.5 CONCLUSIONS

(1) The thermal etch pits on calcite cleavage surfaces are of rhombic shape in the range of temperature 540^{o} to $605^{o}C$.

(2) The activation energies $E_{t\ th}$ and $E_{s\ th}$ of thermal dissolution are larger than the corresponding activation energies $E_{t\ ch}$ and $E_{s\ ch}$ of chemical dissolution of calcite cleavages.

(3) Thermal etch pits are produced at dislocation free places such as kinks, steps, impurity centres etc.

REFERENCES

1. Dash, W.C. — J. Appl. Phys. 27, 1193-8, 1956.

2. Espange, S. — J. Phys. Radium, 21, 97-101, 1961.

3. Spivak, G.V. — Soviet. Phys. Cryst. 16, 213-6, 1961.

4. Shuttleworth, R. — Metallurgia, 38, 125-31, 1948.

5. Hendrickson, A.A. and Machlin, E.S. — Acta. Met. 3, 64-9, 1955.

6. Hirth, J.P. and Vassamillet, L. — J. Appl. Phys. 29, 595, 1958.

7. Shigeta, J. and Hiramatsu, M. — J. Phys. Soc. Japan, 13, 1404, 1958.

8. Bunton, G.V. and Weintroub, S. — J. Cryst. Growth, 2, 91-6, 1968.

9. Smakula, A. and Klein, M.W. — Phy. Rev. 84, 1056, 1951.
   J. Chem. Phys. 21, 100-104, 1953.

10. Patel, A.R.; Bahl, O.P. and Vagh, A.S. — Acta. Cryst. 19, 1025-6, 1965.
    Acta. Cryst. 20, 914-6, 1966.

11. Budke, J. — J. Amer. Ceram. Soc. 5, 238, 1968.

12. Takeda, T. and Kondoh, H. — J. Phys. Soc. Japan, 17, 1315-6, 1962.

13. Voitsekhovskii, V.N. — Sovt. Phys. Cryst. 13, 563-5, 1968.

14. Michell, S.M. ; Lubbart, L. and Levi, L. — Phys. States Solid, 4, 63-70, 1964.

15. Kennedy, S.W. and Paterson, J.H. — Nature, 194, 1072, 1962.

16. Millea, M.F. and Kyser, D.F. — J. Appl. Phys. 36, 308-13, 1965.

17. Singh, K. — Trans. Farad. Soc. 52, 1623-5, 1956.

18. Jach, J. — Nature, 196, 827-9, 1962.

19. Bristow, J.R. and Rees, B.L. — Nature, 198, 178, 1963.

20. Varshavskii, A.V. — Zap. Uses. Min. Obsh. 94, 471-5, 1965.

21. Thomas, J.M. and Renshaw, G.D. — Trans. Farad. Soc. 61, 791-6, 1965.

Nature, 209, 1196-9, 1966.

22. Cutler, I.B. and Kovalenko, E.N. — Mater. Sci. Res. 3, 485-502, 1966.

23. Hirth, J.P. ; L.S. Seacrit and Z.A. Munir — Surface Sci. (Netherlands), 28, no. 2, p. 357-72, 1971.

24. Moller, H.J. and P. Hassen — Phys. Status Solidi A (Germany) 33, no. 1, p.k. 59-62, 1976.

25.	Parsanis, A.S. and D. Saran	Indian J. Pure & Appl. Phys. Vol. 13, no. 11, p. 725-30, Nov. 1975.
26.	Robertson, W.M.	J. Am. Ceram. Soc. (USA) 64, no. 1, p. 9-13, 1981.
27.	Mehta, B.J.	Ph.D. Thesis, M.S. Univ. of Baroda, Baroda 1972.
28.	Shah, R.T.	Ph.D. Thesis, M.S. Univ. of Baroda, Baroda, 1976.
29.	Mehta, B.J. and Pandya, J.R.	Crystal Res. & Tech. 17(4), 485-488, 1982.
30.	Mehta, B.J.	Ind. J. of Pure & Appl. Phys., 19(12), 1206-8, 1981.
31.	Mehta, B.J. and Pandya, J.R.	Surface Tech. (Netherland), 14, 139-42, 1981.
32.	Mehta, B.J.	Surface Tech., 11, 301-4, 1980.
33.	Mehta, B.J.	Surface Tech., 12, 253-56, 1981. Surface Tech., 13, 33-38, 1981.
34.	Mehta, B.J. and Pandya, J.R.	Surface Tech., 14, 391-93, 1981.
35.	Mehta, B.J. and Pandya, J.R.	Surface Tech., 15, 141-46, 1982.

CHAPTER - XI

STUDIES OF ETCH PATTERNS BY MULTIPLE BEAM INTERFEROMETRY AND SCANNING ELECTRON MICROSCOPY

CHAPTER - XI

STUDIES OF ETCH PATTERNS BY MULTIPLE BEAM INTERFEROMETRY AND SCANNING ELECTRONMICROSCOPY

11.1 INTRODUCTION

It is known from earlier studies of chemical dissolution of calcite cleavages by aqueous solution of sodium hydroxide (cf. Chapter IX) that plane shape of pyramidal and flat-bottomed and terraced etch pits is similar to that of a boat. The boundaries of these pits are curvilinear. It is also shown by using multiple beam interferometry and light profile microscopy[1] that the depth varies from one end to the other end of the boat-shaped etch pit. Determination of plane area of the plane shape and volume of such an etch pit presents difficulties. Instead an etch pit with a well-defined geometrical shape amenable for such determinations is desirable. A large amount of data about the various types of plane shapes of chemical and thermal etch pits on cleavage surface[2,3,4,5,6] is now available in this laboratory. From the various shapes the author has selected well-defined elongated pentagonal shape of etch pit which may be pyramidal, flat-bottomed or terraced. This is produced on a calcite cleavage by dissolving it in 60% aqueous solution of glacial acetic acid for a couple of minutes. This shape is highly sensitive to etching temperature.[7] The quantitative studies of changes in dimensions of such pits with etching temperature were made by using techniques of multiple beam

interferometry (MBI) and scanning electron microscopy (SEM). Such a combination of study covers large range of resolution and magnification for studying fine features of etched surfaces.

11.2 EXPERIMENTAL

Doubly distilled glacial acetic acid (GR quality supplied by SARA MERCK INDIA LTD) was used to prepare solution of desired concentration (60%) in distilled water. In what follows this solution will be referred to as the etchant. This etchant reveals dislocations[7] terminating on the surface under observation. The cleavage surfaces were produced in the usual way. The dislocation etch pits were produced by keeping the freshly cleaved surfaces in a still solution of the etchant for a definite time and for a constant etching temperature. The etched surface was washed in running distilled water, dried by an air blower and was optically studied. For obtaining better contrast between etch pits and surrounding areas at high resolution and magnification and also for interferometric study, the freshly cleaved and etched surface was uniformly coated by evaporating silver on the surface under high vacuum (cf. Chapter II). It is shown by Tolansky[8] that the uniform coating of silver film faithfully contours the surface. The silvered etched surface was matched with an optical flat having silver coating of appropriate thickness

Fig. 11.1a (x 95) photomicrograph of a dislocation etch pits by etching the freshly cleaved surface of calcite in 60% acetic acid for 3 min at 43°C.

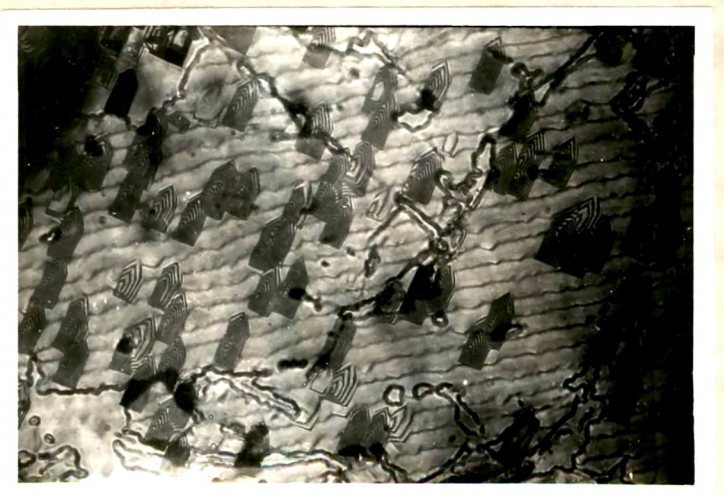

Fig. 11.1b (x 95) MBI interferogram of the surface shown in fig. 11.1a.

so as to satisfy the conditions for the production of good quality multiple beam interferograms. It should be noted that since calcite is chemically highly active and soft, the thin film of silver cannot be removed by chemical or mechanical means. It is therefore not possible to use silvered surface again for further treatment. Unsilvered surface is required to be used for optical study of the same surface for different stages of etching. For SEM study the surface was coated by gold by using ' Advance Sputter Coater ' (cf. Chapter II). The thickness of the gold film should be less than 80 A so that adequate emission of electrons from all major and minor topographical features could be obtained. Due to its chemical activity and softness, removal of gold film from the surface by chemical or mechanical means damages the surface and makes it unsuitable for further treatment.

11.3 OBSERVATIONS, RESULTS AND DISCUSSION

Fig. 11.1a (x950) is a photomicrograph of dislocation etfh pits by etching the freshly cleaved surface for 3 minutes at 43°C in the etchant. The etching is highly preferential, free from micropitting on the surface. The etch pits are well defined elongated pentagonal etch pits having identical orientation with respect to the surface. The line passing through the centre of the base and vertex of the elongated pits has direction [110]. The pits are of

three types : pyramidal, flat-bottomed and terraced. It is also possible to label them as dark and light pits. The terraced and pyramidal etch pits are highly eccentric. The typical characteristics are brought out more clearly by MBI interferogram (fig. 11.1b x 95) taken over the surface shown in fig. 11.1a. The interferogram gives not only depth but also the roughness or smoothness of the surface. The general fringe pattern indicates general etching over the entire surface to be much less than at preferential points. The pits have almost identical structure. The depth to which a pit descends is calculated by counting the number of fringes in a pit and multiplying it by $\lambda/2$ where λ is the wavelength of green light (5350 A). From the studies it is observed that depths of all etch pits are not identical. Some pits are so deep that the fringes inside it are not visible ; hence they remain dark in the interferogram (e.g. a row of etch pits on the left hand side of fig. 11.1b). In view of the varying depths of etch pits it is decided to concentrate on a few etch pits having larger depths. Since the studies are to be carried out at different etching temperatures, the matching characteristics of cleavage counter parts and uttlization of specimens from a single big block of calcite were used. One surface was optically and interferometrically studied at room temperature etching and the other at a higher temperature of etching. This made possible

to concentrate on a few pits. A large number of observations were taken on matched pairs of etched counterparts. Further for all observations etching time of 3 minutes was kept constant. A typical set of optical and interferometric micrographs are presented here. Fig. 11.2a is an optical micrograph of freshly cleavage surface etched at 62.5°C. The pit dimensions increase with etching temperature. Fig. 11.2b (x 95) is MBI interferogram taken over the surface (fig. 11.2a). In addition to the preferential etching, the interferogram sharply reveals shallow pits which were not clear in fig. 11.2a due to their shallower character.

Fig. 11.3a (x 45) exhibits a photomicrograph of a cleavage surface etched at 75°C by the etchant. In order to have more pits in the field of view the photograph was taken at a lower magnification. Although the pits retained their geometrical shapes, their dimensions have increased, with a few prominently scattered pits and a large number of shallow pits. The surface assumes a somewhat mottled character. This is more vividly brought out by MBI picture taken over this surface. The shallower pits are well-defined. In all these cases the eccentric nature of the pits is very clear. The figures also indicate significant effect of etching temperature for fixed time of etching, viz. 3 min. in elongating pit in the direction [110] whereas relatively less increase of the

Fig. 11.2a (x 95) photomicrograph of dislocation etch pits by etching the freshly cleaved surface of calcite in 60% acetic acid for 3 min at 62.5°C.

Fig. 11.2b (x 95) MBI interferogram of the surface shown in fig. 11.2a.

Fig. 11.3a (x 45) photomicrograph of dislocation etch pits by etching the freshly cleaved surface of calcite in 60% acetic acid for 3 min at 75°C.

Fig. 11.3b (x 45) MBI interferogram of the surface shown in fig. 11.3a.

of the base in the direction [110].

Several pairs (optical micrographs and corresponding MBI interferograms) were studied for the measurement of lateral dimensions and depth of etch pits at different etching temperatures. The data is presented in a tabular form (Table 11.1) and the graphs of rates of dissolution of length along [110] (fig. 11.4), of depth approximately along [001] (fig. 11.5), of area (fig. 11.6) and of volume (fig. 11.7). It is remarkable to note that the nature of plots is curvilinear and similar. This indicates that initial preferential dissolution of ledges along the directions of length, breadth and depth of dislocation etch pits have taken place in a way to maintain the etch pit shape even at etching temperature 82°C and the crystallographic symmetry about [110].

Fig. 11.8 (x 1720) represents (SEM) electron micrograph of an etfh pit on a calcite cleavage etched for 4.5 minutes by the etchant at 40°C. The etching time in the present work was kept the same for all observations. The boundaries of etch pit are very sharp and all lie on the surface under observation. Further out of five planes inside the surface forming the pentagonal pit, the inclination of the planes (shown dark) are more with observation plane. Fig. 11.9 (x 372) is SEM micrograph of a cleavage surface etched at 48.5°C and fig. 11.10 presents the magnified electron micrograph of

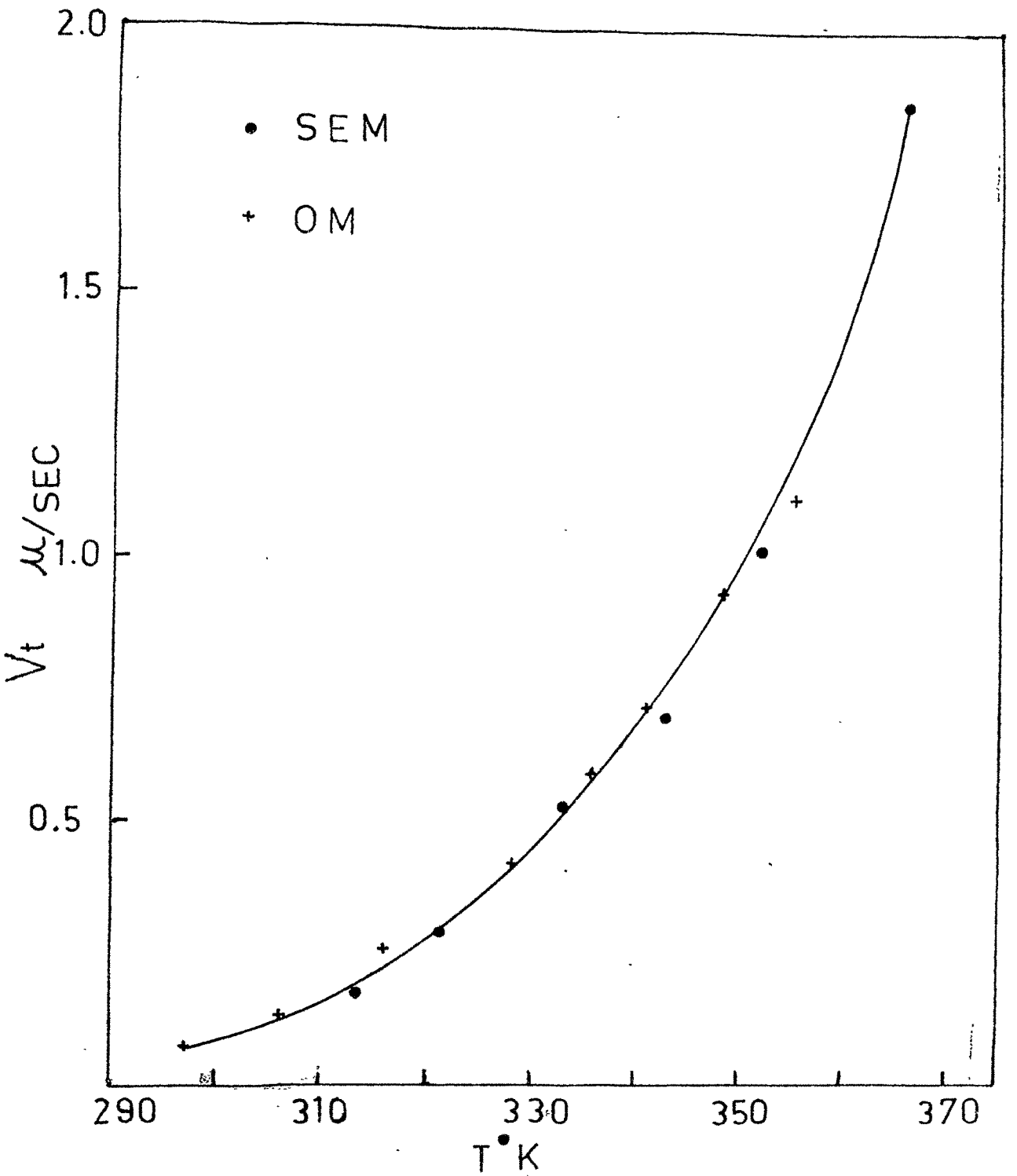

FIG. 11.4 PLOT OF V_t vs T

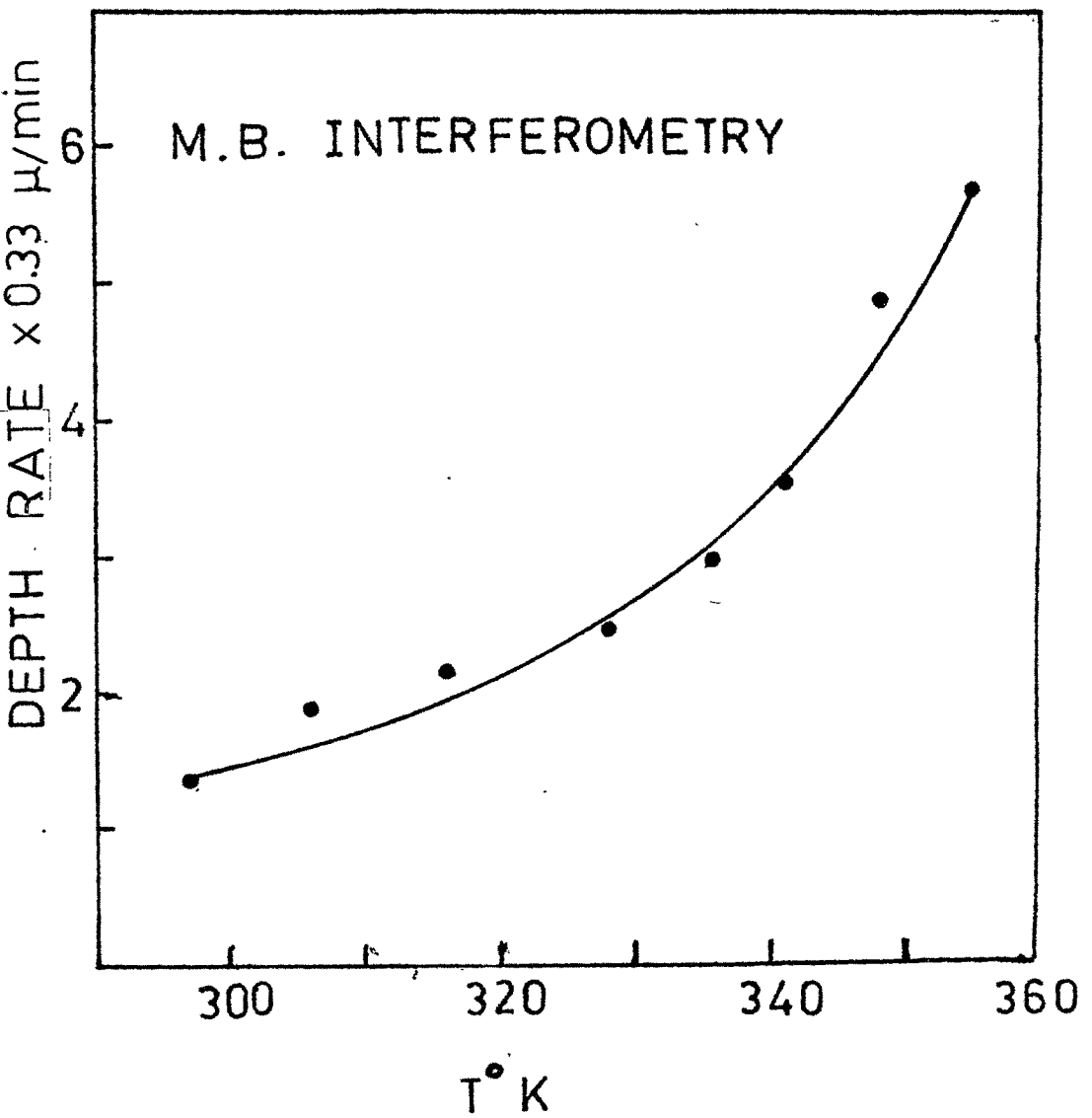

FIG. 11.5 PLOT OF DEPTH vs TEMP.

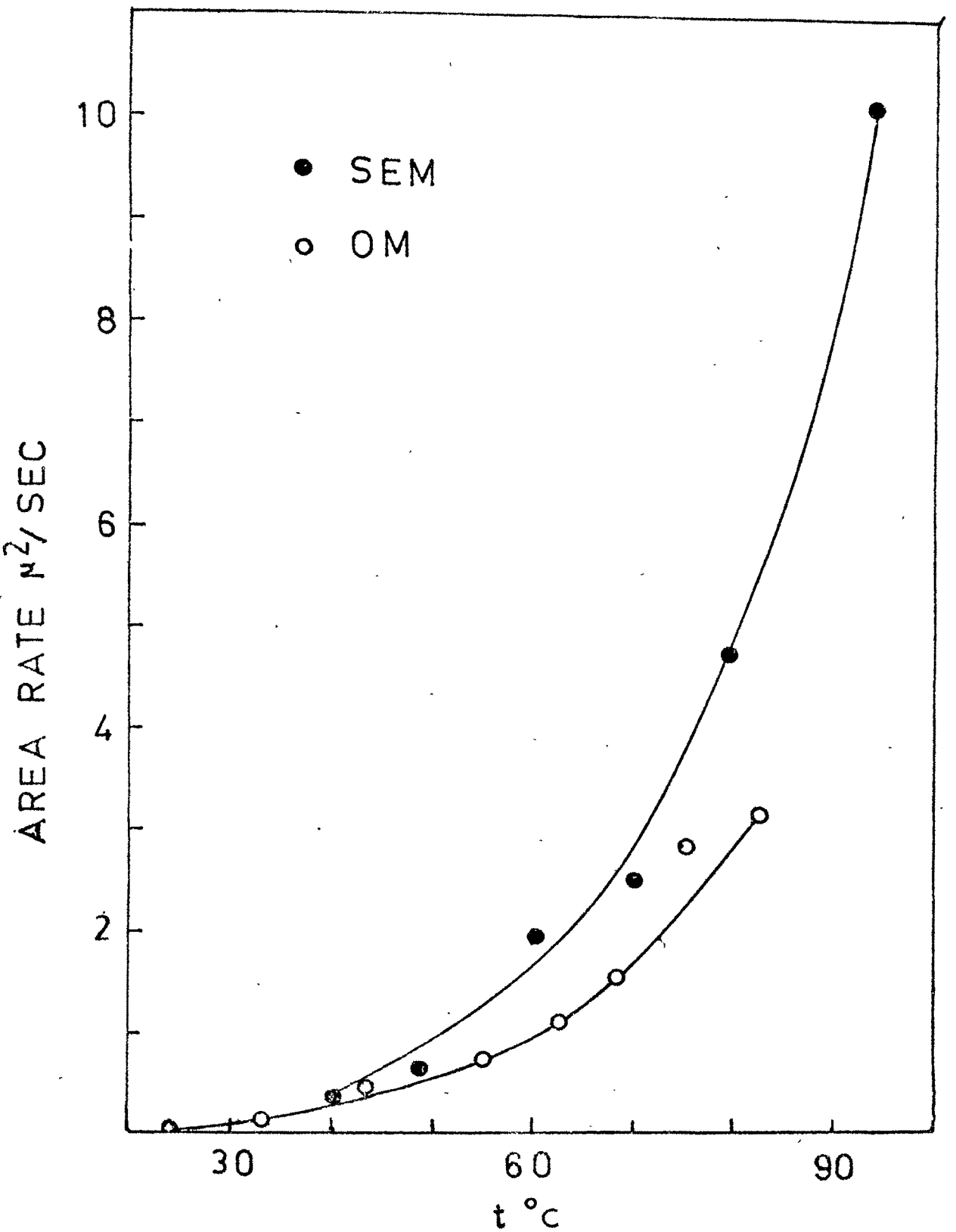

FIG.11.6 PLOT OF AREA RATE vs TEMP.

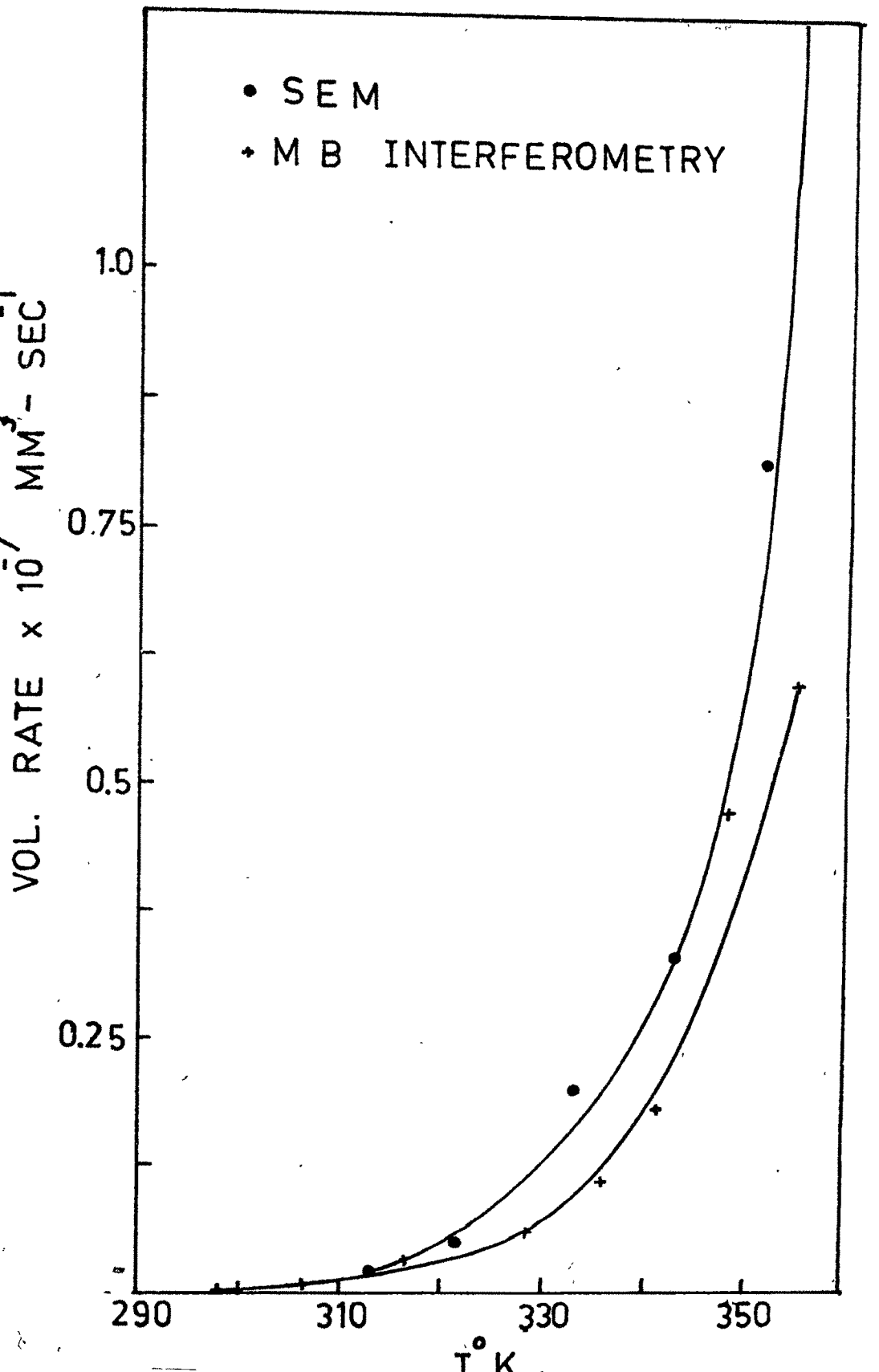

FIG. 11.7 PLOT OF VOL RATE vs TEMP.

Fig. 11.8 (x 1720) (SEM) electron micrograph of an etch pit on a calcite cleavage etched for 4.5 min. by 60% glacial acetic acid at 40°C.

Table 11.2 Scanning Electron Microscope (SEM) Observations

Etching Temperature T °K	Length L μ	L μ/sec	Area A μ^2 x 10^3	A μ^2/sec	Volume V μ^3 x 10^4	V μ^3/sec x 10^2
313	48.5	0.1796	0.903	3.340	0.0571	0.0212
321.5	80.08	0.2965	1.751	6.485	0.1341	0.0497
333	144.85	0.5364	5.392	19.90	0.5481	0.2030
343	190.2	0.7044	6.800	25.18	0.8953	0.3316
352	302.0	1.118	12.849	47.58	2.2056	0.8169
366	502.15	1.8598	27.300	101.11	7.5983	2.8140

one of the etch pits shown in fig. 11.9. Effect of etching at a still higher temperature of 60°C is shown in fig. 11.11 (x 592). Figs. 11.12 (x 295) and 11.13 (x 142) are electron micgrographs of etch pits produced on calcite cleavages by etching them at 79°C and 93°C respectively. In all these electron micgrographs it is clear that the etching is highly preferential at all etching temperatures. The boundaries of pits on cleavage surfaces are fairly sharp. The terracing of pits increases with etching temperature. At high etching temperature the dimensions of pits increase and hence the electron micrographs are taken at lower and lower magnifications. Several observations of the lateral dimensions of etch pits at different temperatures of etching for a fixed etching time (4.5 minutes) were taken whereas their depths were measured by MBI. A typical set of observations is presented in table 11.2 and their graphical plots in figs. 11.4, 11.6 and 11.7.

In these graphs are also plotted the observations taken by MBI technique. It is clear from these plots that although tangential etch rates of dissolution along [110] by SEM and by OM (optical microscopy) are studied at different etching temperatures, the scattering of these points around the same curvilinear plot is very less. Obviously this is not expected of etch rates of dissolution of area and volume of etch pit ; however almost the same type of curvature of plots (figs. 11.6

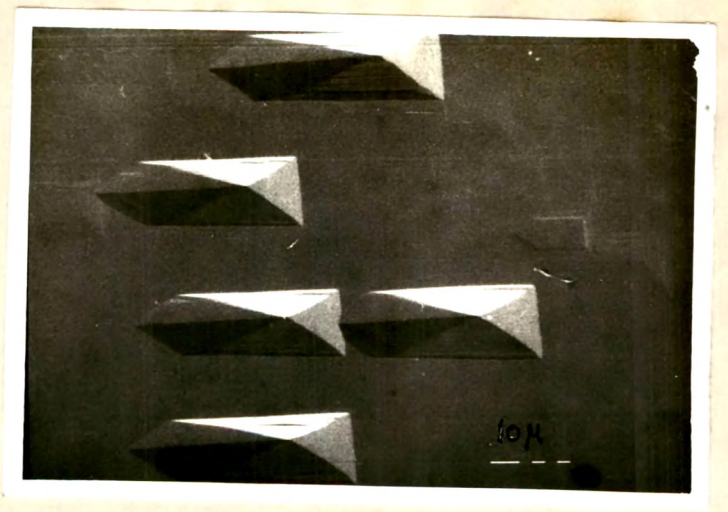

Fig. 11.9 (x 372) SEM micrograph of etch pits on a calcite cleavage, etched for 4.5 min. by 60% glacial acetic acid at 48.5°C.

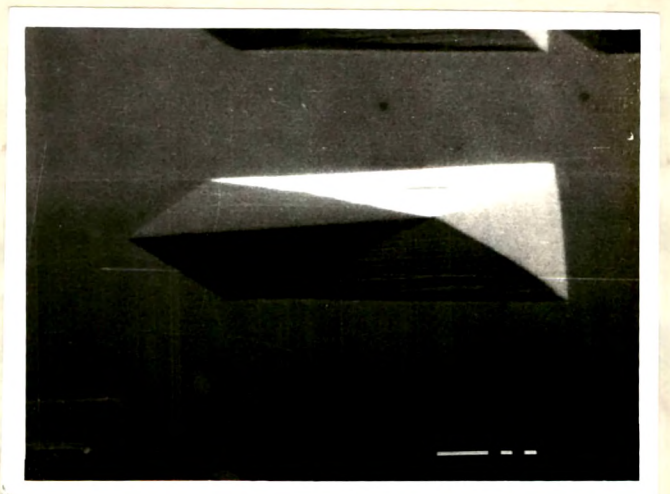

Fig. 11.10 (x 714) SEM micrograph of one of the etch pit of Fig. 11.9

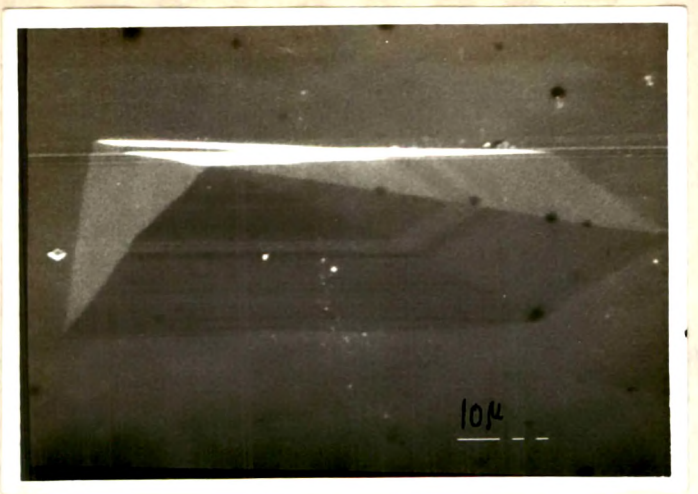

Fig. 11.11 (x 592)

Fig. 11.12 (x 295)

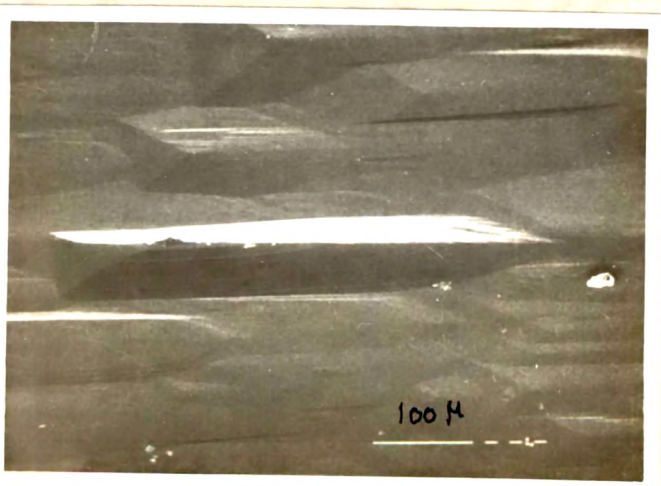

Fig. 11.13 (x 142)

Fig. 11.11, 11.12 and 11.13 electron micrographs of etch pit on calcite cleavages etched for 4.5 min. by 60% glacial acetic acid at 60°, 79°C and 93°C respectively.

Table 11.3

MBI				SEM		
$10^3/T$	Log D	Log L	Log A	$10^3/T$	Log L	Log A
3.367	0.1351	1.1702	2.021	3.194	1.685	2.955
3.267	0.412	1.408	2.470	3.110	1.903	3.243
3.164	0.3392	1.695	2.946	3.003	2.161	3.732
3.048	0.3904	1.892	3.114	2.915	2.279	3.832
2.981	0.4775	2.029	3.311	2.841	2.480	4.108
2.932	0.5501	2.116	3.446	2.732	2.701	4.436
2.873	0.6914	2.231	3.716			
2.817	0.7583	2.309	3.757			

and 11.7) is maintained at high etching temperatures. The etch rates follow Arraheneous equation (cf. Chapter IX, eqn. 9.0). Hence it is possible to determine activation energy of dissolution process. The plots (cf. Table 11.3 for observation) of Log D vs. $10^3/T$ (1), Log V_t vs. $10^3/T$ (2 and 3) and log A vs. $10^3/T$ (4 and 5) are shown in fig. 11.14 where OM, MBI and SEM stand for optical microscopy, multiple beam interferometry and scanning electron microscopy respectively and numbers 1, 2, 3, 4 and 5 in paranthesis denote the plots. The activation energies calculated from these straight line plots along with those obtained by using aqueous solutions of sodium hydroxide (cf. Chapter IX), of potassium hydroxide[9], of glacial acetic acid[10] (0.45% and 60%), ammonium chloride[11] and formic acid[12] (100%) as dislocation etchants are shown in table 11.4. The activation energies obtained from the study of dissolution rates of area, length along [110] and of depth approximately along [001] are different from the value obtained earlier.[10] The reasons for larger value of E_A and smaller value of E_t (SEM) than 0.54 ev are not yet clear. However the lower value of E_n (MBI) for dissolution rate along depth is likeoy to be due to crystal anisotropy and release of strain energy at the preferential etching spots which are most probably at dislocations terminating on a cleavage surface of calcite.[10]

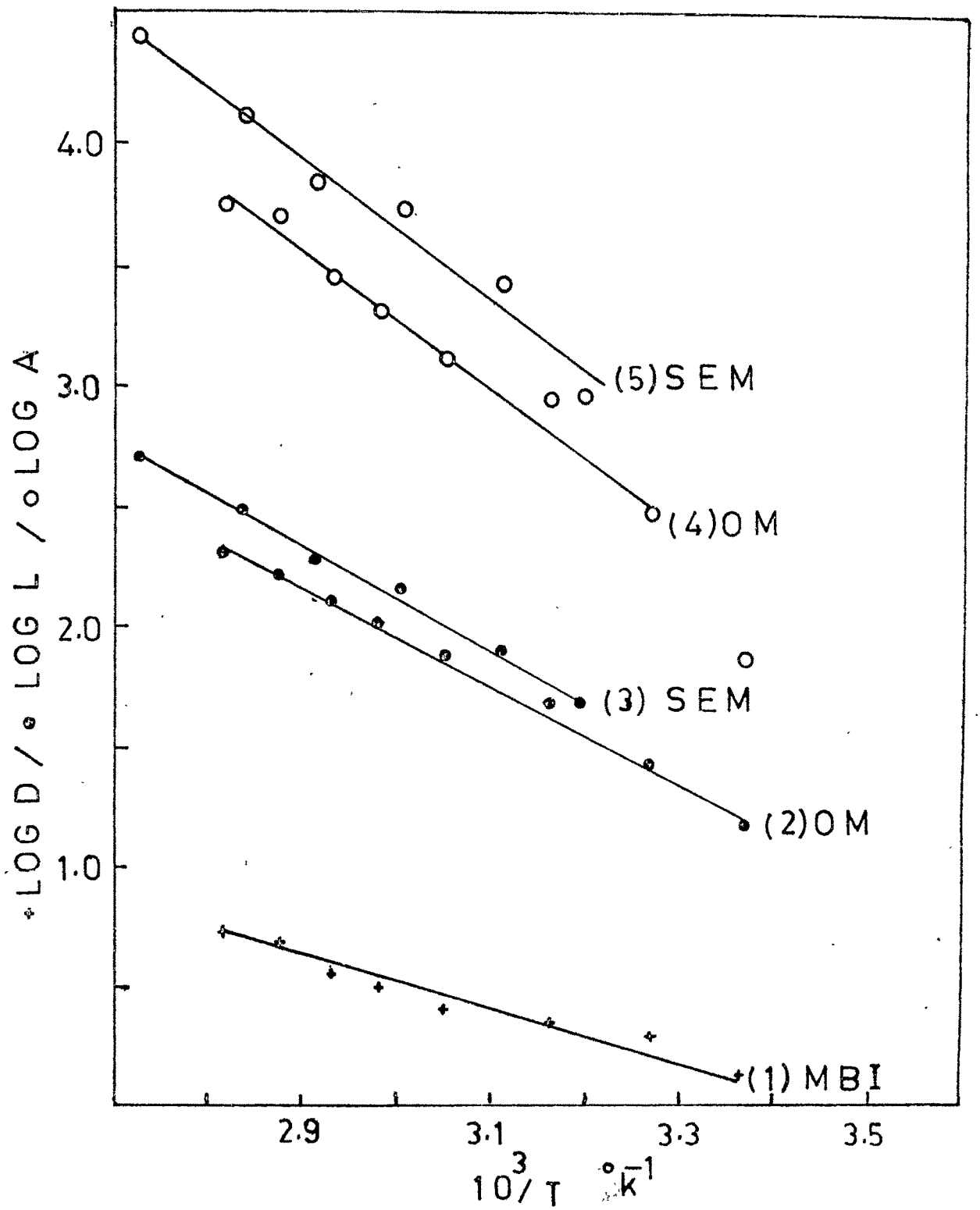
4.0
3.0
2.0
1.0
LOG D / ∘ LOG L / ∘ LOG A
(5) S E M
(4) O M
(3) S E M
(2) O M
(1) M B I
2.9
3.1
3.3
3.5
10³/ T °k⁻¹

FIG. 11.14

It should be noted that graphical analysis (cf. Chapter VII) was also made for these plots and those straight line plots of Chapter IX on dissolution of calcite cleavages in aqueous solutions of sodium hydroxide. The analysis did not reveal significant differences in slope values for a large number of observations except for a very few observations. Hence it is not presented here.

It is known that initial stages of preferential etching of a crystal surface by an appropriate etchant consists of scattered etch pits whose dimensions increase with etching time and with etching temperature. At a constant temperature the increased etching produces pits of larger dimensions which touch each other and begin to coalesce. This gives rise to a block pattern observed on a number of crystal surfaces such as diamond,[13] fluorite[14] etc. Such patterns are readily observable on the surfaces of crystals exhibiting well-defined geometrical etch pits produced by an appropriate chemical etchant. Such patterns are obtainable at those places where there is comparatively heavy deformation such as the edge along which the propagation of cleavage takes due to a light blow on the razor blade kept on this edge. Comparatively low etching or initial etching at high etching temperature can produce etch blocks at such places. It can also be produced at those places such as central part of a cleavage plane having

Table 11.4 Activation Energy Values

Etchant	Activation energy in ev			
	E_t	E_A	E_t (SEM)	E_n (MBI)
Aq. Sodium hydroxide solution	0.62	-	-	-
Aq. Potassium hydroxide solution	0.62	-	-	-
Glacial Acetic acid 0.45%	0.68	-	-	-
Glacial Acetic acid 60%	0.54	0.59 0.57	0.44 0.41	0.23
Formic acid 100%	0.56	-	-	-
NH_4Cl	0.35	-	-	-

less deformation by heavy etching. Fig. 11.15a (x 2350) is an electron micrograph of an etch pattern produced by etching a cleavage face of calcite by 60% glacial acetic acid. This pattern, known as block pattern, can be compared with a growing face of a crystal containing a large number of kinks and steps. It is generally understood that systematic dissolution is a reverse process of growth. However there is no definite experimental evidence. An attempt is therefore made here to correlate the depression of a smallest block with a lattice parameter parallel to direction of depression namely [001]. SEM is used to determine depressions (step heights) of these blocks by studying in detail electron micrograph of a small area taken at higher magnification and resolution (fig. 11.15b x 4440). Determination of depression (heights) was carried out over a large number of surfaces (more than a dozen) etched for a fixed time (4.5 min) and at a constant higher etching temperature (93°C). A typical set of observations is presented here :

Sr.No.	Step height in micron	Number of observations
1	5.157 5.132	Weighted mean of 12 obs.
2	4.132	Weighted mean of 10 obs.
3	3.522 3.467	Weighted mean of 15 obs.

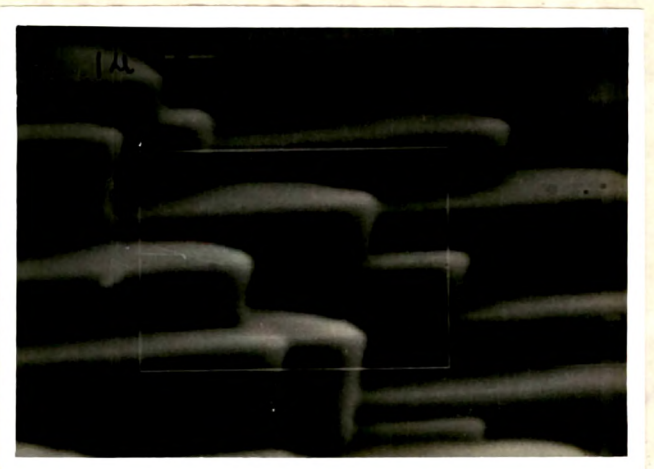

Fig. 11.15a (x 2530) and 11.15b (x4440) electron micrograph of a cleavage surface of calcite etched by 60% glacial acetic acid for 4.5 min. at 93°C.

4	2.650 2.510	Weighted mean of 10 obs.
5	2.040 2.080	Weighted mean of 12 obs.
6	1.479 1.501	Weighted mean of 10 obs.
7	1.017	Weighted mean of 10 obs.
8	0.510	Weighted mean of 10 obs.

It is clear from the above set that the dissolution steps is approximately a multiple of the lowest depression (0.51μ). The lattice parameter representing the spacing between two successive rhombohedral cleavages on an atomic level is 6.1A. The lowest depression (step) of the block 0.51μ can not be connected with the lattice parameter 6.1 A in a simple manner. The reason for this is not yet known. The author had a desire to carry out a large amount of work on topographical study of virgin and etched cleavage surfaces of calcite ; however this could not be realised due to non functioning of SEM over a large period, non-availability of certain accessories required for studying fine etch features and indentations, and other difficulties.

11.4 CONCLUSIONS

(1) Initial preferential dissolution of ledges along three non-coplanar directions takes place in such a way as to

maintain the geometrical shape of an etch pit which exhibits crystallographic symmetry of a cleavage plane of calcite.

(2) In an etch pattern resembling a growth pattern, the etch ledges (depressions) in a direction normal to cleavage plane occur in multiple of the smallest depression. However the lattice parameter along this direction is not a multiple of this depression produced by etching.

REFERENCES

1. Pandya, J.R. — Ph.D. Thesis, M.S. University of Baroda, Baroda, 1961.

2. Pandya, N.S. and Pandya, J.R. — Nature (Lond), 184, 894, 1959.

3. Mehta, B.J. — Ph.D. Thesis, M.S. University of Baroda, Baroda, 1972.

4. Mehta, B.J. — Surface Tech.(Netherlands), 13, 33, 1981.

5. Pandya, J.R. and Mehta, B.J. — Min. Mag. (Lond.), 57, 526, 1969.

6. Mehta, B.J. and Pandya, J.R. — Surface Tech.(Netherlands), 14, 159, 391, 1981.

7. Mehta, B.J. and Pandya, J.R. — Ibid, 15, 141, 1982

8. Tolansky, S. — Multiple Beam Interferometry of Surface and Thin films. Oxfor and Clarendon Press, 1948.

9. Shah, A.J. and Pandya, J.R. — Uppublished work

10. Shah, R.T. — Ph.D. Thesis, M.S. University of Baroda, Baroda, 1982.

11. S.E. Khisti — Private Communication

12. L.J. Bhagia — Ph.D. Thesis, M.S. University of Baroda, Baroda, 1982.

13. Pandya, N.S. and Pandya, J.R. — Curr. Sci., 27, 437, 1958.

14. Pandya, N.S. and Tolansky, S. — Proc. Roy. Soc. A 225, 40, 1954